

THE
LONDON, EDINBURGH, AND DUBLIN
PHILOSOPHICAL MAGAZINE
AND
JOURNAL OF SCIENCE.

[SEVENTH SERIES.]

SEPTEMBER 1934.

XXXVI. *The Preparation of Free Hydroxyl.*

By ERIC M. STODDART *.

SUMMARY.

A BRIEF survey of the previous work on hydroxyl is given, particular attention being given to the work of Lavin and his collaborators on the removal of free hydroxyl from a discharge through water vapour. With a view of studying the chemical properties of hydroxyl the work of Lavin was repeated. It was found that free hydroxyl was not removable from a discharge through water vapour. Possible explanations for the observations of Lavin are dealt with. The quenching of the oxygen afterglow with water vapour was studied in detail, and the formation of hydroxyl was observed as one of the products of the mechanism. It was found that the apparent life-period of hydroxyl was the same as that of the oxygen afterglow, but, since the life-period of free hydroxyl is known to be very short, it was, therefore, clear that the hydroxyl owed its formation to a secondary change brought about by oxygen atoms. Atomic and molecular hydrogen were also used to quench the oxygen afterglow, hydroxyl again being observed as a product. Even so, it was quite impossible to separate the free radicle from active hydrogen

* Communicated by Prof. F. G. Donnan, C.B.E., M.A., LL.D., D.Sc., F.R.S.

or active oxygen, thereby enabling a study of its chemical reactions to be made. Small quantities of hydrogen peroxide were found as a product of the reactions, and a possible explanation of its formation is given.

WATSON (Astrophys. J. iii. p. 145 (1924)) showed that when water vapour was excited by an electrodeless discharge, the principal Balmer lines of atomic hydrogen made their appearance together with certain characteristic bands in the ultra-violet. Since this time a considerable literature has accumulated bearing upon the production of these bands in electrical discharges through water vapour. Fortrat (*J. de Physique*, v. p. 20, (1924)) incorrectly assigned the bands to the oxygen molecule, and later analysis has shown that they belong to the hydroxyl radicle. Bonhoeffer and Reichardt (*Z. physik. Chem. A*, cxxxix. p. 75 (1928)) found it was possible to obtain the 3064 Å.U. hydroxyl band in absorption through heated water vapour, the free radicle being in thermodynamical equilibrium.

Bonhoeffer (*Z. physik. Chem.* cxvi. p. 391 (1925)) noticed that atomic hydrogen caused many substances, including the alkali metals, to phosphoresce, and atomic hydrogen itself was found to emit the "water-vapour band," which is now known to be the characteristic hydroxyl band. He considered that this emission could only be accounted for by the assumption of a triple collision between two hydrogen atoms and a water molecule. The energy of recombination of hydrogen atoms was sufficient to cause dissociation of water molecules with the production of excited hydroxyl radicles. The hydroxyl radicles then lost their excess energy by radiation of the characteristic 3064 Å.U. band. Such was the mechanism proposed by Bonhoeffer in explanation of his experimental observations, but Urey and Lavin (*J. Am. C. S. li. p. 3290 (1929)*) refer to the paper thus: "... the fact that the OH bands are emitted by the gases leaving Wood's tube as used in the production of atomic hydrogen shows that the OH molecule can be pumped to considerable distances from the discharge tube..." Bonhoeffer, in his original paper, however, stressed the idea that the free hydroxyl radicle was being produced by secondary changes, and was not being removed

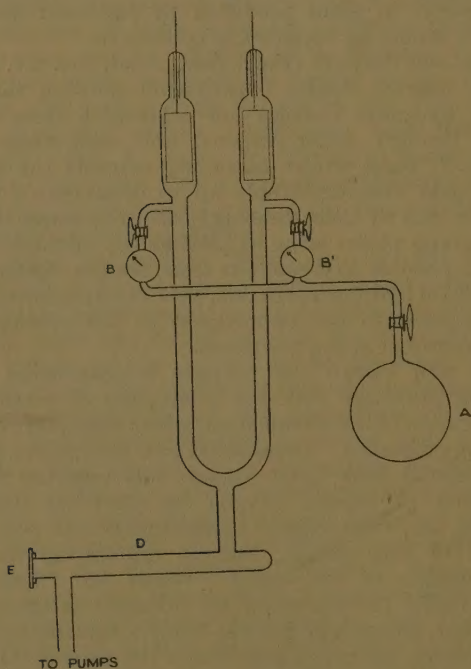
from the discharge-tube. Urey and Lavin were themselves unsuccessful in demonstrating the presence of free hydroxyl in the gases issuing from a discharge-tube by absorption spectrum methods, but considered that such a product was chemically detectable in such gases. They report that free hydroxyl had both powerful oxidizing and powerful reducing properties. Gases resulting from a disruptive discharge through water vapour are known to contain large concentrations of atomic hydrogen and atomic oxygen, a fact to which they made no reference, and consequently their chemical evidence for the presence of hydroxyl in gases produced by electrical discharge methods cannot be regarded as conclusive.

Lavin and Stewart (Proc. Nat. Acad. Sci. xv. p. 829 (1929)) describe similar experiments showing that free excited hydroxyl radicles are removable from a discharge through water vapour, and emit their usual 3064 Å.U. band whilst travelling towards the pumps. Such bands were detectable up to distances of 35 cm. from the exit of their discharge-tube, exposures of their spectrograph plates being as little as ten minutes. They found it possible to freeze out from the gas-stream small quantities of hydrogen peroxide, the concentration of which was supposed to be proportional to the concentration of the hydroxyl in the gas-phase.

It is well known that oxygen is dissociated in an electrical discharge with the production of considerable concentration of the atomic form, which possesses powerful oxidizing properties. Copeland (Phys. Rev. xxxvi. p. 1221 (1930)) found that water vapour was essential for the production of atomic oxygen by electrical discharge methods, the water vapour being supposed to poison the surfaces of the system, thereby minimizing the wall recombination of the atoms. Wrede (*Z. Physik.* liv. p. 53 (1929)) demonstrated by diffusion methods that 25 per cent. monatomic gas was easily attainable by direct or alternating current at pressures of the order of 0.15 mm. It is generally considered that a trace of nitrogen is necessary for the production of an afterglow in oxygen, even when the walls of the system have been poisoned with water vapour, but Lewis (J. Am. C. S. li. p. 654 (1929)) reports that this is not so, the afterglow being easily producible in oxygen free from nitrogen.

The object of the present paper is to describe experiments which show that the free hydroxyl radicle cannot be removed from a discharge through water vapour. It will be shown, however, that when an afterglow is produced in damp oxygen, hydroxyl emission can be detected up to distances of a metre and a half from the exit of the discharge-tube. Evidence will be given showing that this emission is dependent upon the intensity of the oxygen afterglow.

Fig. 1.



Preliminary Experiments.

In fig. 1 is shown the apparatus constructed for the purpose of repeating the experiments of Lavin and Stewart (*vide supra*). The water vapour employed was supplied from the 5-litre bulb A, which contained *vacuo*

distilled water. The water vapour entered the discharge-tube *via* the needle valves B and B', which regulated the rate of flow, the equilibrium pressure in the system being measured by a Pirani gauge (not shown). The discharge-tube was constructed of soft glass in the shape shown, each limb of the U being $2\frac{1}{2}$ feet in length, and the internal diameter of the tubing being 1 inch. The electrodes were cylindrical in shape and constructed from aluminium sheet, this being found to make an electrode which did not sputter as readily as one turned from solid aluminium. Copper-clad wire, as supplied by The Vactite Wire Co., was used for the leading-in wires for these electrodes. The water vapour, after passing through the discharge-tube, traversed the horizontal tube D, which was fitted with a quartz window E, luted in place with de Khotinski cement. The working in parallel of two twin Gaede rotary oil pumps, protected from the water vapour by a liquid-air trap, was the usual method of evacuation, but, if desired, the system could be evacuated by means of a two-stage mercury diffusion pump backed by a "Hyvac" pump. Every part of the apparatus was treated with hot chromic-nitric acid solution and thoroughly washed with tap-water followed by distilled water. The system was evacuated by means of the mercury diffusion pump, and all the essential parts were heated with a soft blow-pipe flame to a temperature just below softening point for the glass. This enabled the surfaces of the system to be freed from any extraneous gas, which might give rise to some unforeseen phenomenon. Since the recombination of the free radicles is possibly a wall reaction, water vapour was streamed through the system for several hours without passage of a discharge, the surfaces thereby being poisoned and enabling this effect to be minimized.

The experimental procedure then consisted of adjusting the streaming velocity of the water vapour so as to maintain a suitable pressure (about 0.2 mm.) in the apparatus in spite of the withdrawal of gas by the pumping system, the horizontal tube D being examined through the quartz window E by means of a spectrograph, whilst an alternating current of 80 ma., supplied by a 1 kw. transformer, was maintained through the vapour in the discharge-tube. Lavin and Stewart observed strong hydroxyl emission up to distances of 25 cm. from the

exit of their discharge-tube, the exposures of their spectrograph plates being ten minutes. In the present apparatus the observation tube D was 15 cm. long, and was separated from the discharge-tube by a connecting tube 6 cm. long. Consequently it was anticipated that no difficulty would be experienced in the detection of the hydroxyl bands in emission along the horizontal tube D. No such emission was ever detectable however, even with exposures as long as twelve hours. Various equilibrium pressures between 0.05 mm. and 0.8 mm. were tried, but success was never attained. The liquid-air trap inserted into the system for the protection of the pumps was examined for the presence of hydrogen peroxide, but only very small quantities were obtained.

Two possible explanations were found which could account for the observations of Lavin and Stewart. Firstly, no mention is made in their paper of using air-free water for their experiments, and, as will be shown later, the presence of oxygen enables the detection of free hydroxyl in emission away from a discharge. A second, and more likely, explanation is that a stray discharge may have been present throughout their apparatus. Whether the latter explanation be the true one or not, it was found that when a small earthed electrode was inserted into the system near the pumps a stray discharge of sufficient magnitude was thereby produced through the system which rendered it possible to detect the 3064 Å.U. hydroxyl band in emission along the observation tube D. Elimination of both these factors, however, rendered it impossible to repeat the observations of Lavin and Stewart.

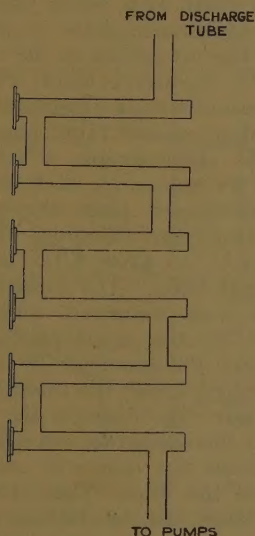
The Oxygen Afterglow.

In a note to 'Nature' (cxxxiii. p. 607 (1929)) Lavin and Stewart mentioned that when oxygen was added to water vapour in their experiments much larger quantities of free hydroxyl appeared to be removed from the discharge-tube than in previous experiments employing water vapour alone. They found that the oxygen afterglow was produced when the mixture admitted to the discharge-tube was comparatively rich in oxygen.

With the object of repeating these experiments, the apparatus shown in fig. 1 was modified so that the water

vapour could be adulterated with electrolytic oxygen before being passed through the discharge-tube. The hydroxyl bands did not make their appearance outside the discharge-tube as had been reported. When the gases employed in these experiments were comparatively rich in oxygen, thereby producing its afterglow, the appearance of the 3064 Å.U. hydroxyl band was noticed in emission along the observation tube D. Addition of larger quantities of oxygen increased the intensity of

Fig. 2.



its afterglow, and at the same time increased the intensity of the hydroxyl emission.

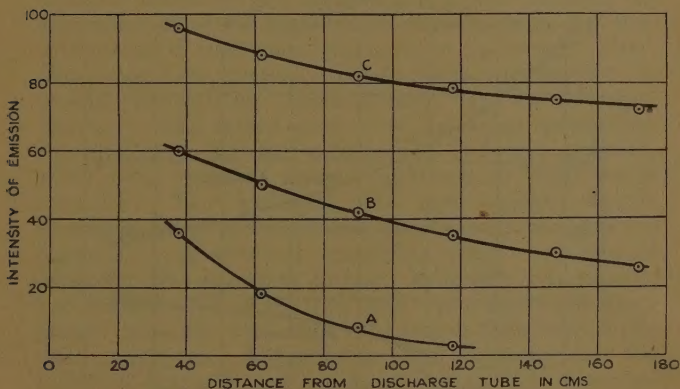
Considerable modification was made to the apparatus for the purpose of closely investigating the relation between the intensity of the oxygen afterglow and the intensity of the hydroxyl emission. The gases leaving the discharge-tube traversed six horizontal tubes, each 12 cm. long and $2\frac{1}{2}$ cm. internal diameter, fitted with quartz windows luted in place (see fig. 2). The pumping system remained unaltered, but the pressure in the system

was measured with a McLeod gauge. Since large quantities of oxygen were needed for the experiments about to be described, electrolytic gas in cylinders as supplied by The British Oxygen Co. was employed. This gas was found to be very pure, and highly suitable for the purpose. It was passed through two bubblers containing *vacuo* distilled water, followed by an empty trap which was connected to the discharge-tube *via* the usual two regulating valves. By immersing the empty trap in various cold liquids the amount of water vapour being carried into the system could be controlled. The walls of the system were poisoned, as usual, with water vapour, a necessary condition for the appearance of the oxygen afterglow.

The decays of the intensities of the oxygen afterglow and the 3064 Å.U. hydroxyl band were observed by examination in turn of the six observation tubes with the spectrograph. Ilford special rapid panchromatic plates were used in the spectrograph, a single plate being employed for all six exposures, each being of six hours' duration. The developed plate showed in each case the spectrum of the oxygen afterglow, which was continuous from 6700 Å.U. to 4200 Å.U., together with the 3064 Å.U. hydroxyl band. The densities of the images of these spectra were measured with a Zeiss microphotometer, and by the usual photographic methods (see 'Photographic Photometry,' by Dobson, Griffith, and Harrison: Oxford Press) the intensities of the radiations were deduced. The distance the glowing gas had travelled between the exposures was measured by taking the distance between the centre of one horizontal tube and the centre of the next. This necessitated making the assumption that the intensities of the emissions remained constant throughout the length of each individual tube, and, since it was not practicable to reduce the lengths of these any further without unduly increasing the time of exposure, the measurements are only approximate. Nevertheless, the results of such measurements were very reproducible. Owing to the cleaning-up action of the discharge, difficulty was at first experienced in obtaining identical surface conditions for all the exposures. This was finally solved by filling the apparatus with damp oxygen after each exposure and allowing it to stand overnight, the surfaces being thereby restored to a reproducible state.

The experimental results are shown graphically in fig. 3. The intensity of the spectrum of the oxygen afterglow is plotted in arbitrary units against the distance the gas had travelled from the exit of the discharge-tube. All the curves are for an equilibrium gas pressure of 0.18 mm. in the apparatus. Curve A illustrates the decay of the oxygen afterglow when the oxygen was saturated with water vapour at 15° C.; curve B illustrates the decay when the oxygen was saturated with water vapour at 0° C., and curve C illustrates the decay when water vapour was eliminated from the gas-stream by

Fig. 3.



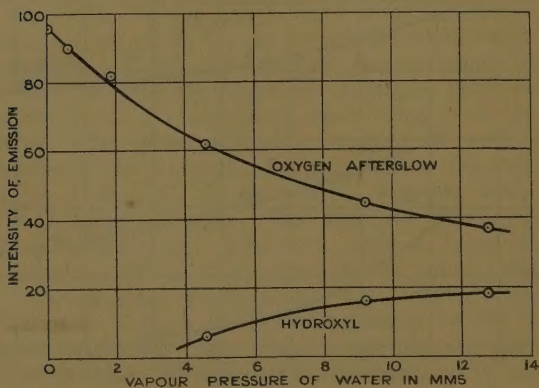
cooling the control trap to -78°C . The curves clearly show the quenching effect of water vapour on the oxygen afterglow.

It was of great importance to observe that the intensity of the hydroxyl emission had the same rate of decay as that of the afterglow of oxygen. When the experiment was carried out with oxygen saturated with water vapour at 15° C., the hydroxyl intensity was always 0.48 times that of the oxygen afterglow intensity. Similarly, with water vapour at 0° C. the hydroxyl intensity was 0.1 times that of the oxygen afterglow, whilst no emission due to hydroxyl was observed when the oxygen stream was free from water vapour. Since the two emissions have the same rate of decay, it is clear that the free hydroxyl

observed owes its formation to the presence of the excited oxygen. If the hydroxyl had been removed from the discharge-tube, as stated by Lavin and Stewart, the rate of its decay would not have been dependent upon the rate of the decay of the oxygen afterglow, but would have been very much greater than observed, since it has been shown by Bonhoeffer and Pearson (*Z. physik. Chem. B*, xiv. p. 1 (1931)) that free hydroxyl has a very short life period.

The effect of the concentration of the water vapour upon the intensities of the emissions was investigated by varying the quantity of water vapour admitted to the

Fig. 4.



gas-stream and making the usual spectrographic observations on the first of the horizontal tubes. Fig. 4 shows these relationships, and it will be noticed that the intensity of the oxygen afterglow diminishes with increasing concentration of water vapour, whereas the reverse is true in the case of hydroxyl.

The Action of Atomic and Molecular Hydrogen on the Oxygen Afterglow.

Two discharge-tubes were employed, one for oxygen and the other for hydrogen, both being of the same dimensions as the one used in the previous experiments. The effluent gases from both discharge-tubes entered

the same horizontal observation tube, fitted, as usual, with a quartz window. Glass baffles were sealed into the exits of both discharge-tubes for the purpose of preventing any back diffusion of gas. Surface poisoning was maintained by adulterating the gases with water vapour until it was desired to study the effect of one gas on the other, whereupon all the water vapour was rigorously removed from the gas-streams by passing them through traps immersed in solid carbon dioxide-ether mixture. This procedure was essential, since both active hydrogen and active oxygen luminesce with the 3064 Å.U. hydroxyl band when water vapour is present. The gas-streams were adjusted by needle valves so that about twice as much oxygen as hydrogen passed through the apparatus, the total equilibrium pressure being 0.2 mm. The action of molecular hydrogen on the oxygen afterglow was first studied. The oxygen was excited in passing through its discharge-tube, but the hydrogen was not. The mixed gases were examined away from the discharge for the presence of hydroxyl emission, which was always present although in very feeble intensity. The hydrogen was then excited, atomic hydrogen being produced and mixing with the glowing oxygen. A pronounced quenching effect was noticed whenever the discharge through hydrogen was started, and the 3064 Å.U. hydroxyl band was observed in much greater intensity with atomic hydrogen than with molecular hydrogen. Nevertheless, the intensity of the hydroxyl emission was no greater than that observed in the previous experiments. Variation in the gas mixture, the equilibrium pressure in the system, and the discharge currents did not result in any pronounced increase in the hydroxyl emission.

Discussion.

The presence of atoms in the oxygen afterglow has been demonstrated by Crewe and Hulbert (Phys. Rev. xxx. p. 124 (1927)) and also by Copeland (*ibid.* xxxi. p. 1113 A (1928)). J. J. Thomson (Phil. Mag. xxxii. p. 321 (1891)) expressed the opinion that the oxygen afterglow is due to the emission accompanying atomic recombination. From the experiments just described it has been shown that a stream of active oxygen not only

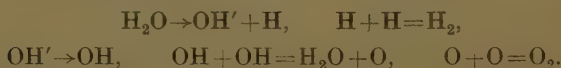
emits its afterglow, but also the 3064 Å.U. hydroxyl band when water vapour is present. It is clear that the necessary activation of this hydroxyl emission cannot be brought about by electronic bombardment outside the discharge-tube, but must result from energy transfer by ternary collision with two oxygen atoms, or by collision with an oxygen molecule produced by combination of oxygen atoms. The available energy for this process, given by the heat of dissociation of oxygen into atoms, is sufficient to produce the observed excitation.

It is clear that recombination of oxygen atoms can take place on the walls of the system and also as a result of employing oxygen atoms and molecules as third-body agencies. Hence the complete recombination in these experiments can be expressed by an equation, thus :

$$-\frac{\partial O}{\partial t} = K_1[O]^2[H_2O] + K_2[O]^2 + K_3[O]^2[O] + K_4[O]^2[O_2],$$

which is the sum of all these individual quantities. The hydroxyl emission observed in all these experiments was very weak, and, therefore, the radicle could only have been present in very small concentrations. It would have been quite impossible to attempt any study of the chemical properties of hydroxyl using these gas mixtures.

Bonhoeffer and Pearson (*Z. physik. Chem.* B, xiv. p. 1 (1931)) propose the following reactions in discharges through water vapour :



If this mechanism is correct, it is clear that the hydroxyl radicle can never be separated from hydrogen and oxygen atoms, and that this is the case has been shown in the present experiments. The chemical properties reported by Lavin and his collaborators for free hydroxyl are, in reality, due to a mixture of atomic hydrogen and oxygen. Many investigators have taken exception to the scheme of Bonhoeffer and Pearson, largely because they have observed the formation of hydrogen peroxide in similar experiments. Consequently the decay of hydroxyl has often been represented thus :

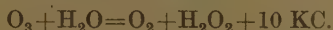


It is difficult to understand how the hydrogen peroxide molecule is capable of radiating this energy, and von Elbe (J. Am. C. S. lv. p. 62 (1933)), in order to get over this difficulty, suggested the following alternative :



Such a mechanism has one inherent difficulty, fully realized by von Elbe : no explanation is given for the initial production of hydrogen peroxide.

In the present work, small quantities of hydrogen peroxide were found from time to time. A careful consideration of the literature reveals the fact that hydrogen peroxide is always found as a product of reactions in which the conditions favour the formation of ozone. The following mechanism for the formation of the hydrogen peroxide is, therefore, suggested :



Consequently there is no need to assume that the decay of hydroxyl leads to the formation of hydrogen peroxide, and the scheme originally put forward by Bonhoeffer and Pearson clearly embraces the main mechanisms in such experiments.

The author wishes to record his thanks to Prof. F. G. Donnan, C.B.E., F.R.S., for the interest with which he has followed this work.

Summary of Conclusions.

1. The experiments of Lavin and Stewart on the removal of free hydroxyl from a discharge through water vapour have been repeated, but their results and theories not confirmed.

2. The quenching of the afterglow of oxygen by means of water vapour has been studied, hydroxyl being found to be one of the products of the reaction.

3. Glowing oxygen has also been treated with atomic and molecular hydrogen, hydroxyl again being produced.

4. It has not been possible to separate the hydroxyl from atomic hydrogen and oxygen.

XXXVII. *Note on Methods of Computing Modulation Products.* By W. R. BENNETT and S. O. RICE *.

IN a recent paper † Mr. A. C. Bartlett has described an operational method of computing the response of a non-linear device when sinusoidal waves of different frequencies are simultaneously applied. The amplitude of the typical frequency in the output is expressed in terms of products of series resembling those defining Bessel functions, except that the argument is replaced by an operator which differentiates successively the instantaneous current versus voltage characteristic of the device. It appears that Bartlett's method is particularly suitable for cases in which the first few derivatives suffice to give the accuracy required. When a large number of derivatives must be evaluated, or when the characteristic is not differentiable throughout the entire operating range, a more easily interpreted form of the symbolic result is needed.

One method of approach to the problem of obtaining an alternative form of the solution is suggested by the relations demonstrated by Bromwich between operational formulas and certain contour integrals. Expressions for modulation products in terms of contour integrals have been obtained previously ‡ by the present authors. In this note it will be shown that Bartlett's result can be derived from a contour integral provided that the derivatives of the characteristic of the device are continuous, a restriction that need not be satisfied if the modulation products are computed from the contour integral directly. The contour integral thus appears to have a more general field of application than the operational formula.

For purposes of illustration, consider the modulating device in which the current I is related to the applied voltage E , as follows :

$$\left. \begin{aligned} I(E) &= A_1 E + A_2 E^2 + \dots + A_n E^n, & E > 0, \\ &= 0, & E < 0. \end{aligned} \right\} \quad (1)$$

* Communicated by the Authors.

† Bartlett, *Phil. Mag.*, Oct. 1933.

‡ Bennett, *Bell System Technical Journal*, April 1933.

Suppose the voltage E to consist of the sum of a constant term and two sinusoidal components with incommensurable frequencies

$$E = b + v_1 \cos \omega_1 t + v_2 \cos \omega_2 t, \quad b > 0. \quad . \quad . \quad (2)$$

We wish to calculate the amplitude of the component of I which has the frequency $(n_1 \omega_1 + n_2 \omega_2)/2\pi$. This may be done by expanding $I(E)$ in a double Fourier series in $\theta_1 = \omega_1 t$ and $\theta_2 = \omega_2 t$, thus :

$$I = \sum_{n_1=0}^{\infty} \sum_{n_2=0}^{\infty} \frac{\epsilon_{n_1} \epsilon_{n_2}}{4} a_{n_1 n_2} \cos n_1 \theta_1 \cos n_2 \theta_2, \quad . \quad . \quad (3)$$

where ϵ_k is Neumann's discontinuous factor, which is equal to unity when k is zero and is equal to two for other values of k , and

$$a_{n_1 n_2} = \frac{1}{\pi^2} \int_{-\pi}^{\pi} \int_{-\pi}^{\pi} I(b + v_1 \cos \theta_1 + v_2 \cos \theta_2) \times \cos n_1 \theta_1 \cos n_2 \theta_2 d\theta_1 d\theta_2. \quad (4)$$

Equation (1) may be written in the form

$$I(E) = \frac{1}{2\pi i} \int_C \frac{dz}{z} e^{iEz} \sum_{k=1}^n \frac{k! A_k}{(iz)^k}, \quad . \quad . \quad (5)$$

where C is a contour consisting of the real axis indented downward at the origin. Substituting (5) in (4), and interchanging the order of integration, we obtain

$$a_{n_1 n_2} = \frac{2i^{n_1+n_2}}{\pi i} \int_C \frac{dz}{z} e^{ibz} J_{n_1}(v_1 z) J_{n_2}(v_2 z) \sum_{k=1}^n \frac{k! A_k}{(iz)^k}. \quad (6)$$

The integral (6), which is closely related to the Weber-Schafheitlin integral*, is a very useful device in itself for the computation of modulation products. Its relation to Bartlett's result may be brought out by means of Bromwich's contour integral† for the interpretation of operational formulas :

$$\Phi(p)H(b) = \frac{1}{2\pi i} \int_L \frac{e^{b\lambda}}{\lambda} \Phi(\lambda) d\lambda. \quad . \quad . \quad (7)$$

* Watson, 'Theory of Bessel Functions,' chapter xiii.

† Jeffreys, 'Operational Calculus,' Cambridge Tract No. 23, 1927, p. 19.

In (7) L is an infinite contour from $c-i\infty$ to $c+i\infty$, $c>0$, passing to the right of all singularities of $\Phi(\lambda)$. The function $H(b)$ is defined by

$$H(b) = \left. \begin{aligned} &= 1, & b > 0, \\ &= 0, & b < 0. \end{aligned} \right\} \dots \dots \dots (8)$$

We may transform the integral (6) to the form (7) by substituting $\lambda = iz$. The result is

$$a_{n_1 n_2} = \frac{2}{\pi i} \int_L \frac{d\lambda}{\lambda} e^{b\lambda} I_{n_1}(v_1 \lambda) I_{n_2}(v_2 \lambda) \sum_{k=1}^n \frac{k!}{\lambda^k} A_k \dots \dots (9)$$

Therefore, by comparison with (7),

$$a_{n_1 n_2} = 4 I_{n_1}(v_1 p) I_{n_2}(v_2 p) \sum_{k=1}^n \frac{k!}{p^k} A_k H(b), \dots \dots (10)$$

where the operator p is to be interpreted in accordance with operational rules. If $b > |v_1| + |v_2|$, it may be shown that correct results may be obtained by replacing $1/p^k$ by $b^k/k!$ in the summation and p by d/db in the arguments of the Bessel functions. This gives Bartlett's result :

$$a_{n_1 n_2} = 4 I_{n_1} \left(v_1 \frac{d}{db} \right) I_{n_2} \left(v_2 \frac{d}{db} \right) I(b). \dots \dots (11)$$

(11) is obtained from (9) by closing the contour L by an infinite semicircle on the left, a procedure which is invalid if $b - |v_1| - |v_2| < 0$. The Bessel functions and the exponential are expanded in power series, and the residues are evaluated.

Referring to (2), we see that the restriction

$$b - |v_1| - |v_2| > 0 \dots \dots \dots (12)$$

is equivalent to stipulating that the voltage never becomes negative, and, therefore, by (1), the current is represented by a polynomial throughout the entire operating range. Thus the integral (9) may be applied to cut off characteristics such as (1), for which the operational method fails because it requires differentiation of the current-voltage relation.

XXXVIII. *The Influence of the Crystal Forces on the Vibration of a Complex Ion.* By M. BLACKMAN, M.Sc., Ph.D., Otto Beit Research Scholar, Imperial College of Science and Technology*.

RUBENS and Hertz †, in a fundamental investigation into the absorption of crystals, divided the molecular vibrations of a crystal into two types. The first type of vibration was such that the absorption in its neighbourhood was susceptible to the influence of temperature (falling off very rapidly with temperature), whereas in the case of the second type of vibration, which was found to lie at higher frequencies, the absorption was found to vary very little with temperature. As an example of the first type we can take the $60\ \mu$ absorption band of NaCl, as an example of the second type the $7\ \mu$ absorption band of calcium carbonate. The investigators rightly supposed that the first type was due to lattice vibrations ("outer vibrations"), whereas the latter were characteristic of a tightly bound collection of atoms, practically uninfluenced by the lattice and its structure.

Since then a large number of investigations ‡ have been carried out on the inner vibrations of crystals containing complex ions, such as the carbonates, sulphates, and the ammonium compounds. It has been found that though the inner vibration is characteristic of a group of atoms, there are slight differences from crystal to crystal.

No attempt seems to have been made to calculate even in the roughest way the influence of the lattice structure on the inner vibrations. It is clear that the variation in the frequency is due to the presence of the other molecules. There are, however, two possible ways in which the frequency can be affected. Firstly, it is possible that the binding forces between the atoms building up the complex molecule may be influenced by the surroundings; secondly, the inner vibration is coupled to the lattice vibrations, and this will produce a shift of the frequency.

* Communicated by the Author.

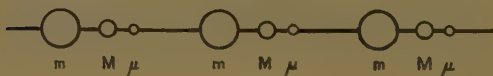
† Berl. Berichte, 1912, p. 256.

‡ See, for example, Schaefer and Matossi, 'Das ultrarote Spektrum'; Rawlins and Taylor, 'Infra-red Analysis of Molecular Structure.'

In this paper an attempt is made to show that this latter coupling gives the order of magnitude of the effects observed. It is, of course, to be remembered that the direct influence of the surroundings on the binding of the complex ions will also play a part; but it is found from X-ray work that the distance between the carbon and oxygen atoms* varies extremely little from compound to compound in the case of the uniaxial carbonates.

The only previous paper on this type of work appears to be that due to Lewis †, whom we follow in considering a linear chain of atoms. Lewis took different bindings between groups of atoms and obtained, in consequence, rather complicated results, which have not found application to the question dealt with here ‡. In particular the simplification introduced by the consideration of a periodic lattice could not be used in the problems there considered.

Fig. 1.



As a very rough approximation we consider the one dimensional case, *i. e.*, we replace the group of atoms by a hypothetical oscillator and couple this to the atoms in the lattice. This is justified in the case of a vibration which is parallel to the axis, and it is only such vibrations which we wish to consider. The problem is essentially one of the coupling of two vibrations, the frequency of one being small relative to the other. We obtain the right order of magnitude for the vibrations considered, and it is doubtful whether an extension to three dimensions would add anything to the physical side of the question unless the rigid treatment is given taking the actual form of the lattice structure and all the forces into account.

We consider a linear lattice consisting of $3N$ particles. There are three different types of particles having the masses m , M , μ respectively and arranged as shown above.

* See P. P. Ewald and G. Hermann, 'Strukturbericht,' 1913-28: Leipzig, 1931.

† A. B. Lewis, Phys. Rev. xxxvi. p. 568 (1930).

‡ K. Herzfeld, 'Handbuch der Physik,' xxiv. (2 Auflage), 1933.

We assume α to be the binding factor between the particles of mass m and M , β that between those of mass M and μ . The displacements of the particles m , M , μ are represented by u_{2n} , u_{2n+1} , ξ_{2n+1} respectively where n varies from 0 to N ; the charges on the particles are $+e$, $-e$, $+e$ respectively. The essential point is that the particle of mass μ is connected only to that of mass M ; we can now write down the equations of motions of the particles

$$\left. \begin{aligned} m\ddot{u}_{2n} &= \alpha(u_{2n+1} - u_{2n}) + \alpha(u_{2n-1} - u_{2n}), \\ M\ddot{u}_{2n+1} &= \alpha(u_{2n} - u_{2n+1}) + \alpha(u_{2n+2} - u_{2n+1}) + \beta(\xi_{2n+1} - u_{2n+1}), \\ \mu\ddot{\xi}_{2n+1} &= \beta(u_{2n+1} - \xi_{2n+1}). \end{aligned} \right\} \quad \dots \quad (1)$$

To solve these equations we use the usual periodic solutions

$$\left. \begin{aligned} u_{2n} &= u' e^{i(\nu t + 2n\phi)}, \\ u_{2n+1} &= u'' e^{i(\nu t + (2n+1)\phi)}, \\ \xi_{2n+1} &= \xi' e^{i(\nu t + (2n+1)\phi)}, \end{aligned} \right\}$$

where $\phi = \frac{\pi\kappa}{N}$ and $\begin{matrix} 1 < \kappa \leq N \\ 0 < \phi \leq \pi \end{matrix}$.

This gives the secular equation for the frequencies

$$\begin{vmatrix} -m\nu^2 + 2\alpha & -2\alpha \cos \phi & 0 \\ -2\alpha \cos \phi & -M\nu^2 + 2\alpha + \beta & -\beta \\ 0 & -\beta & -\mu\nu^2 + \beta \end{vmatrix} = 0,$$

which leads to the equation

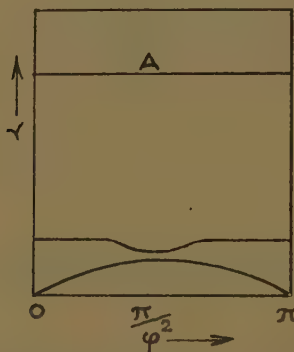
$$\begin{aligned} \nu^6 - \nu^4 \left[2\alpha \left(\frac{1}{m} + \frac{1}{M} \right) + \beta \left(\frac{1}{\mu} + \frac{1}{M} \right) \right] \\ + \nu^2 \left[2\alpha\beta \left(\frac{1}{\mu m} + \frac{1}{mM} + \frac{1}{\mu M} \right) + \frac{4\alpha^2}{mM} \sin^2 \phi \right] \\ - \frac{4\alpha^2\beta}{\mu m M} \sin^2 \phi = 0. \quad \dots \quad (2) \end{aligned}$$

There are, of course, three frequency branches. A consideration of (2) shows that the curves are symmetrical about $\phi = \frac{\pi}{2}$. This is also a point where the curves have

extreme values. The general shape can be seen from the curve given. The highest branch corresponds to the inner vibration and is practically monochromatic. The second branch corresponds to the optical branch of the crystals of the NaCl type, and is in this case responsible for the "outer" vibrations.

The vibrations which interest us are those which possess an electric moment. These are the vibrations for

Fig. 2.



Frequency curve for a linear chain with three types of particles.

which $\phi=0$, i. e., the vibrations which will appear in the infra-red spectrum are given by the roots of the equation

$$\nu^4 - \nu^2 \left[2\alpha \left(\frac{1}{m} + \frac{1}{M} \right) + \beta \left(\frac{1}{\mu} + \frac{1}{M} \right) \right] + 2\alpha\beta \left[\frac{1}{mM} + \frac{1}{\mu m} + \frac{1}{\mu M} \right] = 0,$$

i. e.,

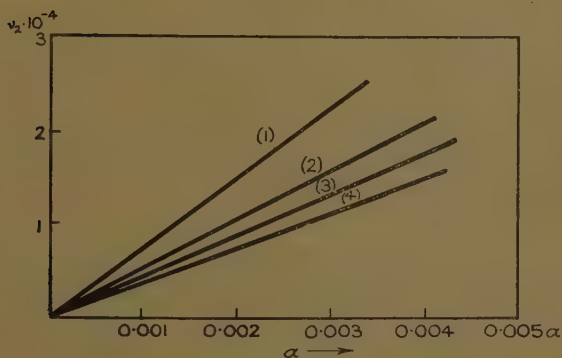
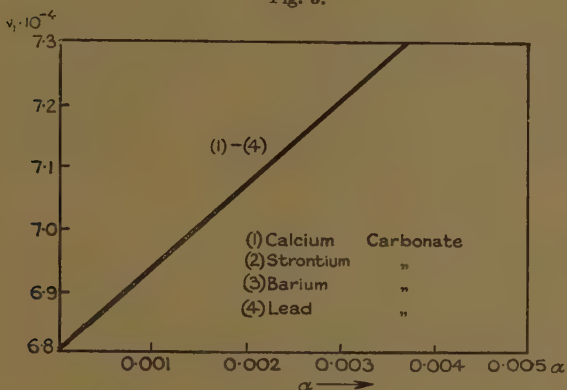
$$2\nu^2 = 2\alpha \left(\frac{1}{m} + \frac{1}{M} \right) + \beta \left(\frac{1}{\mu} + \frac{1}{M} \right) \pm \sqrt{\left[2\alpha \left(\frac{1}{m} + \frac{1}{M} \right) + \beta \left(\frac{1}{\mu} + \frac{1}{M} \right) \right]^2 - 8\alpha\beta \left(\frac{1}{mM} + \frac{1}{\mu m} + \frac{1}{\mu M} \right)}.$$

We can now calculate the effect of the lattice coupling. In general we see (fig. 3) that for a given binding constant α , the heavier the mass M the greater is the shift towards

longer wave-lengths; this is especially true for the smaller vibration (ν_2); the effect of the mass is extremely small in the case of the higher frequency. An increase in α means an increase in both frequencies.

If we consider a series such as the carbonates CaCO_3 , BaCO_3 , SrCO_3 , etc., both parameters α and M vary.

Fig. 3.



The frequency as a function of the bending factor.

In order to show that the shift found can be accounted for by taking both variations into account, we proceed in the following way.

We take a fixed value of β , and α as variable; we then obtain two series of curves for the frequency with different

values of the parameter M ; then, given the value of ν_1 (the observed value of the inner vibration of a particular compound) and the parameter M , we can read off immediately the value of α and ν_2 . We can do this for the whole carbonate series for example. ν_2 is, of course, the "outer" vibration associated with ν_1 as "inner" vibration.

The curves and the tables given below show the results of such a calculation. (The units chosen are such that $1/\nu$ gives the wave-length in μ .) The frequency used in this case was the 11.5μ vibration of the biaxial carbonates. No attempt was made to obtain a close relationship between the calculated and experimental work.

For the purpose of comparison the optical vibrations of the carbonates are given below*.

TABLE I.

	λ (observed).	λ_2 (calcul.).	α (calcul.).
CaCO_3	11.55 μ	51.0 μ	0.0010
BaCO_3	11.61	64.7	0.0045
SrCO_4	11.62	70.0	0.0045
PbCO_3	12.00	120	0.0051

The vibrations here used are in the fourth column of the biaxial carbonates. The outer vibrations are seen in the fifth, sixth, and seventh columns. It is seen that the shifts are roughly of the same order except in the case of lead carbonate.

3. The effect of temperature on the inner and outer vibrations can also be estimated, using the relations given, it being assumed that the expansion carried with it a change in α . It is clear that the change in the inner vibration is extremely small, this being a second order effect as the change in α is only a first order effect. The effect on the "outer" vibration will be much larger in comparison.

In the case of CaCO_3 the calculation gives a shift for the 10μ vibration of about 1/100 per cent. per $100^\circ \text{C}.$ and for the 40μ outer vibration about 1/4 per cent.

* Schaefer and Matossi, 'Das ultraiore Spektrum.'

TABLE II.

	Inner vibrations.				Outer vibrations.			
	$o.$		$o.$	$a.o.*$	$o.$		$a.o.$	
Uniaxial	{ $MgCO_3$							
	$CaCO_3$...				13.78	11.25		28.0
	{ $(Mg)CO_3$				6.7-7.0	11.38	30.3 (55)	94
	$FeCO_3$				6.9	11.45	29	27
					6.77	11.53	30 (51)	46
Biaxial	{ $CaCO_3$				$b.$	$c.$	$b.$	$a.$
	$BaCO_3$				6.7	6.65	14.06	14.17
	{ $SrCO_3$				6.78	—	14.28	—
	$PbCO_3$				6.85	—	14.48	—
					7.64	7.28	15.04	64
						11.55	36.5 (56) (100)	34 (56) (100)
						11.62	42	47
						11.61	46.5	56
						12.09	64	64
								94

* $a.o.$ = extraordinary ray; $o.$ = ordinary ray.

The experimental work on the temperature shift of the inner vibrations by Rubens and Hertz * and Rusch † has shown that this is indeed very small. The former found no shift; the latter, using very sensitive methods, found only a very slight one; a rough estimate shows that it is of the order given above, but probably somewhat greater. There are no measurements on the temperature shift of the "outer" vibrations. We must, however, expect the above values to be only lower limits, as there are other effects which will also play a part; the damping constant will change with temperature (as is shown by the work of Rubens and Hertz), and this will also cause a shift in the same direction as that given by the expansion.

4. An application of the above idea can be made to correlate some of the observations on the properties of the Ammonium Compounds. It has been found that the ammonium-salts show a change of their properties at about -50°C . This is particularly evident in the specific heats ‡, in the expansion † and in the behaviour of the vibrational frequency ‡. It is with the two latter phenomena that we will deal.

It was shown by Pohlman §, following earlier work by Hettner and Simon ||, that the 7μ absorption band of NH_4Cl showed a shift towards longer wave-lengths while in the case of NH_4Br the shift is towards shorter wave-lengths as the critical point was passed.

An investigation of the expansion of the lattice by Simon and Bergmann ¶ showed that the NH_4Cl lattice expanded, while the NH_4Br lattice contracted on passing this point.

An expansion of the lattice means that the binding becomes smaller. This means that the inner vibration ν_1 will become smaller, *i. e.*, there will be a shift towards longer wave-lengths. A contraction of the lattice has the opposite effect.

* Berl. Berichte, 1912, p. 256.

† *Ann. d. Phys.* lxx. p. 373 (1929).

‡ P. P. Ewald, *Naturw.* xlv. p. 1213 (1914); F. Simon, *Naturw.* lxviii. p. 263 (1922); F. Simon, Cl v. Simson, u. M. Ruhemann, *Zeit. f. Phys. Chemie*, cxxix. p. 339 (1927).

§ R. Pohlman, *Zeit. f. Phys.* lxxix. p. 394 (1932).

|| G. Hettner and F. Simon, *Zeit. f. Phys. Chemie* (B), i. p. 293 (1928).

¶ F. Simon and R. Bergmann, *Zeit. f. Phys. Chemie* (B), viii. p. 225 (1930).

We can estimate roughly the effect of the change in length on the inner vibration, assuming that the change in α is roughly proportional to twice the change in the length (as is usual in the case of expansion of a lattice). Then the change in α is about 6 per cent., and the effect on ν_1 is about 1/4 per cent., while the observed change is about 1/3 per cent.

XXXIX. *Skin Effect in Rectangular Conductors at High Frequencies.* By W. JACKSON, M.Sc., Magdalen College, Oxford *.

Introduction.

WHEN an alternating current is caused to flow through a conductor eddy currents are generated in a manner tending to prevent the setting up of a magnetic field within the conductor. The current distribution over the cross-section and the effective resistance of an isolated conductor are therefore functions of the frequency of the current flowing. As the frequency increases the current tends to be concentrated more and more on the surface, until at very high frequency the distribution is such as to make the contour of the cross-section coincident with a stream-line of the magnetic field. The magnetic-field distribution is then equivalent to that of the electric field of a charged cylinder of the same shape, the current density in the former case corresponding to the electrostatic surface density in the latter. If, therefore, the cylinder has a shape for which the electrostatic field and charge distribution can be determined, the limiting distribution of current density is also determinate and the effective resistance per unit length can be evaluated.

This analogy has been applied by Cockcroft † to calculate the high-frequency resistance of isolated cylindrical conductors of rectangular section, the dimensions of which are assumed to be large compared with the effective depth of penetration, $\frac{1}{m} = \frac{1}{(2\pi\omega/\rho)}$, for the case of both sharp

* Communicated by Prof. R. V. Southwell, M.A., F.R.S.

† J. D. Cockcroft, Proc. Roy. Soc. A, cxxii. p. 533 (1929).

and rounded corners (fig. 1). In both cases the ratio of the high-frequency resistance per unit length R_n to the D.C. resistance R_0 is obtained in the form

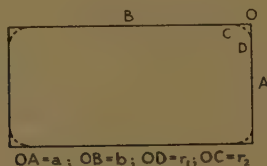
$$\frac{R_n}{R_0} = f\left(\frac{b}{a}\right) \cdot \frac{1}{\pi} \sqrt{2\omega/R_0} \dots \dots \dots (1)$$

For sharp corners

$$f\left(\frac{b}{a}\right) = \frac{2}{\sqrt{\pi}} (E - \kappa_1^2 F)^{\frac{1}{2}} (E' - \kappa^2 F')^{\frac{1}{2}} (F + F'),$$

where F and F' are the complete elliptic integrals of the first kind and E and E' those of the second kind, to

Fig. 1.



OA = a; OB = b; OD = r₁; OC = r₂

moduli κ and $\kappa_1 = \sqrt{1 - \kappa^2}$, and where κ is given in terms of the conductor shape by

$$a = (E - \kappa_1^2 F) / \kappa,$$

$$b = (E' - \kappa^2 F') / \kappa.$$

For rounded corners $f\left(\frac{b}{a}\right)$ is a much more complex function taking account of r_1 and r_2 . Due to the diminution of the current density at the corners caused by slight rounding the ratio R_n/R_0 is somewhat lower in the latter case, although, according to Cockcroft, only to the extent of about 5 per cent. for a series of conductors for which $2a/(r_1 + r_2)$ was approximately 10 and b/a varied from 9.7 to 43 as compared with the corresponding values for sharp corners.

The experimental verification of this theoretical work has been delayed, mainly because of the difficulty experienced in building a measuring circuit in which proximity effects are avoided and where the conductor resistance required forms a sufficiently large proportion of the total circuit resistance to permit of its accurate

determination. This has now been made possible, however, by use of a special low-loss air condenser. A description of this condenser and an experimental analysis of its equivalent series resistance at high radio frequencies has been given elsewhere *.

Description of the Measurements.

The measurements to be described consisted in determining the effective resistance per unit length of a series of copper conductors of rectangular cross-section, each of thickness $\frac{1}{8}$ inch, but of $\frac{b}{a}$ ratio from 1 to 8, at the same high frequency 6.67×10^6 cycles per second (45 metres). For this purpose each of the several conductors was bent along its width b into the form of a large single-turn rectangle, and employed as the inductive part of a resonant circuit tuned by means of the low-loss air condenser mentioned previously. This condenser was locked at a constant capacitance value of 725 micro-microfarads, so that for resonance to occur at the same frequency in each case the several coils were required to be of the same inductance value. The breadth of each coil was made 5 inches, but change in the conductor internal inductance with the sectional dimensions caused them to be of different length. Thus for the conductor of $1 \times 1/8$ inch section the coil was 22.4 inches long, as compared with 14.2 inches for the $1/8 \times 1/8$ inch conductor. Since the ratio of the spacing between the coil sides and the conductor thickness $2a$ was 40 throughout, no question of proximity effect arose, and the conductors could be regarded as isolated.

The circuit so formed was loosely coupled to an oscillation generator, and, with each coil connected in turn, the power factor of the whole circuit was deduced from the fractional width of the resonance curve delineated by varying the frequency of the injected E.M.F. over the requisite range about the resonant value by means of a fine adjustment condenser on the generator †. The differences in setting of this condenser were convertible to frequency changes from a calibration performed by a double-beat process.

* W. Jackson, J. Inst. Rad. Eng. vol. xxii. (Aug. 1934).

† E. B. Moullin, 'Radio Frequency Measurements,' p. 273.

The circuit power factor thus derived represents the sum of the coil and condenser power factors and that added by the connexion across the condenser of the indicating thermionic voltmeter. In arranging for the several coils to be of equal inductance, and thus for the measurements to be carried out with fixed capacitance as well as at constant frequency, the contributions of the condenser and voltmeter to the total power factor are constant and can be evaluated and separated from the desired coil power factor by making use of a further coil of the same inductance value and of accurately calculable resistance. This coil was formed from a copper conductor of circular section of diameter $d=0.64$ cm., bent into a rectangle of breadth $D=20d$, for which, as has been verified by Moullin*, the resistance per unit length can be calculated from the well-known formula for an isolated conductor of this form,

$$\frac{R_n}{R_0} = \frac{\sqrt{2Z+1}}{4}, \quad (2)$$

where

$$Z^2 = \frac{\pi \omega d^2}{\rho}, \quad \omega = 2\pi n.$$

The resulting resistance values for the coils of rectangular section conductor are therefore direct comparisons with this expression, and are given to an accuracy determined by that of the above acceptance.

It remains to be mentioned that two sources of error attach to the use of equation (2), due respectively to inherent coil self-capacitance and radiation resistance. The self-capacitance of coils of this rectangular form cannot be calculated with accuracy, but it is possible to assign an upper limit †, which is such that it could not increase the coil resistance by more than 2 per cent. at a wave-length of 45 metres. Since, however, this error arises in the same order of magnitude for each of the test coils, it will be eliminated, along with the condenser losses, in the above process. This applies equally to the coil radiation resistance, which, however, is less than 0.001 ohm at 45 metres, and as such is negligibly small.

* E. B. Moullin, Proc. Roy. Soc. A, cxxxvii. p. 116 (1932).

† E. B. Moullin, *loc. cit.*

The following table gives a statement of the experimental results :—

Frequency = 6.67×10^6 cps. ($\lambda = 45$ metres) ; $C = 725 \mu\text{F}$.						
$\frac{b}{a}$	Con- ductor length (cm.).	Circuit power factor (10^{-3}).	Resultant condenser power factor (10^{-3}).	Coil power factor (10^{-3}).	Coil resist- ance (ohms).	Conductor resistance per cm. : R_n (abs. units).
Round conductor 0.64 cm. diam. }	105.7	1.620	0.525	1.095	.0355	—
8	130.0	1.290	„	0.765	.0245	1.90×10^5
6	120.0	1.400	„	0.875	.0280	2.33×10^5
4	109.2	1.505	„	0.980	.0320	2.82×10^5
3	99.7	1.600	„	1.075	.0345	3.46×10^5
2	93.0	1.770	„	1.245	.0400	4.30×10^5
1.5	91.0	1.935	„	1.410	.0460	5.10×10^5
1	88.0	2.250	„	1.725	.0565	6.43×10^5

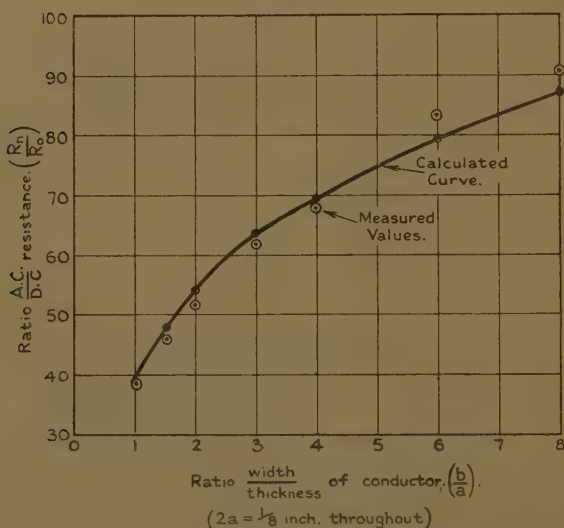
Discussion of the Results.

The curve of fig. 2, connecting the ratio R_n/R_0 of the high-frequency to the D.C. resistance with the width to thickness ratio b/a of the conductor, has been calculated from Cockcroft's formula (1) for the case of sharp corners. It is seen that the experimentally obtained values follow the curve closely. The corners of the actual conductors were not ideally sharp, so that it is to be expected, as previously mentioned, that the experimental points should lie slightly below this theoretical curve. With the exception of the points corresponding to $b/a=6$ and $b/a=8$ this indeed occurs, so that the agreement can be regarded as very satisfactory.

In noting this good agreement it is important to see whether the conditions of test constitute an approach to those on which Cockcroft's equation (1) is based. That this is the case is shown by the fact that the effective depth of current penetration $1/m$ at the testing frequency is only 0.0025 cm., or 8 thousandths of the conductor thickness.

The physical significance of the results is readily understandable from the curves of fig. 3. Here curve (A) shows the calculated resistance per unit length R_n , at a frequency of 6.67×10^6 cycles per second, plotted against the inverse of the perimeter for rectangular section conductors of constant thickness $2a=1/8$ inch and of b/a ratios extending from unity to large values. Curve (B) gives the calculated resistance per unit length at the same frequency of a strip forming part of the surface of

Fig. 2.

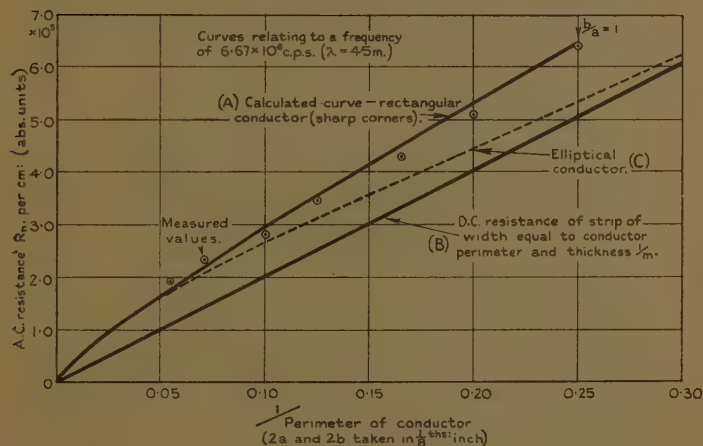


an infinitely wide and infinitely thick copper plate. The surface width of this strip is taken as $2(a+b)$, that is a width equal to the perimeter of the rectangular conductor. The current distribution over the surface of such a plate is uniform and the depth of current penetration is $\frac{1}{m} = \left(\frac{\rho}{2\pi\omega} \right)^{\frac{1}{2}}$. This high-frequency resistance is the same as the resistance to steady currents of a strip of the same width and of thickness $1/m$, i. e., $R_n = \frac{\rho m}{2(a+b)}$.

Due to the non-uniform current distribution the resistance of the rectangular conductor is throughout higher than that of a strip of flat plate of the same surface area, but the ratio of the two resistances becomes continuously less as the b/a ratio of the section decreases to unity, indicating a tendency towards greater uniformity of current distribution as the rectangle approaches a square.

This does not mean that the square section is the most efficient for practical use, since the equivalent perimeter

Fig. 3.

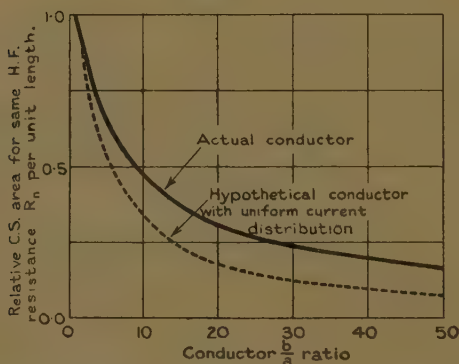


for a given sectional area is the significant factor, and this increases as the section is elongated. Fig. 4 shows how the area of cross-section required for the same resistance per unit length, taken relative to the square, varies over the range of b/a of the section from 1 to 50. For comparison the curve which would apply if the current distribution over the surface were uniform is also shown. It is seen that the amount of copper required decreases continuously with increase in b/a , although the effect of the corners becomes more and more marked with departure from the square section.

It is of interest to compare curve (A) of fig. 3 with the corresponding curve for elliptical section conductors,

since for large values of b/a this section forms a good approximation to the rectangular conductor, and for $b/a=1$ (circular section) approximates closely for the purposes of current flow to a flat plate, provided that the radius of the circular section is very large compared with $1/m$. Thus curve (C) shows the resistance per unit length at 6.67×10^6 cycles per second plotted against the inverse of the perimeter for elliptical conductors of major and minor axes $2b$ and $2a$ respectively, for constant $2a=1/8$ inch and variable b/a ratio. The formula for the high-

Fig. 4.



frequency resistance of conductors of elliptical section has been given by Strutt * as

$$R_n = F \left(1 - \frac{a^2}{b^2} \right)^{\frac{1}{2}} \left(\frac{a}{b} \right)^{\frac{1}{2}} \frac{1}{\pi} \sqrt{2\omega} R_0,$$

where F denotes the complete elliptic integral of the first kind. For large values of b/a curve (C) follows closely that for the rectangular section, but approaches curve (B) as b/a tends to unity. The abscissa for $b/a=1$ is .319, and here curve (C) lies above curve (B) to the extent of only 4 per cent. This close approach is due to the fact that for a circular conductor of $1/8$ inch diameter at a frequency of 6.67×10^6 cycles per second the conductor radius is 63 times the effective depth of current penetration.

* Strutt, *Ann. d. Phys.* lxxxv. p. 781 (1928).

Finally, it might be mentioned that equation (1) for the rectangular section is given to within 3 per cent. for copper by the simple relation

$$R_n = 72(1 - 0.18b/a) \sqrt{\frac{n}{A}} \times 10^{-8} \text{ ohms per. cm. length,}$$

where n = frequency in cps. and A = C.S. area in sq. cm. over the range of b/a which is of most practical interest ; $b/a > 5 < 20$.

Acknowledgment is due to the Advisory Council of the Department of Scientific and Industrial Research for a grant which made this investigation possible. It was carried out in the Engineering Laboratory, Oxford.

XL. On the Intensity Distribution of Sound from a Tuning-Fork. By GENTARO ARAKI, Research Fellow in the Tokyo University of Science and Literature *.

Introduction.

IN text-books of physics and acoustics it is customary, almost without exception, to represent the direction of the minimum sound intensity due to a tuning-fork by two branches of a hyperbola, in a plane perpendicular to the prongs of the tuning-fork †. The reason for it seems to be that the directional variation of the sound intensity in this case has been regarded by most authors as if it were due to interference of sound-waves coming from the two prongs ; thus an example of phenomenon that is familiar to us in dealing with a pair of synchronous sources of waves, so that it seems to be tacitly agreed that our hyperbola branches represent the loci of a point for which the distances from the two prongs differ by an odd multiple of half a wave-length.

By an ordinary tuning-fork, however, the wave-length is so large in comparison with the distance between the

* Communicated by Prof. U. Doi.

† Grimsehl, 'Lehrbuch der Physik,' i. pp. 603, 668 (1929); W. Watson, 'A Text-book of Physics,' 1927, p. 388; Müller-Pouillels, 'Lehrbuch der Physik,' i. part 3, p. 185 (1929); A. Winkelmann, 'Handbuch der Physik,' Bd. ii. p. 602 (1909); Lommel, Wied. Ann. der Phys. xxvi. p. 156 (1885).

two prongs that the above condition for the interference evidently cannot be satisfied. This point has been noticed by Chwolson* and Togino†, among others. Accordingly the problem should be attacked from another side. Only what we can rely on presumably is that the loci of a point of the minimum sound intensity in question do not deviate far from the straight lines inclined 45° against the line connecting the two prongs of the tuning-fork, the fact‡ which is unfailingly experienced by everyone who has ever experimented in this direction.

§ 1. *The Wave from a Line Source with an Axiality.*

Suppose an infinitely long, circular cylinder of radius r_0 , moving with a constant velocity U perpendicular to its length in an infinite mass of fluid, which is at rest at infinity. The motion of the fluid belongs to a two-dimensional problem, and its velocity potential§ is given by

$$\phi(r, \theta) = U \frac{r_0^2}{r} \cos \theta, \quad . \quad . \quad . \quad (1)$$

where r and θ are polar coordinates with their origin on the axis of the cylinder, and $\theta=0$ is defined by the direction of the velocity U . Thus, for the normal component of the velocity of fluid on the surface of the cylinder we have

$$\left[-\frac{\partial}{\partial r} \phi(r, \theta) \right]_{r=r_0} = U \cos \theta. \quad . \quad . \quad . \quad (2)$$

In case of oscillating U , such as $U = a_0 \cos 2\pi vt$, too, we may take (1) for our velocity potential, and consequently (2) for the normal component of the velocity of fluid on the surface of the cylinder, only if we confine our attention to a sufficiently narrow neighbourhood of the surface of the cylinder. Accordingly the displacement of fluid on the surface is given by

$$a_0 \cos \theta \sin 2\pi vt.$$

The last amount remains unaltered in the limit $r_0=0$, where we have a case of line source, coinciding with the

* O. D. Chwolson, 'Lehrbuch der Physik.' ii. p. 49 (1904).

† S. Togino, Bulletin of the Tokyo Butsuri Gakko, xxxvi. p. 364 (1927). (Edited in the Japanese Language.)

‡ O. D. Chwolson, *loc. cit.*

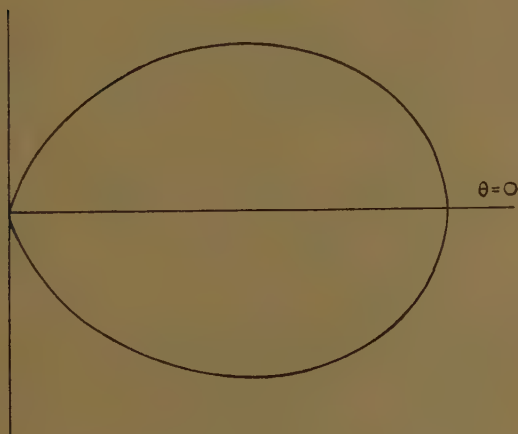
§ H. Lamb, 'Hydrodynamics,' p. 72 (1924).

axis of the so far considered cylinder, with an axiality in the direction of $\theta=0$. The cylindrical waves propagating from such a line source will be of the type

$$\frac{a_0}{r} \cos \theta \sin 2\pi \left(\nu t - \frac{r}{\lambda} \right), \quad . \quad . \quad . \quad (3)$$

where λ stands for the wave-length. The angular distribution of the intensity of our waves, in a plane perpendicular to the line of source, is represented in fig. 1.

Fig. 1.



§ 2. *The Wave from a Plane Source.*

Consider a plane source of breadth $2c_0$ and infinite length, vibrating perpendicular to its plane; AB in fig. 2 represents a cross-section of the source perpendicular to it. Take, now, a sufficiently small interval dx on AB at a point D, distant x from its middle point C. Take, further, an arbitrary point P in the plane of figure, and let $PC=r$, $PD=r'$, $\angle PCN=\theta$, $\angle PDN'=\theta'$, and $\angle CPD=\phi$, in which CN and DN' are the perpendiculars to AB at C and D respectively. The r -component of the wave at P due to the source dx is, by (3),

$$\frac{A dx}{2c_0 r'} \cos \theta' \sin 2\pi \left(\nu t - \frac{r'}{\lambda} \right) \cos \phi. \quad . \quad . \quad . \quad (4)$$

Taking into account the first order of $\frac{2c_0}{r}$ only, we have

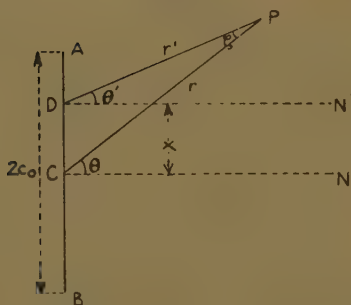
$$r' = r \left(1 - \frac{x}{r} \sin \theta \right),$$

$$\frac{1}{r'} = \frac{1}{r} \left(1 + \frac{x}{r} \sin \theta \right),$$

$$\cos \theta' = \cos \theta \left(1 + \frac{x}{r} \sin \theta \right),$$

$$\cos \phi = 1.$$

Fig. 2.



Substitution of these values in (4) gives

$$\frac{A \cos \theta}{2c_0 r} \left(1 + 2 \frac{x}{r} \sin \theta \right) \sin 2\pi \left(vt - \frac{r}{\lambda} + \frac{x}{\lambda} \sin \theta \right),$$

which simplifies, in consideration of $\frac{2c_0}{\lambda} < 1$, to

$$\begin{aligned} & \frac{A \cos \theta}{2c_0 r} \sin 2\pi \left(vt - \frac{r}{\lambda} + \frac{x}{\lambda} \sin \theta \right) dx \\ & + \frac{A \sin 2\theta}{2c_0 r} \sin 2\pi \left(vt - \frac{r}{\lambda} \right) \cdot \frac{x}{r} \cdot dx. \end{aligned}$$

Now, the total effect at P due to the whole plane source AB will be given by

$$\begin{aligned} w &= \frac{A \cos \theta}{r} \frac{1}{2c_0} \int_{-c_0}^{+c_0} \sin 2\pi \left(vt - \frac{r}{\lambda} + \frac{\sin \theta}{\lambda} x \right) dx \\ &= \frac{A \cos \theta}{r} \frac{\sin \left(2\pi \frac{c_0}{\lambda} \sin \theta \right)}{2\pi \frac{c_0}{\lambda} \sin \theta} \sin 2\pi \left(vt - \frac{r}{\lambda} \right), \quad . \quad . \quad (5) \end{aligned}$$

where the integral of the second term vanishes. In fig. 3 the angular distribution of the intensity of such a wave is plotted.

Fig. 3.

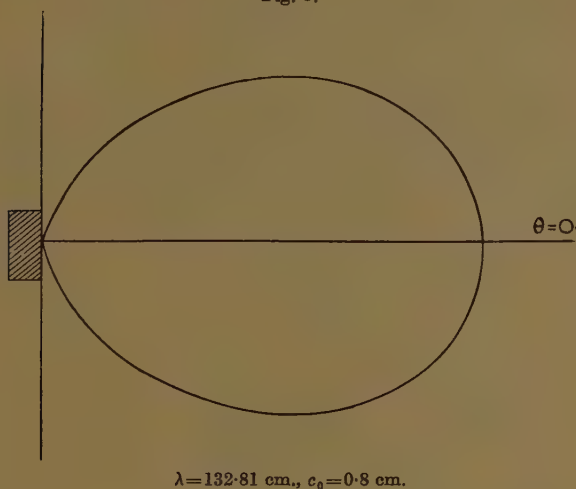
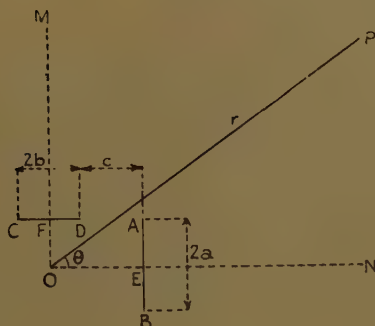


Fig. 4.



§ 3. *Two Plane Sources Perpendicular to each other with a Phase Difference of π .*

Let AB and CD in fig. 4 represent the section of two plane sources, which are supposed to be perpendicular

to each other and to the plane of figure, and the phase difference of their vibrations be π . As is shown in the figure, we shall take $AB=2a$, $CD=2b$, $DA=c$. At E and F, the middle points of AB and CD respectively, draw the perpendiculars EN and FM intersecting each other at O. Take, now, a point P in the quadrant MON, and let $OP=r$ and $\angle PON=\theta$. If we assume that $\frac{2a}{r}$, $\frac{2b}{r}$ and $\frac{b+c}{r}$ are all sufficiently small in comparison with unity, the superposed effect at P due to our two plane sources AB and CD will be expressed, to a first approximation, by

where
$$W=A_1 \sin \psi_1 + A_2 \sin \psi_2, \quad . . . (6)$$

$$A_1 = \frac{A\lambda}{2\pi ar} \cot \theta \left(1 - \frac{b+c}{r} \tan \theta \sin \theta \right) \sin \left\{ \frac{2\pi a}{\lambda} \sin \theta \left(1 + \frac{b+c}{r} \cos \theta \right) \right\},$$

$$A_2 = \frac{A\lambda}{2\pi br} \tan \theta \left(1 - \frac{a}{r} \cot \theta \cos \theta \right) \sin \left\{ \frac{2\pi b}{\lambda} \cos \theta \left(1 + \frac{a}{r} \sin \theta \right) \right\}, \quad . (7)$$

$$\psi_1 = 2\pi \left(vt - \frac{r}{\lambda} + \frac{b+c}{\lambda} \cos \theta \right),$$

$$\psi_2 = 2\pi \left(vt - \frac{r}{\lambda} + \frac{a}{\lambda} \sin \theta \right) + \pi.$$

The intensity of the superposed wave (6) will be given by

$$I = A_1^2 + A_2^2 + 2A_1 A_2 \cos (\psi_2 - \psi_1). \quad . . . (8)$$

Now let us proceed to look for a nodal surface for the vanishing intensity $I=0$. In case $c=0$ and $a=b$, $I=0$ for $\theta=\frac{\pi}{4}$, so that we shall be able to go further in search of the nodal surface by putting $\theta=\frac{\pi}{4}+\delta$ in (6) combined with (7), where δ is supposed to be small. (8) can be reduced, thus, in terms of δ in our approximation, to

$$I = \frac{A^2}{r^2} \left\{ \left(\sqrt{2} + 2 \frac{a+b+c}{r} \right) \delta - \left(\frac{1}{3\sqrt{2}} + \frac{4}{3} \frac{a+b+c}{r} + \frac{\pi}{2\sqrt{2}} \cdot \frac{a+b}{\lambda} \right) \delta^3 + \dots \right\}^2, \quad . (9)$$

whose minimum is given by $\delta=0$.

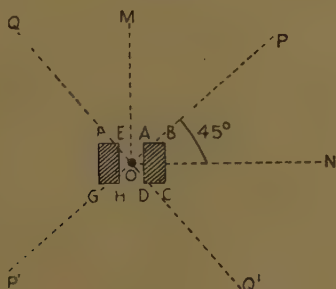
Hence, the nodal curve in the plane of figure is, up to our approximation, the straight line

$$\theta = \frac{\pi}{4}.$$

§ 4. *Vibration of a Tuning-Fork.*

Suppose fig. 5 represents a cross-section of the two prongs of a tuning-fork cut by a plane perpendicular to them, near their extremities. The vibration of a tuning-fork takes place in such a way that the air in front of BC and FG is condensed, while the air between AD and EH is rarefied, and *vice versa*. Accordingly it

Fig. 5.



may be agreed that, since AD is very small as compared with the wave-length in our ordinary case, the phase difference between the waves propagating from BC and those from AE amounts just to π ; moreover, it follows from what has been studied in § 2 that the effect in the quadrant NOM in fig. 5 is the superposition of the contributions only from the sources AE and BC. So that the results obtained in the preceding articles can be applied at once to our present case; thus we have, for example, as the loci of a point of the minimum intensity of sound from the tuning-fork, not hyperbolas, but the straight lines PP' and QQ', inclined 45° to the faces of the prongs. In fig. 6 is plotted the angular distribution of the intensity of sound, computed according to equations (7) and (8), for a tuning-fork of a frequency 256 per

448 *Intensity Distribution of Sound from a Tuning-Fork.*

sec. (i. e., the note c' on the musical scale). In the computation the following data have been adopted :—
 $a=0.8$ cm., $b=0.45$ cm., $c=0.8$ cm., the actual dimensions of the above-mentioned tuning-fork, and sound velocity $=3.4 \times 10^4$ cm./sec., $r=100$ cm.

Fig. 6.



The author wishes to express his hearty thanks to Prof. U. Doi for the kind interest he has taken in the present treatment.

Note added in proof.—Recently a paper entitled “Oscillations de solides dans l’air ou dans l’eau” was published by Marty*, in which is reported an experimental study on the surface of silence in the neighbouring

* L. Marty, *J. de Phys. Rad.* iv. p. 537 (1933).

vicinity of two large disks oscillating with audible frequencies with opposite phase to each other. No need, however, of modification seems to be called on our present argument.

XLI. The Atomic Diamagnetic Susceptibility of Hydrogen.

*By Prof. S. S. BHATNAGAR, D.Sc., F.Inst.Phys., Director,
University Chemical Laboratories, Lahore, N. G. MITRA,
M.Sc., and GOPAL DAS TULI, B.Sc.(Hons.) *.*

ALTHOUGH different workers in the field of magnetism have not seldom found deviations from the old-time values of Pascal ⁽¹⁾ for the magnetic susceptibilities of organic compounds, no systematic attempt has so far been made to put the whole matter on a surer footing. Considering the gravity of Pascal's work, and the fact that many important conclusions have been derived from it, it was felt desirable to investigate this whole subject with the help of the more sensitive and accurate instruments and the purest materials now available.

The atomic diamagnetic susceptibility of hydrogen can be determined only by the methods employed by Pascal. The procedure adopted here has been to determine the value of χ for the CH_2 group from the magnetic susceptibilities of a large number of homologous series of compounds, both aliphatic and aromatic. By subtracting from this constant the value for carbon the value for molecular hydrogen can be easily obtained, from which the atomic diamagnetic susceptibility of hydrogen can be calculated by dividing this result by the number of atoms in a molecule of hydrogen.

Pascal's value for carbon (corrected for the latest value for water) has been retained, for the simple reason that Pascal determined this with great precision and it coincided exactly with the value obtained indirectly by magnetic analysis. His measurements were made upon the carbon obtained from recrystallized white sugar containing no trace of any metal whatsoever. The crystals were decomposed at red heat, and the carbon of sugar obtained after porphyrization was heated for

* Communicated by the Authors.

several hours at red heat in a current of chlorine, washed, and then dried at red heat. These operations were repeated until a constant value of magnetic susceptibility was obtained. The same sample was heated at white heat for six hours in a quartz tube full of argon, and the value was found not to change.

The apparatus employed for the determination of magnetic susceptibility was the magnetic interference balance devised by Bhatnagar and Mathur ⁽²⁾ and manufactured by Messrs. Adam Hilger, Ltd., London. The sensitivity of this apparatus can be judged from the fact that a deflexion of the tube of the order of 1/500 cm. corresponds to 600 divisions on the drum of the interferometer, and the accuracy of observation can easily be said to be one in one thousand. As such, a change in the diamagnetic susceptibility of the order of 0.2 per cent. or even less can be easily detected.

For the susceptibility value of each substance a large number of observations, never less than three, were taken, and the mean of all the concordant readings was taken as the value for that substance.

The substances employed were of a very high standard of purity, and no substance was used unless its purity was made sure of. Kahlbaum and Merck's extra pure specimens were re-purified, and their physical constants determined. The alcohols, for example, were purified by the methods put forward by Brunel, Crenshaw, and Tobin ⁽³⁾, Wildermann ⁽⁴⁾, Young and Fortey ⁽⁵⁾, and Andrews ⁽⁶⁾. The values of the physical constants as determined by us and given in the tables below compare favourably with the values of other observers as given in the International Critical Tables and the Tables of Bornstein, showing thereby that the specimens used were quite pure. Scrupulous cleanliness was observed throughout.

The values of χ given in the following tables have been calculated according to the formula :

$$\chi M = \chi_a M_a + (\chi_w m_w - \chi_a m_a) \frac{r - r_1}{r_2 - r_1}$$

(Bhatnagar and Mathur, *loc. cit.*),

where

χ = the magnetic susceptibility of the unknown substance.

M = the mass of the substance taken.

χ_a = magnetic susceptibility of air at that temperature.

M_a = the mass of air which fills the same volume as the substance.

χ_w = magnetic susceptibility of water.

m_w = the mass of water taken.

m_a = mass of air which fills the same volume as occupied by water.

r = deflexion with the unknown substance in the tube.

r_1 = deflexion due to the tube alone.

r_2 = deflexion with the tube containing water.

The specific susceptibilities of water χ_w and of air χ_a were as -0.72×10^{-6} and 24.0×10^{-6} respectively.

It was found that better results could be obtained by keeping the weight constant throughout.

The current was kept constant at 1.5 amps. The temperature was maintained constant throughout the experiment, and the balance was standardized from time to time in course of this investigation, against the accepted values of two or three substances given in the standard tables.

By subtracting the value for carbon (-6.00×10^{-6}) from the mean value for one CH_2 group (-11.36×10^{-6}) obtained in the case of aliphatic compounds (Table I.) the value for χ_{H} comes out to be -2.68×10^{-6} .

In the case of aromatic hydrocarbons (Table II.) the mean value for one CH_2 group is -11.35×10^{-6} , wherefrom χ_{H} comes out to be -2.675×10^{-6} .

The value for the atomic diamagnetic susceptibility of hydrogen in the case of the aliphatic compounds has been determined from the mean of fifteen practically concordant values of CH_2 , and comes out to be -2.68×10^{-6} . It is remarkable to observe that this value is in excellent agreement with the one obtained from the aromatic hydrocarbons.

Pascal's value for χ_{H} is -3.05×10^{-6} , which, when corrected for the now generally recognized value for water, comes out to be -2.98×10^{-6} , a value appreciably higher than the one obtained by us.

TABLE I.

1. Aliphatic Alcohols.

Serial no.	Name of the substance.	Boiling-point.	Refractive index.	Density.	Molecular weight.	$-\chi \times 10^{-6}$.	$-\chi_m \times 10^{-6}$.	$-\chi_{CH_2} \times 10^{-6}$.
1.....	Ethyl alcohol	77.5° C.	1.3625	0.7967	46.046	0.7474	34.42	
2.....	<i>n</i> -Propyl alcohol ...	96.5° C.	1.3835	0.8003	60.062	0.764	45.88	11.46
3.....	<i>n</i> -Butyl alcohol	116.5° C.	1.3990	0.808	74.077	0.772	57.18	11.30

2. Aliphatic Monocarboxylic Acids.

4.....	Acetic acid	Melting-point. 15.75° C.	1.3705	1.054	60.03	0.528	31.63	
5.....	<i>n</i> -Propionic acid ...	Boiling-point. 141.0° C.	1.3859	0.993	74.046	0.580	42.93	11.30
6.....	<i>n</i> -Butyric acid	1.3930	0.959	88.06	0.618	54.43	11.50

3. Aliphatic Esters.

(a) *Ethyl Esters.*

7.....	Ethyl formate	54.5° C.	1.3590	0.908	74.046	0.5886	43.43	
8.....	Ethyl acetate	77.0° C.	1.3719	0.900	88.062	0.6208	54.66	11.23
9.....	Ethyl propionate...	99.0° C.	1.3840	0.892	102.08	0.6468	66.02	11.36
10.....	Ethyl butyrate	101.5° C.	1.3925	0.880	116.09	0.668	77.54	11.52

TABLE II.
Benzene Hydrocarbons.

No.	Substance.	Boiling-point.	Density.	Refractive index.	Molecular weight.	$-\chi \times 10^{-6}$.	$-\chi_m \times 10^{-6}$.	$-\chi_{CH} \times 10^{-6}$.
1.....	Benzene	79.5° C.	0.878	1.5010	78.04	0.713	55.64	
2.....	Toluene	110.5° C.	0.8659	1.4975	92.06	0.729	67.10	11.46
3.....	Ethyl benzene	135.5° C.	0.868	1.4960	106.08	0.740	78.49	11.39
4.....	<i>p</i> -Xylene.....	136.0° C.	0.866	1.4950	106.08	0.7387	78.36	11.26
5.....	<i>m</i> -Xylene	138.5° C.	0.868	1.4970	106.08	0.7390	78.39	11.29

It is interesting to recall here the theoretically predicted value of hydrogen on the new mechanics.

Van Vleck ⁽⁷⁾, in considering diamagnetism from the standpoint of quantum mechanics, supposes the atoms to be in singlet states, and neglecting the second term in

$$\chi_{\text{mol.}} = -\frac{Ne^2}{6mc^2} \Sigma \bar{r}_k^2 + \frac{2}{3} N \sum_{n' \neq n} \frac{[m_0(n'; n)]^2}{h\gamma(n'; n)}$$

restores the classical formula of Langevin, according to which

$$\chi_{\text{mol.}} = -\frac{Ne^2}{6mc^2} \Sigma \bar{r}^2 = -2.832 \times 10^{10} \Sigma r^2. \quad (1)$$

On the old quantum theory the value of \bar{r}^2 was given by

$$\bar{r}^2 = a_0^2 \frac{n^2}{z^2} \left(\frac{5}{2} n^2 - \frac{3}{2} k^2 \right), \quad (2)$$

where $a_0 = 0.5284 \times 10^{-8}$, and refers to the radius of the innermost (1—1) orbit in hydrogen.

Substituting the value of \bar{r}^2 so obtained in equation (1) in form for both the theories, the old theory yields the results for hydrogen :

$$\begin{aligned} \chi_{\text{mol.}} &= -2.832 \times 10^{10} \times a_0^2 \left(\frac{5}{2} n^2 - \frac{3}{2} k^2 \right) \frac{n^2}{z^2} \\ &= -2.832 \times 10^{10} \times (0.5284 \times 10^{-8})^2 \\ &= -0.79 \times 10^{-6}. \end{aligned} \quad (3)$$

On the new quantum mechanics the value of $\Sigma \bar{r}^2$ for hydrogen-like atoms is given by

$$\left[\frac{h^2}{4\pi^2 z e^2 m} \right]^2 \cdot \left[\frac{5}{2} n^4 - \frac{3}{2} n^2(l+1) + \frac{1}{2} n^2 \right]. \quad (4)$$

Substituting these values in equation (1), we get

$$\begin{aligned} \chi_{\text{mol.}} &= -2.832 \times 10^{10} \left(\frac{h^2}{4\pi^2 z e^2 m} \right)^2 \left[\frac{5}{2} n^4 - \frac{3}{2} n^2(l+1) + \frac{1}{2} n^2 \right] \\ &= -0.790 \times 10^{-6} \left[\frac{5n^4 - 3n^2l(l+1) + n^2}{2z^2} \right]. \end{aligned}$$

For the normal state of atomic hydrogen

$$\begin{aligned} n &= 1, \\ l &= 0, \\ z &= 1. \end{aligned}$$

Substituting these values in equation (1), we get

$$\begin{aligned}\chi_{\text{mol.}} &= -0.79 \times 10^{-6} \times 3 \\ &= -2.37 \times 10^{-6}\end{aligned}$$

The value for χ_{H} (-2.68×10^{-6}) obtained from our measurements is in much better accord with the theoretical value (-2.37×10^{-6}) than the original value of Pascal. Exact agreement cannot of course be expected, as the additivity rules taken for granted here may not always furnish true atomic properties.

Work on halides, phosphorus, etc. is in progress.

References.

- (1) Pascal, *Compt. Rend.* cxlix. p. 342 (1909); *Bull. Soc. Chim.* ix. pp. 6-12 (1911).
- (2) Bhatnagar and Mathur, *Phil. Mag.* viii. pp. 1041-1055 (1929).
- (3) Brunel, Crenshaw, and Tobin, *Journ. Amer. Chem. Soc.* xliii. p. 561 (1921); xlv. p. 1334 (1923).
- (4) Wildermann, *Zeit. Physik. Chem.* xiv. p. 232 (1894).
- (5) Young and Fortey, *Journ. Chem. Soc.* lxxxi. p. 723 (1902).
- (6) Andrews, *Journ. Amer. Chem. Soc.* xxx. p. 353 (1908).
- (7) Van Vleck, 'Electric and Magnetic Susceptibilities,' p. 207.

University Chemical Laboratories,
Lahore (India).

XLII. *The Elastic Bending of a Curved Rectangular Bar under Direct Stress.* By ERIC JONES, M.Sc., and R. J. CORNISH, M.Sc.*

THE formula usually given in text-books for the bending of a curved rectangular bar under a uniformly distributed direct stress neglects the alteration in depth of the bar, and is, therefore, considerably in error.

In fig. 1, ABCD represents a short sector of the bar before being stressed. The length of the central filament EF is ds , subtending an angle $d\theta$ at the centre of curvature O. R is the radius of curvature of the central filament, and the depth of the bar is $2h$. Fig. 2 shows the same sector under a compressive stress p , the new dimensions being indicated by dashes.

Then

$$\frac{A'B'}{AB} = \frac{(R' + h')d\theta'}{(R + h)d\theta} = 1 - \frac{p}{E}; \quad \dots (1)$$

* Communicated by the Authors.

Fig. 1.

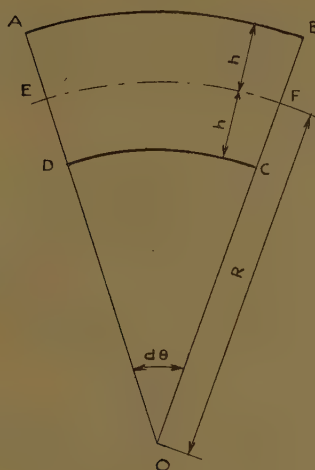
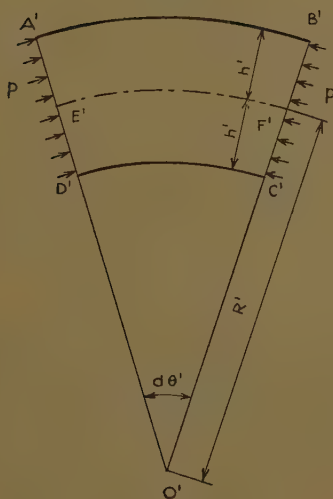


Fig. 2.



$$\frac{E'F'}{EF} = \frac{R'd\theta'}{Rd\theta} = 1 - \frac{p}{E}; \quad \dots \dots \dots (2)$$

$$\frac{A'E'}{AE} = \frac{h'}{h} = 1 + \frac{p}{mE}. \quad \dots \dots \dots (3)$$

In the above equations E is Young's Modulus and $1/m$ is Poisson's Ratio.

Dividing (1) by (2), we have

$$\frac{1 + \frac{h'}{R'}}{1 + \frac{h}{R}} = 1.$$

Therefore $\frac{R'}{R} = \frac{h'}{h} = 1 + \frac{p}{mE}$ (from (3)).

Substituting for R'/R in (2), we get

$$\begin{aligned} \frac{d\theta'}{d\theta} &= \frac{1 - \frac{p}{E}}{1 + \frac{p}{mE}}, \\ &= 1 - \frac{p}{E} - \frac{p}{mE}, \end{aligned}$$

neglecting the squares of small quantities.

Hence

$$\frac{d\theta - d\theta'}{d\theta} = \frac{p}{E} + \frac{p}{mE} = \frac{P}{AE} \left(1 + \frac{1}{m} \right),$$

where P is the total compressive force and A is the cross-sectional area of the bar.

But $d\theta = ds/R$, and, therefore, the relative angular movement of the two ends is given by

$$d\theta - d\theta' = \frac{P}{AE} \left(1 + \frac{1}{m} \right) \frac{ds}{R}.$$

The above formula has a practical application in the calculation of the total energy of bent beams, arches, crane-hooks, and the like. If the bending moment at any point is M , the expression for the total energy should include the term

$$\int \frac{MP}{2AE} \left(1 + \frac{1}{m} \right) \frac{ds}{R}.$$

XLIII. *The Relation between Vibration Frequency and Nuclear Separation for some simple non-Hydride Diatomic Molecules.* By C. H. DOUGLAS CLARK, M.Sc., A.R.C.S., D.I.C., Assistant Lecturer in Chemistry in the University of Leeds *.

I. Introduction.

IT is often advantageous, in spectroscopic work on diatomic molecules, to possess a convenient means of estimating r_e , the equilibrium nuclear separation, from a known value of ω_e , the equilibrium nuclear vibration frequency for small amplitudes. For different electronic levels of a given molecule, Birge ⁽¹⁾ and Mecke ⁽²⁾ found the empirical result that

$$\omega_e r_e^2 = \text{a constant.} \quad . \quad . \quad . \quad . \quad (1)$$

Morse ⁽³⁾ found that the deviations from the above rule might be considerable. Moreover, since the value of the constant on the right-hand side of equation (1) varies with different molecules, the relation can only be applied in estimating r_e for a state for which ω_e is known, provided that both r_e and ω_e are known for at least one other state of the molecule considered. Morse introduced a more general empirical relation, applicable to different molecules of a similar kind, as follows:—

$$\omega_e r_e^3 = \text{a constant.} \quad . \quad . \quad . \quad . \quad (2)$$

Equation (2) was found to give the most satisfactory agreement with experiment in cases where the two atoms composing the molecule did not differ very greatly in mass. For such cases it was found that, with very considerable approximation,

$$\omega_e r_e^3 = 3 \times 10^{-21}, \quad . \quad . \quad . \quad . \quad (3)$$

where ω_e , r_e are in cm.^{-1} and cm. respectively. The constant term on the right-hand side of equation (3) tends to take higher values in the case of less symmetrical molecules. Morse considered that the deviations might be corrected for by means of an "asymmetry factor," involving M_1 , M_2 , the masses of the vibrating nuclei. It is the purpose of the present paper to suggest that,

* Communicated by Prof. R. W. Whytlaw Gray, F.R.S.

at any rate for simple types of molecules, there is another way of approaching the question of correcting the relation (3), and that this method is capable of yielding generally good agreement with results derived from spectroscopic measurements.

II. *The Periodicity of non-Hydride Diatomic Molecules.*

In a recent paper, the author ⁽⁴⁾ has considered the appropriate classification of diatomic molecules of the non-hydride type, and a periodic arrangement has been suggested which appears to be suited to describe their properties. The picture, provided by the spectroscopic evidence, of such a molecule appears to be quite simple. An atom, in general, consists of a completed group of electrons, together with a certain number of "valency" electrons. When two atoms unite to form a homopolar non-hydride molecule, the completed groups of electrons remain more or less appropriated by their individual nuclei, and form a "non-bonding" group in two parts. The valency electrons, however, tend to become shared between the two atoms, and have their quantum designations more or less strongly modified. The group of shared electrons, according to Mulliken ⁽⁵⁾, contains "bonding" and "anti-bonding" electrons, the bonding electrons tending to link the two atoms together, and the anti-bonding electrons tending to have the opposite effect. On paper at least, any combination of non-bonding groups may become associated with any given set of shared electrons. The problem of classification then consists in combining three sets of practically independent variables. The principles governing such classification have been suggested by the author ⁽⁶⁾ and carried into effect for every molecule of the specified type thus far examined ⁽⁴⁾. The classification follows the lines laid down by Mendel'jéeff for atoms, though it differs in being essentially three-dimensional. The molecules are divided into periods, according to their pair of non-bonding groups, and into periodic groups, depending on the number of shared electrons. Thus, for example, the molecule CO falls into the symmetrical two-complete K ring period (designated KK or 4S), and into group number 10, since it derives four and six electrons from the constituent atoms carbon and oxygen respectively, to form the shared, considerably modified group. If

He₂ and H₂⁺ may be regarded from this point of view as belonging to groups 0 and 1 respectively, then a complete set of periodic groups of molecules may be described, numbered from 0 to 14. The classification on this basis (1) brings together in a single table a great deal of information derived from experiment, (2) places in close association molecules of the same kind in groups and periods, enabling previously unnoticed relations between them to be more easily discovered, and (3) leaves gaps for cases thus far not investigated, for which it becomes possible to forecast the leading spectroscopic features in many cases with a considerable measure of probability. The present paper provides a possible application of the suggested arrangement.

III. A simple Modification of Morse's Rule.

In the light of the classification outlined in the foregoing paragraph, according to data collected by Jevons⁽⁷⁾, it appears that Morse's rule, as expressed in equation (3), applies best in the period of non-hydride diatomic molecules containing two completed K rings associated with each atomic nucleus. Even in this period, however, the rule in its simplest form definitely breaks down for Li₂, where the nuclei are of equal mass and where the rule might be expected to hold pretty accurately. Table II. shows this, and also clearly indicates that the errors from observed values of r_e tend to pass from large negative values to smaller negative values, and finally to increasingly positive values *with increasing group number*. It thus happens that the rule fits best in the middle groups, where the errors tend to pass from negative to positive. This definitely seems to suggest that the group number n should enter into the expression connecting r_e and ω_e . A search was therefore made for a value of x which should make the expression $\omega_e r_e^3 n^x$ as nearly constant as possible, which yielded $x=0.47$. It appeared that no very serious error would be introduced by taking $x=\frac{1}{2}$, whence the following empirical modification of Morse's rule was reached:—

$$\omega_e r_e^3 \cdot \sqrt{n} = k - k', \quad (4)$$

where k is a constant for a given molecular period, and k' is a correction for the case of an ionized molecule. The value of k' will be different for singly, doubly . . . ionized

states in the given period, and will be zero for uncharged molecules. Values of these constants, so far as they have been determined, are shown in Table I.

TABLE I.
Values of Period Constants in the Modified
Morse Expression.

Period.	$k' (\times 10^{21}).$	k' (singly ionized, positive) $(\times 10^{21}).$
KK (4S)	9.55	0.50
KL (12)	12.85
KM (20B)	(13.50)

IV. *Application to the KK Molecular Period.*

For neutral molecules of the KK period, where $k'=0$, the modified Morse expression takes the form⁽⁸⁾

$$\omega_e r_e^3 \cdot \sqrt{n} = 9.55 \times 10^{-21}. \quad . \quad . \quad . \quad (5)$$

Results for thirty electronic states of ten molecules of the KK period are collected together in Table II.

The errors are expressed as percentages, and the mean errors are calculated without reference to sign. It is observed that the mean error is reduced from 5.2 per cent. to 1.3 per cent. by the modification introduced, the new formula showing a marked improvement in accuracy on the tested cases. The results are possibly within the general experimental uncertainty. Moreover, the individual errors show no tendency to progress in one direction, and they are about evenly distributed between positive and negative values. The agreement with experiment is as good as that obtained by the Morse relation in the middle part of the table, where this relation gives the best results. It may be noted that a certain proportion of the ω_e values are derived from band-head data.

Let us next consider the case of molecule-ions of the KK period. Using Table I. in connexion with equation (4), we have

$$\omega_e r_e^3 \cdot \sqrt{n} = 9.05 \times 10^{-21} \quad . \quad . \quad . \quad (6)$$

TABLE II.
Equilibrium Internuclear Distances in the KK Period
(Neutral Molecules).

Molecule.	Periodic group. n.	Electronic state.	ω_e cm. ⁻¹ .	r_e (Å.U.) (expt.)	r_e (Å.U.)		r_e percentage errors.	
					Morse.	Clark.	Eq. (3).	Eq. (5).
					Eq. (3) (calc.).	Eq. (5) (calc.).		
Li ₂	2	C ¹ Π_u	H 269.7	2.93	2.232	2.926	-23.8	-0.2
		B ¹ Σ^+_u	H 253.2	3.11	2.280	2.989	-26.7	-3.9
		G A ¹ Σ^+_g	H 351.6	2.67	2.044	2.678	-23.5	+0.3
C ₂	8	d ¹ Π_g	1832.5	1.251	1.179	1.226	-5.8	-2.0
		B ³ Π_g	1792.6	1.261	1.189	1.235	-5.7	-2.1
		b ¹ Π_u	1608.3	1.315	1.231	1.280	-6.4	-2.7
		G A ³ Π_u	1641.6	1.308	1.223	1.272	-6.5	-2.8
BeO	8	C ¹ Σ^+	H 1370.8	1.359	1.298	1.350	-4.5	-0.7
		B ¹ Π	H 1079	1.50	1.406	1.463	-6.3	-2.5
		G A ¹ Σ^+	H 1487.5	1.328	1.266	1.316	-4.7	-0.9
BeF	9	A ² $\Pi_{reg.}$	1172.6	1.390	1.368	1.395	-1.6	+0.4
		G X ² Σ^+	1265.6	1.357	1.333	1.360	-1.8	+0.2
BO	9	B ² Σ^+	1280.3	1.301	1.328	1.355	+2.1	+4.2
		A ² $\Pi_{inv.}$	1259.1	1.348	1.336	1.362	-0.7	+1.0
		G X ² Σ^+	1885.4	1.199	1.168	1.191	-2.6	-0.7
CN	9	B ² Σ^+	2164.2	1.148	1.115	1.137	-2.9	-1.0
		A ² $\Pi_{inv.}$	1788.7	1.236	1.188	1.212	-3.9	-1.9
		G X ³ Σ^+	2068.8	1.169	1.132	1.154	-3.2	-1.3
N ₂	10	B ³ $\Pi_{reg.}$	H 1732.8	1.201	1.200	1.203	-0.1	+0.2
		A ³ Σ	H 1460.4	1.291	1.272	1.275	-1.5	-1.2
		G X ¹ Σ^+_g	H 2359.6	1.094	1.083	1.086	-1.0	-0.7
CO	10	B ¹ Σ	H 2182	1.118	1.112	1.114	-0.5	-0.4
		A ¹ Π	H 1516.7	1.232	1.255	1.258	+1.9	+2.1
		G X ¹ Σ^+	H 2167.4	1.15(r_0)	1.114	1.117
NO	11	B ³ $\Pi_{reg.}$	1037.6	1.413	1.424	1.406	+0.8	-0.5
		A ² Σ^+	2375.3	1.060	1.081	1.066	+2.0	-0.6
		G X ² $\Pi_{reg.}$	1906.5	1.146	1.163	1.148	+1.5	-0.2
O ₂	12	B ³ Σ^-_u	710.1	1.599	1.616	1.571	+1.1	-1.8
		A ¹ Σ^-_u	1432.6	1.223	1.279	1.244	+4.6	+1.7
		G X ³ Σ^-_g	1584.9	1.204	1.237	1.202	+2.7	-0.2
Average percentage error (neglecting sign)							5.2	1.3

H.—Band-head measured.
G.—Ground state.

for singly positively charged molecule-ions. Using this relation for cases where data are available, Table III. is obtained.

It is observed from Table III. that fairly large positive errors tend to appear in values calculated from Morse's unmodified formula in Group 11. The results by the modified formula are generally slightly better than those using the equation (3) without change. Morse's formula

TABLE III.

Equilibrium Internuclear Distances in the KK Period
(Ionized Molecules).

Molecule-ion.	Periodic group. <i>n.</i>	Electronic state.	ω_e	r_e (Å.U.)	r_e (Å.U.)		r_e percentage errors.	
			cm. ⁻¹ .	(expt.)	Morse.	Clark.	Eq. (3).	Eq. (6).
					Eq. (3) (calc.).	Eq. (6) (calc.).		
CO ⁺	9	B $^2\Sigma^+$	1722.1	1.16	1.203	1.206	+3.6	+3.8
		A $^2\Pi_{inv.}$	1564.5	1.24	1.243	1.245	+0.3	+0.4
		G X $^2\Sigma^+$	2212	1.11	1.107	1.109	-0.3	-0.1
N ₂ ⁺	9	B $^2\Sigma_u^+$	2417.7	1.071	1.074	1.076	+0.3	+0.5
		G X $^2\Sigma_g^+$	2206.8	1.113	1.108	1.110	-0.5	-0.3
O ₂ ⁺	11	A $^2\Pi_u$	H 898.9	1.41	1.494	1.447	+6.0	+2.6
		G X $^2\Sigma_{g,reg.}$	H 1876.4	1.14	1.168	1.133	+2.5	-0.6
Average percentage error (neglecting sign)							1.9	1.2

H.—Band-head measured.

G.—Ground state.

has already been observed to give the best results in the middle groups. The rather large positive errors in two cases of excited states may be partly connected with experimental uncertainty, the figures being given in Jevons' table to two decimal places only. Apart from this discrepancy, the errors of the unmodified Morse expression show the tendency to become increasingly positive with increasing group number. This tendency was noted in the earlier period, and again disappears in the figures derived from the modified formula.

V. Application to the KL Molecular Period.

For neutral molecules of the KL period, by equation (4) and Table I., the appropriate relation is

$$\omega_e r_e^3 \cdot \sqrt{n} = 12.85 \times 10^{-21}. \quad (7)$$

Results using this equation are shown in Table IV.

In including calculations based on Morse's unmodified equation (3), it must be remembered that this author

TABLE IV.

Equilibrium Internuclear Distances in the KL Period
(Neutral Molecules).

Molecule.	Periodic group.	Electronic state.	ω_e	r_e Å.U.	r_e (Å.U.)		r_e percentage errors.			
	n .				cm. ⁻¹ .	(expt.)	Morse.	Clark.	Eq. (3).	Eq. (7).
							Eq. (3) (calc.).	Eq. (7) (calc.).		
AlO	9	B $^2\Sigma^+$	868.2	1.663	1.512	1.702	-10.0	+2.3		
		G X $^2\Sigma^+$	977	1.614	1.453	1.637	-10.0	+1.4		
SiN	9	B $^2\Sigma^+$	1034.4	1.576	1.426	1.604	-9.5	+1.1		
		G X $^2\Sigma^+$	1151.7	1.568	1.376	1.549	-12.3	-1.2		
SiO	10	A $^1\Pi$	H 848.1	1.621(r_0)	1.524	1.686		
		G X $^1\Sigma$	H 1240.5	1.505	1.342	1.485	-10.9	-1.3		
SO	12	B $^3\Sigma$	H 628.7	1.769	1.684	1.807	-4.8	+2.1		
		G X $^3\Sigma$	1123.7	1.489	1.387	1.489	-6.8	0.0		
Average percentage error (neglecting sign)							9.2	1.3		

H.—Band-head measured.

G.—Ground state.

considered that a correction would be necessary where considerable difference existed between the masses of the two nuclei concerned. Morse⁽³⁾, however, included the molecule SiN of Table IV. in his Table I. (p. 62). The errors using equation (3) show some tendency to become decreasingly negative with increasing group number, but they do not become positive in any of the cases noted in Table IV. The errors using equation (7) are, on the other hand, about evenly distributed between positive and negative values, and show no inclination to progress

steadily in one direction. The degree of applicability of the present author's relation is as good as in Tables II. and III. for rather simpler molecules, as judged by the mean error. It should be noted, however, that in two cases where the calculations have been carried through the values of ω_e upon which they depend are derived from measurements on band-heads (see section VII.).

VI. Example in the KM Molecular Period.

The only molecule of the KM period for which the requisite data are recorded by Jevons⁽⁷⁾ appears to be the neutral TiO. It would evidently be unsafe to

TABLE V.
Equilibrium Internuclear Distances of TiO.

Mole- cule.	Periodic group.	Electronic state.	ω_e	r_e (Å.U.)		Per- centage errors.	
	n .			cm. ⁻¹ .	(expt.).		(calc.).
					Eq. (8).		
TiO	10	C ³ Π	H 837.9	1.690	1.721	+1.8	
		G X ³ Π	H 1008.1	1.617	1.618	+0.1	
Average error (per cent.)						1.0	

H.—Band-head measured.

G.—Ground state.

generalize from one instance, but provisionally the constant for the period may be assumed to lie in the neighbourhood of the value enclosed in brackets in Table I., whence the appropriate relation would be

$$\omega_e r_e^3 \cdot \sqrt{n} \approx 13.50 \times 10^{-21}. \quad . \quad . \quad . \quad (8)$$

The r_e values for two electronic states of TiO are calculated by this formula, results being shown in Table V.

VII. Some "Predicted" Values of r_e .

The measure of agreement between experimental values of r_e and those calculated with the aid of the modified

Morse expression would appear to justify calculation being made in cases where ω_e , but not r_e , has been determined by experiment. Unfortunately the cases to which this method can at present be applied are all those in which the ω_e data are derived from measurements on band-heads. Tables II., III., IV., and V. of this paper contain cases of this kind (marked H), and *on the whole* it would appear that the errors inherent in calculation in these cases is about the same as those in other cases. Encouraged by this observation, the author has considered it worth while to prepare Table VI., showing "predicted" values of r_e for cases where $\omega_e(\text{H})$ has been determined, and where no direct experimental check on the calculation is yet possible. It will be of interest to observe, if the necessary experiments are carried out, whether the previous measure of agreement between calculation and observation is maintained. If such comparison is ever made, however, it should be remembered that the values of ω_e used in calculating r_e 's in Table VI. are derived entirely from band-head measurements.

So far as the calculated values of Table VI. may be compared with approximate experimental estimates, the agreement appears satisfactory. Thus the r_e values for MgF, for instance, tend to lie between those of BeF and CaF: similar results apply in other cases, as inspection reveals. The agreement for the "C" level of N_2 with the estimated value is excellent: 1.14 (expt.), 1.139 Å.U. (calc.). In other cases, where values of r_0 have been determined, the agreement appears satisfactory so far as orders of magnitude are concerned. The equilibrium internuclear distance of F_2 in the $^1\Pi$ state is calculated by the modified Morse formula as 1.331 Å.U.; Jevons⁽⁷⁾ (see p. 113) gives the estimate of 1.5 Å.U. Several cases are included in Table VI. for which no value of r_e has been determined for any state: F_2 , MgF, SiF, CP, CS, PO, and NS. The accuracy of calculation in all tables is that obtainable by the use of four-figure logarithms.

VIII. Concluding Remarks.

It is probably unwise, in the nature of the case, to emphasize the significance of a rule very much for which, up to the present, no theoretical justification has been found; nevertheless, from the general agreement of Morse's expression in its modified form with experiment,

TABLE VI.
Calculation of Equilibrium Internuclear Distances.

Mole- cule.	Group. <i>n.</i>	Electronic state.	$(k-k')$ $\times 10^{21}$.	ω_e .	r_e (calc.).	Equa- tion no.
				cm. ⁻¹ .	A.U.	
BeO	8	E ? Σ D ? Σ	9.55	H 1016 H 1136	1.492 1.438	(5)
CO	10	a $^3\Pi$ a' $^3\Sigma?$ F $^1\Pi?$ G X $^1\Sigma^+$	9.55	H 1739.3 H 1182 H 2112 H 2167.4	1.202 1.367 1.127 1.117	(5)
N ₂	10	a $^1\Pi_u$ C $^3\Pi$	9.55	H 1692.3 H 2044.7	1.213 1.139	(5)
NO	11	D	9.55	H 2351	1.070	(5)
O ₂	12	b E D C	9.55	H 1121 H 1454 H 1524 H 1494	1.350 1.238 1.218 1.227	(5)
F ₂	14	$^1\Sigma$ $^1\Pi$	9.55	H 1107.8 H 1081.4	1.321 1.331	(5)
O ₂ ⁺	11	a $^4\Pi_u?$ b $^4\Sigma_g?$	9.05	H 1037.2 H 1198.1	1.349 1.315	(6)
MgF	9	B $^2\Sigma?$ A $^2\Pi$ G X $^2\Sigma$	12.85	H 757.8 H 718.9 H 690.8	1.781 1.813 1.838	(7)
SiN	9	C $^2\Pi?$ A $^2\Pi?$	12.85	H 697.3 H 1031.0	1.831 1.608	(7)
CP	9	B $^2\Sigma$ G X $^2\Sigma$	12.85	H 832.4 H 1239.0	1.727 1.512	(7)
SiO	10	A $^1\Pi$	12.85	H 848.1	1.686	(7)
CS	10	A $^1\Pi$ G X $^1\Sigma$	12.85	H 1072.2 H 1282.5	1.559 1.469	(7)
SiF	11	β α G X	12.85	H 1020.5 H 716.5 H 865.0	1.560 1.755 1.648	(7)
PO	11	A $^2\Sigma$ G X $^2\Pi$	12.85	H 1393.2 H 1235	1.406 1.464	(7)
NS	11	B $^2\Pi$ G X $^2\Pi$	12.85	H 944 H 967 H 1220	1.601 1.588 1.470	(7)
TiO	10	A $^2\Sigma$	13.50	H 866.2	1.702	(8)

H.—Band-head measured.

G.—Ground state.

it is difficult to escape the conclusion that the function $\omega_e r_e^3$ has some fundamental significance. Further, so far as it is possible to argue from results obtained from an empirical relation, it would appear that the conception of molecular periods and groups of diatomic molecules has an importance of its own. The fact that the value of the "period constant" k varies discontinuously from one period to another, whilst remaining approximately constant within a given period, suggests that the right kind of classification has been chosen. It also appears that the square root of the group number of a molecule, a magnitude which has not apparently been considered elsewhere, may enter into the relations between the spectroscopic constants of diatomic molecules.

Morse⁽³⁾, following a suggestion made by Mulliken, considered that the deviations from the requirements of the rule might be connected with increasing differences in the masses of the separate atomic nuclei of a diatomic molecule, and might be allowed for by an appropriate "asymmetry factor." It is observed, however, that large deviations occur in the case of Li_2 , where the nuclear masses are equal (Table II.). In the present author's view, therefore, the discrepancies are preferably interpreted, at any rate in the case of simpler molecules, in terms of the fact that the molecules fall into different periods, requiring characteristic period constants, allowance being also made for the group number of a molecule by using the modified function $\omega_e r_e^3 \sqrt{n}$.

The author holds that the results support his contention that the properties of diatomic molecules should be considered in relation to the natural classification of the molecules in groups and periods.

IX. Summary.

It has been found that Morse's rule (equation (3)) may be modified by the introduction of the appropriate group number and a period constant, with an allowance for ionized states of diatomic molecules of non-hydride type (equation (4)). The average error from the experimental results is slightly greater than 1 per cent. (Tables II., III., IV., and V.). The modification has only been applied to cases where at least one of the two constituent atoms of a non-hydride diatomic molecule has no more than one K ring in its completed group.

Out of twenty-eight cases for which data concerning both ω_e and r_e are recorded by Jevons⁽⁷⁾ for ground states of diatomic molecules of non-hydride type, eighteen are here taken into account.

Assuming the validity of the method, and its more general applicability, r_e values for thirty-six electronic states of diatomic molecules of the prescribed type, where no direct experimental check is at present possible, have been "predicted" in Table VI.

From the results communicated it would appear that the suggested modification of Morse's rule possesses considerable usefulness, in the cases to which it may be applied, in relating together the two fundamental molecular magnitudes concerned.

Note added in Proof.—The author ('Nature,' cxxxiv. p. 99 (1934)) has observed that the atomic radius of fluorine (calculated from the r_e value for the 1I state of F_2 in Table VI.) is in satisfactory agreement with the radius derived from crystal data.

References.

- (1) R. T. Birge, *Phys. Rev.* (ii.) xxv. p. 240 (1925).
- (2) R. Mecke, *Zeit. Physik*, xxxii. p. 823 (1925).
- (3) P. M. Morse, *Phys. Rev.* (ii.) xxxiv. p. 57 (1929).
- (4) C. H. Douglas Clark, *Proc. Leeds Phil. Soc.* ii. p. 502 (1934).
- (5) R. S. Mulliken, *Chemical Reviews*, ix. p. 348 (1931).
- (6) C. H. Douglas Clark, *Chemical Reviews*, xi. p. 231 (1932).
- (7) W. Jevons, 'Report on Band-Spectra of Diatomic Molecules' (Appendix II.). Camb. Univ. Press, 1932.
- (8) C. H. Douglas Clark, 'Nature' cxxxiii. p. 873 (1934).

Department of Inorganic Chemistry,
The University of Leeds.
May 12th, 1934.

XLIV. *The Temperature Variation of the Thermoelectric Properties and the Specific Heat of Nickel-Chromium Alloys.* By ALAN W. FOSTER, Ph.D.*

INTRODUCTORY.

FERROMAGNETIC substances possess an intrinsic magnetization which varies in a characteristic manner with temperature. At low temperatures the magnetiza-

* Communicated by Prof. R. Whiddington, F.R.S.

tion approaches the absolute saturation value, but as the temperature is raised it falls with increasing rapidity to zero at the Curie point. Other properties of ferromagnetics show abnormal temperature variations in the Curie point region, and attempts have been made to correlate such variations with the magnetization ⁽¹⁾. Accurate data, however, for a range of properties are available only for nickel.

Knowledge of the effects of the addition of foreign metals to ferromagnetic elements on the low temperature saturation magnetization has proved invaluable in the theoretical interpretation of the low temperature atomic moments, and investigation of the effects on other properties of ferromagnetics near the Curie point may also throw new light on the complex magnetic behaviour at higher temperatures. The present measurements were undertaken to provide accurate data on the variation with temperature of the specific heat, thermoelectric power, and Thomson coefficients of nickel-chromium alloys, containing 1 and 2 per cent. of chromium, in the vicinity of their Curie points.

The specific heat (s) of pure nickel has been accurately determined over a wide temperature range by Lapp ⁽²⁾ and the thermoelectric power and Thomson coefficient (σ), near the Curie point, by Dorfman and Jaanus ⁽³⁾. Grew ⁽⁴⁾ has investigated the effect of the addition of copper to nickel on both σ and s . The present work differs from that of Grew in that the added metal atom has an incomplete d group of electrons, whereas copper atoms have a complete "core" and one s electron. The saturation magnetic moment of dilute alloys of chromium in nickel has been investigated by Sadron ⁽⁵⁾. No satisfactory magnetic data for the Curie point region have yet appeared, though Safranek ⁽⁶⁾ has measured the paramagnetic susceptibility of the same alloys above the Curie point.

Measurements of the total e.m.f. of platinum, nickel-chromium alloy thermocouples have been made by Chevenard ⁽⁷⁾, and thermoelectric power curves obtained by differentiation. The validity of the second differentiation required to give σ is questionable, particularly in view of the smoothing of the curves as given by the e.m.f. recorder. Chevenard also measured the mean specific heat of some of these alloys; that differentiation, giving

the true specific heat, may lead to considerable errors is evidenced by the discrepancies between the accurate measurements on nickel of Weiss and Forrer ⁽⁸⁾, on the mean s , and Lapp on the true s .

The experimental methods adopted are based upon the principles of previously successful methods with a number of modifications which may be found useful in work of this character. The results for the thermoelectric power measurements are believed to be of considerable accuracy, but those on the specific heat had to be left at a provisional stage.

Measurements have been made on nickel and on two alloys of nickel with low chromium content. The expense of chemically pure nickel was considered unnecessary, since sufficient measurements on such nickel already exist. Commercially pure nickel (99.5 per cent.) obtained as wire 0.11 cm. diameter was used; it shows effects due to common impurities. As the effect of the addition of chromium is being considered the same type of nickel can be used for the manufacture of the alloys, and, with the low concentration of chromium, commercially pure metal (99 per cent. Cr) is quite adequate. With these materials alloys of nickel with 1 and 2 per cent. by weight of chromium were made by British Driver-Harris Co., Manchester, and supplied in wire form 0.11 cm. diameter. The impurity of the materials used might be thought to introduce some uncertainty into the interpretation of results, but for the thermoelectric properties, where impurities have the greatest effect, the action of chromium additions is known to be abnormally large and swamps the effects of other metals.

THERMOELECTRIC PROPERTIES.

Thomson Coefficient.

As a property solely of the metal under test, and probably because of its less complex theoretical derivation, the variation of the Thomson coefficient, or "specific heat of electricity," with temperature has been primarily considered in the literature of the subject. It is obtained experimentally most simply from the thermoelectric power by the thermodynamically derived equation

$$\sigma_A - \sigma_B = T \frac{\partial^2 ({}_A E_B)}{\partial T^2},$$

where σ_A and σ_B are Thomson coefficients of metals A and B between which the thermoelectric power is $\partial({}_A E_B)/\partial T$; T is the absolute temperature. A is the test metal and B a convenient nonferromagnetic substance; in these experiments copper was used. The abnormal variations of σ_A with temperature are considered as being those of $\sigma_A - \sigma_B$ in the Curie point region.

Measurement of Thermoelectric Power.

A fairly complete discussion of methods of measuring thermoelectric powers of metals has been given by Galibourg⁽⁹⁾, from whose account it is evident that differential methods are almost essential for the accurate determination of thermoelectric powers which vary at all rapidly or irregularly with temperature. Previous to the commencement of this work measurements on pure nickel by differential methods had been made by Dorfman and Jaanus⁽³⁾ and by Grew⁽¹⁰⁾ in this laboratory. The method adopted in both cases consisted in measuring the e.m.f. given by a reference metal (specimen) reference metal thermocouple due to a small difference of temperature between the junctions, recorded by a standard differential thermocouple. The specimen and standard thermocouple junctions were separated by thin mica for electrical insulation, which procedure is open to two possible objections. In the first place mica becomes appreciably surface conducting at moderate temperatures, although the effect is probably negligible for low voltage work. Secondly, appreciable temperature differences may persist between the two sides of the mica, and preliminary tests confirmed the possible seriousness of this effect.

Another source of error lies in the inhomogeneity of the wires used for the thermocouples involving the probability of a potential difference between the ends of a differential couple when the junctions are at exactly the same temperature. Such errors may be eliminated by measuring the *change* in the e.m.f. of the couple produced by a small change in the temperature difference of its junctions.

The following arrangement was finally adopted after trial of less complicated methods. Copper constantan thermocouples (26 s.w.g.) were silver-soldered to a specimen wire about 10 cm. in length at points 3 cm. from each end, excess solder being removed. The free ends of the

specimen were then coated with thin films of glass by melting on to these portions thin tubing and drawing off the main part of the soft glass. Similar heating coils of thin nichrome-wire were wound on each glass film, the latter serving only to insulate the turns of the coil. All thermocouple and lead-wires were encased in pyrex tubing and the whole arrangement placed inside a 1-cm. bore pyrex tube, and supported in a small horizontal resistance furnace. Since the furnace was suitably wound and lined with an iron tube, the thermocouple junctions were very nearly at the same temperature when the furnace attained steady conditions, and any temperature fluctuations of the furnace scarcely affected the relative temperatures of the junctions. A non-inductive furnace winding enabled the furnace current to be taken from large capacity accumulators without setting up appreciable magnetic fields.

By connecting, in turn, each of the small heating coils on the specimen in series with the same battery and rheostat the temperature gradient along the specimen can be varied and reversed at will. The appropriate differential e.m.f. are measured before and after reversal, and subtraction gives the change in each of these quantities produced by the measured change in the temperature difference. Since this was made of the order of one degree the smallness of the e.m.f.'s involved necessitated considerable care in protecting the leads from the furnace from fluctuating temperatures and leakage currents. Also the method of measurement must be such that the introduction of parasitic e.m.f. is avoided, as was effected by the following "compensation" method.

An oil-immersed mercury-cup switch connected appropriate leads from the furnace through a sensitive low resistance galvanometer to wires from the ends of a resistance constructed of a short length of copper wire (26 s.w.g.), which was kept at a steady temperature in a vacuum flask. An adjustable current of the order of milliamps., read on an accurate Weston instrument, passed through the copper resistance, and could be varied until the galvanometer indicated balance. The balancing e.m.f. was directly proportional to the current through the milliammeter, and, relative measurements only being required, the readings of the instrument were used in calculation.

The e.m.f. of both thermocouples, with cold junctions in ice and water, were measured before and after reversal of the temperature gradient, and the mean of the four measurements was used to find the mean temperature of the determination from the calibration of the thermocouples. The other e.m.f. measured are (1) between the copper leads, the change of which on "reversal" may be represented as $\Delta({}_A E_C)$ [A, specimen; C, copper], (2) between the constantan leads, change on reversal $\Delta({}_A E_K)$ [K, constantan].

Then the additive rule gives

$$\Delta({}_A E_K) - \Delta({}_C E_K) = \Delta({}_C E_A).$$

The right-hand side represents the change in the temperature difference produced by "reversal," and the thermoelectric power of the specimen against copper, $d({}_A E_C)/dT$, is given by

$$\frac{\Delta({}_A E_C)}{\Delta({}_C E_K)} \cdot \frac{d({}_C E_K)}{dT}.$$

The first part of this expression was found in terms of the milliammeter readings, and the thermoelectric power of the copper constantan couples was derived from their calibration.

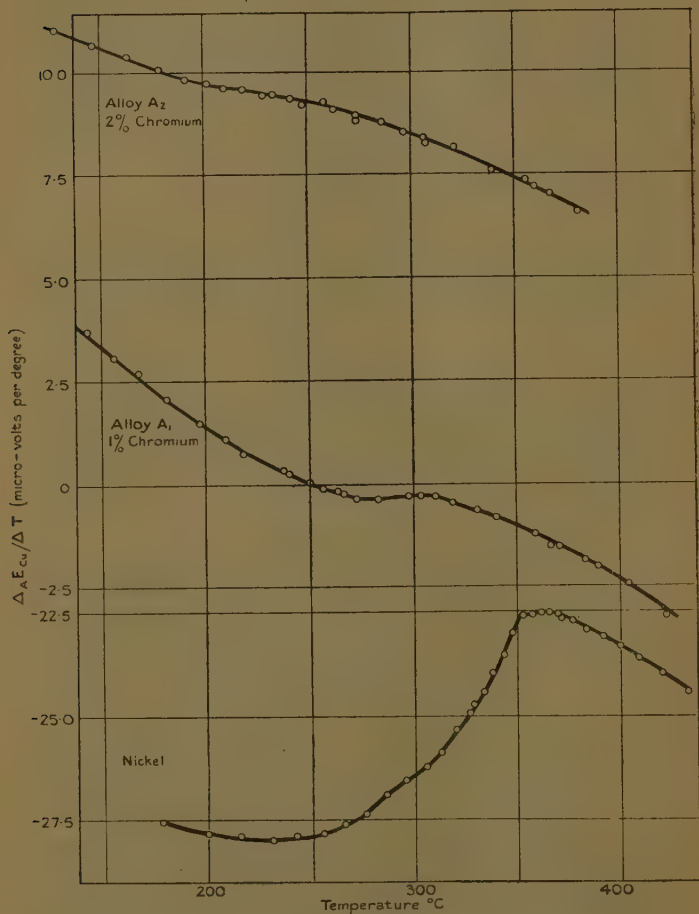
Measurement of Temperature.

The e.m.f. given by the thermocouples were measured on a 5-metre wire potentiometer, previously calibrated, with a range of 0–450° C. The thermocouples were detached from the specimen at the end of the experiment and calibrated at the melting-points of tin, lead, and zinc with the boiling-points of water, aniline, naphthalene, and benzophenone as checks. An accuracy to 0.3° C. was probably attained over the range 150–420° C. Since the thermocouples mounted on the specimen were first treated to several hours heating at a rather higher temperature, and readings were taken in descending order, the chance of error due to deterioration was only slight.

An equation, cubic in T, was constructed to fit the fixed points of the calibration for the first couple of a batch drawn from the same sample of wire, and a difference table constructed giving the e.m.f. for every ten degrees. Each first difference is ten times the mean thermoelectric power over its temperature interval, and the table

enables the power at any temperature to be found by interpolation. Calibration of subsequent couples was

Fig. 1.



Thermoelectric powers of nickel and nickel-chromium alloys against copper.

effected by means of curves showing the deviation of their fixed point e.m.f. from those of the first couple.

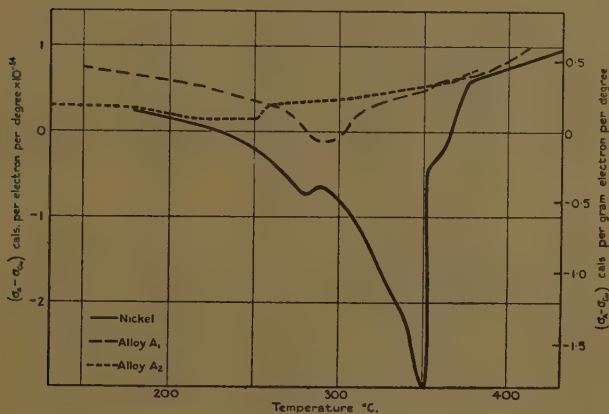
The absolute probable error of each value obtained for the thermoelectric power is estimated to be 0.7 per cent., and the relative error about 0.4 per cent.

Experimental Results.

The thermoelectric powers against copper of each of the alloys and of nickel are given in Table I. and shown graphically in fig. 1, and the variation of the Thomson coefficient in fig. 2.

The specimens had all been heated for fifty hours at 900° C. ; comparison with preliminary results shows that

Fig. 2.



The variation with temperature of the Thomson coefficient of nickel and nickel chromium alloys.

this treatment renders the change of slope at the Curie point less abrupt, though it scarcely affects the value of the change in the Thomson coefficient at the Curie point ($\Delta\sigma_s$). Values for $\Delta\sigma_s$ are given later in Table III.

MEASUREMENT OF SPECIFIC HEAT.

Introduction.

For the present purpose the method required is one which enables the variation of the specific heat with temperature to be followed closely, but absolute accuracy

is a secondary consideration. A complete investigation should aim at determining (1) the magnitude of the change at the Curie point, (2) the shape of the curve in the region of the Curie point, (3) the value of the specific heat in the paramagnetic state. The present measurements were intended as provisional, and can throw light on the first

TABLE I.

Thermoelectric Powers against Copper in micro-volts per degree.

Nickel. Temp. °C.	$-\frac{d(\epsilon_{Ni}E_{Cu})}{dT}$	Temp. °C.	$\frac{d(\epsilon_{A_1}E_{Cu})}{dT}$	Temp. °C.	$\frac{(d\epsilon_{A_2}E_{Cu})}{dT}$
432.0	24.41	422.8	-3.060	379.0	6.76
419.9	23.91	405.0	-2.420	365.7	7.17
408.6	23.56	390.5	-1.730	353.8	7.44
391.4	23.03	370.6	-1.465	343.0	7.65
376.2	22.64	359.0	-1.150	319.3	8.23
369.3	22.52	350.6	-0.919	304.7	8.47
364.8	22.43	340.5	-0.739	295.7	8.63
357.0	22.50	331.4	-0.583	185.3	8.84
352.3	22.50	319.3	-0.380	271.8	9.01
347.7	22.96	311.2	-0.286	260.5	9.22
343.4	23.47	304.2	-0.260	257.8	9.31
334.0	24.42	298.3	-0.265	240.3	9.39
321.6	25.32	284.0	-0.330	231.8	9.48
305.7	26.21	266.8	-0.203	227.3	9.47
296.4	26.53	250.4	+0.025	217.8	9.60
286.3	26.86	231.1	0.464	208.5	9.67
267.4	27.59	208.8	1.100	199.8	9.78
243.8	27.91	197.1	1.470	176.9	10.07
216.8	27.94	180.9	2.060	161.1	10.39
200.6	27.86	155.5	3.055	144.5	10.66
179.0	27.58	142.2	3.660	126.0	11.04

two points only. The method adopted, which was developed to overcome special difficulties, is not new in principle, but it probably presents an original combination of features.

Previous Work.

The work of Lapp ⁽²⁾ on the specific heat of nickel indicated the advantages of electrical methods, which

can determine the *true* specific heat (s) at a given temperature, over the method of mixtures, giving the *mean* specific heat, for metallic substances possessing irregular properties. For specimens in wire form electrical methods are also more suitable.

Lapp's method consisted in measuring the rate of rise of temperature of a specimen in rod form for the calculable rate of input of heat provided by an electric current. The nickel specimen (2 mm. diameter), supported in a vertical electric furnace, had a small thermocouple sunk into it, and also thin potential leads of nickel wire which enable the rate of rise of temperature and the wattage dissipation respectively in a given length of specimen to be measured. Heating and cooling curves were found by a semiautomatic method, rendered necessary by the shortness of the time of heating, about 30 seconds, and the smallness of the rise of temperature, about one degree. The slope of the log (excess temperature) time curve was used in the usual manner to correct the heating curve for normal heat losses.

Present Method.

Lapp's method could not be followed exactly in the present investigation, and the necessary modifications led to alterations in principle and in the method of obtaining cooling curves. Adapting a method developed by Ferguson and Miller ⁽¹¹⁾ for liquids, it is possible to dispense with the determination of the rate of heating curves.

If a current I_0 is sufficient to keep the temperature of the specimen at a small amount θ_0 above the surroundings

$$I_0^2 r / J = -dQ/dt = -ms \cdot d\theta/dt,$$

where dQ/dt is the rate of loss of heat from the surface of the part of the specimen under consideration (mass m , resistance r , specific heat s). Assuming θ_0 is small enough for Newton's Law to be obeyed,

$$dQ/dt = k\theta,$$

where k is closely independent of θ but in general is a function of the surrounding temperature. Then

$$d\theta/dt = \theta \cdot k/m \cdot s,$$

$$d(\log \theta)/dt = k/m \cdot s,$$

where

$$k = I_0^2 r / J \cdot \theta_0.$$

Two experiments are now necessary. First, k is found, with the furnace heated to a series of temperatures, by measuring at each the rise of temperature θ_0 produced by a known current I_0 . In the second a cooling curve is taken at each temperature at which the specific heat is required. The slope of the $\log \theta, t$ curve gives k/s for that temperature, and hence s from the interpolated value of k .

Resistance Method of determining Temperature Changes.

The wire specimens used in the present investigation were of insufficient diameter to allow thermocouple junctions to be sunk into them without causing serious disturbance of the local conditions. Hence copper and constantan wires 0.2 mm. diameter were lightly hard-soldered to the specimen and similarly copper-wire potential leads. The specimen was coiled and mounted centrally in a region of uniform temperature in a vertical resistance furnace.

This arrangement did not allow the temperature of the specimen to be expressed accurately in terms of the e.m.f. of the thermocouple unless the temperature is slowly varying and moderately uniform. The heating and cooling curves obtained were very imperfect, pointing to a marked lag of the thermocouple temperature behind that of the specimen. This difficulty was overcome by using the variation of the resistance of the specimen to record its temperature. Unfortunately this property in ferromagnetics is very irregular at the temperatures requiring most careful investigation. The experimental procedure detailed below is an attempt to overcome this difficulty by using the resistance change as an intermediary which is eliminated in the process.

A constant current was maintained through the specimen in order that the change of resistance of the part between the potential leads should be accurately represented by the change in e.m.f.; by neutralizing the potential difference at any given temperature a galvanometer can be made to record the change of resistance by the movement of a spot of light. If the "spot" is a fine vertical line and the lamp current producing it is switched on, momentarily, only at regular intervals of time, given by a pendulum, then a strip of bromide paper

in the path of the spot will record the change of resistance with time as a row of vertical lines. Hence if, when the furnace is at a steady temperature, a current is passed through the specimen for a short time, and a photographic record taken as the specimen cools, a precise cooling curve can be obtained with the temperature expressed in terms of resistance.

Since the quantity to be found is $d \log \theta / dt$, any quantity may replace θ which bears a constant ratio to θ . The change in e.m.f. of the thermocouple satisfies this condition satisfactorily if θ is small and if the couple follows exactly the temperature of the specimen. This was approximated to in the experiment quite closely when the whole furnace tube was slowly heated after a cooling record had been taken. Exposing the bromide paper to the galvanometer light spot as the e.m.f. of the thermocouple changed by definite amounts therefore gave a calibration of the resistance change in terms of the thermocouple e.m.f. change (e) superposed upon the previous cooling record. This enables the calibration lines (in terms of e) to be used in conjunction with the interpolated time in the cooling record corresponding to each calibration line for constructing a cooling curve; an arbitrary time zero is sufficient. This procedure entirely eliminates the effect of irregularities in the electrical properties of the specimen provided these are reversible and the furnace temperature remains steady during the taking of the cooling record.

Experimental Arrangements.

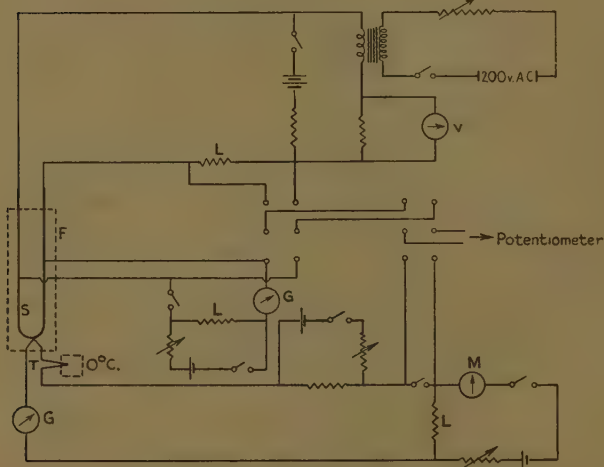
The mounting of the specimen, complete with thermocouple and potential leads, in the furnace has already been sufficiently described. It remains to deal with the measurement of temperature and resistance of the specimen, and the detailed process of recording the resistance change (see circuit diagram, fig. 3).

Lapp used direct current from accumulators to pass through the specimen, and was compelled to provide compensation for the small potential drop introduced across the thermojunction. Alternating current was used in the present measurements to avoid this effect, and could be obtained sufficiently steady for the length of time required from a converter fed from large capacity accumulators.

Steady temperatures were measured on the wire potentiometer, as in the thermoelectric measurements. The same instrument served to measure the e.m.f. between the potential leads on the specimen and those from a fixed resistance, through both of which the same steady current was passed; the ratio of these (r) gives the resistance of the specimen in arbitrary units.

When the change in resistance of the specimen was to be recorded the initial e.m.f., corresponding to the steady temperature and resistance of the specimen, were

Fig. 3.



Circuit for measurement of specific heat.

L, fixed low resistances (shielded); G, low resistance galvanometer; S, specimen; T, thermocouple; M, milliammeter; V, A.C. voltmeter; F, furnace.

balanced out by steady opposing e.m.f. These were provided by the potential drops across low resistances of manganin due to adjustable currents from accumulators, and balance was indicated by sensitive low-resistance galvanometers in each circuit; that in the resistance-measuring circuit served for photographic recording of the resistance change, requiring constant sensitivity and zero only during the taking of each separate record.

The e.m.f. produced by small temperature changes were balanced by using a separate low resistance, passing through it a current sufficient to give a "null" galvanometer reading, and measuring the currents on the Weston milliammeter as in the thermoelectric measurements. Thus " e " could be expressed in terms of the readings of the milliammeter scale. Hence the process of calibration by slow heating of the furnace consisted in setting the milliammeter pointer on each main division in turn, each time exposing the bromide paper as the spot of light passed through its mean position.

The bromide strips were processed in the usual manner, using high contrast developer, and no special precautions taken in drying, since no lengths were actually measured on the strip, only the position of each calibration line with respect to its nearest neighbours on the cooling record, which could be estimated by inspection. $\log e$ was then plotted against t , and the slope of the curve, usually linear over the main part, used to calculate s .

Experimental Results.

It was found that linear $\log e$, t curves were obtained when the furnace temperature was sufficiently steady and at temperatures where the specific heat was not exceptionally variable with temperature. This was only true, of course, for excess temperatures low enough for Newton's Law to hold sufficiently well.

Since measurements on all the specimens were made on the same instruments and in terms of the same resistances, it was merely necessary to find the mass of the part of each specimen between its potential leads in order to have the specific heat for all specimens in the same arbitrary units. Using Lapp's value for the specific heat of nickel at 150° C., the results have been converted to atomic units. The results are given in Table II. and shown graphically in fig. 4.

For nickel the number of determinations made was insufficient, and, being the first measurements with this method, are liable to inaccuracies resulting from insufficiently practised technique. Unfortunately this inaccuracy directly affects the absolute values for the alloys A_1 and A_2 . It may also account for the differences between the Curie points as given by the specific heat

(340° C.) and thermoelectric power measurements (350° C.) in the case of nickel only.

DISCUSSION.

Thermoelectric Properties.

The general slopes of the thermoelectric power curves are confirmed by the curves given by Chevenard ⁽⁷⁾,

TABLE II.

Specific Heats, in Approximate Atomic Units.

Temp. °C.	s_{Ni} .	Temp. °C.	s_{A1} .	Temp. °C.	s_{A2} .
397.0	8.22	341.0	7.03	354.0	6.34
357.0	8.07	326.0	7.19	309.0	5.99
347.0	8.10	312.5	7.12	278.0	5.86
342.0	8.99	302.0	7.29	265.0	5.75
342.0	9.26	298.0	8.06	258.5	5.80
338.0	9.96	293.5	8.18	248.5	6.00
331.0	10.13	290.5	8.38	246.0	6.10
329.0	9.96	283.0	8.11	244.0	6.12
307.5	8.65	276.5	7.81	241.0	6.00
269.0	7.70	235.0	6.98	229.0	5.90
144.0	6.88	213.0	6.78	208.0	5.72
—	—	195.0	6.50	183.0	5.65
—	—	107.0	6.15	127.0	5.40

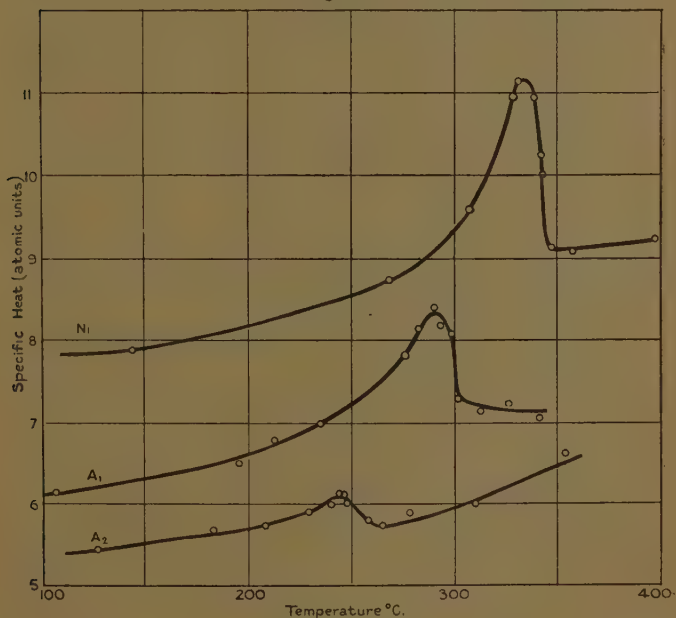
who made measurements on alloys of nickel with chromium, manganese, aluminium, and copper. His results for the cupronickels agree with the accurate determinations made more recently by Grew ⁽⁴⁾ by a sensitive differential method, using very pure materials. From these results it may be concluded that small percentages of copper and aluminium in nickel produce little change in the Thomson coefficient change ($\Delta\sigma_e$, referred to the gram electron), whereas chromium, and to a lesser extent manganese, have the effect of reducing quite rapidly the "ferromagnetic" part of the thermoelectric power and Thomson coefficient. Although the shapes of the curves prohibit

accurate deductions, the figures in Table III. indicate the approximate values of $\Delta\sigma_s$ for nickel and the two alloys; that for (say) 10 per cent. Cu 90 per cent. Ni may be taken as inappreciably different from the value for pure nickel.

Specific Heat.

The absolute accuracy of the specific heat determinations are liable to considerable error, and no definite

Fig. 4.



Specific heats of nickel and nickel chromium alloys.
(Nickel curve raised one unit.)

conclusions can be based upon the values given here. Also the curve for nickel, compared with that given by Lapp, shows a positive difference as the temperature rises, which may easily be variably reproduced in the alloy curves, and points to a systematic error which is a function of the temperature.

Lapp separated the true specific heat of nickel into the following terms :—

(1) Quantum term c_q ; calculable on the Debye theory from the characteristic temperature, which is deduced from the specific heat at low temperatures.

(2) Dilation factor, which corrects the specific heat at constant pressure to that at constant volume.

(3) "Terme croissant," common to all metals, and particularly evident at high temperatures; assumed to be the same for nickel as for copper.

(4) The ferromagnetic term, calculable from the intrinsic magnetization of the material; zero above the Curie point.

(5) The "unknown" term, peculiar to ferromagnetics, which rises to a value $\frac{1}{2}R$ at and above the Curie point.

TABLE III.

Approximate Values of $\Delta\sigma$ and ΔS_A for Nickel and the Alloys A_1 (1 per cent. Cr) and A_2 (2 per cent. Cr).
Units of σ_e , cal. per gram electron.
Units of S_A , cal. per gram atom.
 θ is the Curie point given by the thermoelectric measurements.

	$\Delta\sigma_e$.	ΔS_A .	θ .
Nickel	2.1	2.0	353° C.
Alloy A_1	0.7	1.1	310° C.
Alloy A_2	0.2	0.6	254° C.

Some measurements by Searle's method showed that the mechanical properties of the alloy-wire specimens were not sufficiently different from those of nickel to give material differences in their quantum and dilation terms. Unfortunately the lack of magnetic data above room-temperature prevents calculation of the ferromagnetic term for the alloys in the Curie point region. Approximate values for the drop in the specific heat (ΔS_A refer to the gram atom) at the Curie point are given, along with those for $\Delta\sigma_e$, in Table III.

The uncertainty in the absolute values of the specific heat determinations prevents definite deductions as regards the values of the "unknown" and "growing" terms, but decreases in these for the alloys may help to account for the smallness of the relative values of s for A_1 and A_2 compared with nickel.

The most striking result which emerges from these measurements is that the addition of small amounts of chromium to nickel produces a relatively enormous decrease in the Curie point changes in the Thomson coefficient and in the specific heat. The addition of copper produces decreases which are at least roughly proportional to the change in the low temperature saturation moment. With chromium, however, whereas the decrease in saturation magnetization due to the addition of 1 per cent. to nickel is about 7 per cent., the decrease in $\Delta\sigma_e$ and $\Delta\sigma_A$ is of the order of 50 per cent. (see Table III.). No satisfactory interpretation of these peculiar results can be offered at present, and a fuller discussion would be of little value in the absence of more complete data on the magnetic properties of the alloys near the Curie point. The results serve to illustrate the complexity in detail of the properties of ferromagnetics at the higher temperatures. Apart from the peculiarities in those specific heat and thermoelectric properties which are undoubtedly associated with the intrinsic magnetization, the large positive change produced in the thermoelectric power at room-temperature by the addition of 1 per cent. of chromium is of interest; it may be contrasted with the much smaller negative change produced by copper. Effects such as this, no less than the special "ferromagnetic" effects, call for further theoretical and experimental investigation.

SUMMARY.

Accurate measurements of the thermoelectric power of nickel and two alloys of nickel with 1 and 2 per cent. of chromium have shown that these alloys show only 30 per cent. and 10 per cent. respectively of the change in the Thomson coefficient at the Curie point found in nickel.

A method for the measurement of the specific heats of metals in wire form has been developed and applied

to the present problem. In it the inaccuracy of using the irregularly varying resistance of the metal wire to measure its temperature has been overcome. The two alloys show respectively 55 per cent. and 30 per cent. of the drop in the specific heat at the Curie point measured in nickel.

In conclusion, the writer desires to express his sincere thanks to Professor R. Whiddington and Dr. E. C. Stoner for their help during the progress of this work; also to the University of Leeds and the Durham County Council for maintenance grants.

References.

- (1) E. C. Stoner, *Phil. Mag.* ci. p. 1018 (1933).
- (2) E. Lapp, *Ann. de Physique*, xii. p. 442 (1929).
- (3) J. Dorfman, R. Jaanus, I. Kikoin, *Zeits. f. Phys.* liv. pp. 277 and 289 (1929).
- (4) K. E. Grew, *Phys. Rev.* xli. p. 356 (1932).
- (5) C. Sadron, *Ann. de Physique*, xvii. p. 371 (1932).
- (6) J. Safranek, *Rev. de Metall.* xxi. p. 86 (1924).
- (7) P. Chevenard, *Chal. et Ind.* iv. p. 157 (1923).
- (8) P. Weiss and R. Forrer. See Lapp (2).
- (9) J. Galibourg, *Rev. de Metall.* xxii. pp. 400, 527, 610 (1925).
- (10) K. E. Grew, *Proc. Leeds Phil. Soc.* ii. p. 217 (1931).
- (11) A. Ferguson and J. T. Miller, *Proc. Lond. Phys. Soc.* xlv. (2) p. 194 (1933).

Physics Laboratories,
University of Leeds.

XLV. *On the Ratio of the Maximum to the Mean Velocity, and the Position of the Filament of Mean Velocity, in the Laminar Motion of an Incompressible Viscous Fluid through a Pipe of Rectangular Cross-section.* By J. ALLEN, M.Sc., Assoc.M.Inst.C.E.*

List of Symbols.

a = half width of rectangular pipe } as in fig. 3.
 b = half depth of rectangular pipe }

p = pressure.

Q = quantity flowing through pipe, per unit time.

w = velocity of a particle parallel to the axis of the pipe.

* Communicated by the Author.

x =coordinate of particle, taking the centre of the section as origin and measuring parallel to the width.

y =coordinate, measuring parallel to the depth.

z =distance parallel to the longitudinal axis of the pipe.

μ =coefficient of viscosity.

$$\tau = -\frac{1}{2\mu} \cdot \frac{dp}{dz}.$$

a_c =radius of a circular pipe.

r =radius to a particle inside a circular pipe.

I.

IN the steady flow of an incompressible, viscous fluid through a circular pipe, the velocity of a particle at a distance r from the centre is given by

$$w = -\frac{1}{4\mu} \cdot \frac{dp}{dz} \cdot (a_c^2 - r^2), \quad . \quad . \quad . \quad (1)$$

while the rate of discharge of fluid through the pipe is

$$Q = -\frac{\pi a_c^4}{8\mu} \cdot \frac{dp}{dz} \cdot . \quad . \quad . \quad . \quad (2)$$

The manipulation of these equations leads readily to the well-known results that

(a) the maximum velocity=twice the mean velocity ;

(b) the filament of mean velocity is found at a radius $0.707a_c$.

II.

The corresponding equations for laminar flow through a rectangular pipe * are, however, more complex, viz.,

$$w = -\frac{32\tau b^2}{\pi^3} \left\{ \frac{\cosh(\pi x/2b)}{\cosh(\pi a/2b)} \cdot \cos \frac{\pi y}{2b} - \frac{1}{3^3} \cdot \frac{\cosh(3\pi x/2b)}{\cosh(3\pi a/2b)} \right. \\ \left. \times \cos \frac{3\pi y}{2b} + \dots \right\} + \tau(b^2 - y^2); \quad (3)$$

* See Cornish, "Flow in a Pipe of Rectangular Cross-section," *Proc. Roy. Soc. A*, cxx. pp. 691-700 (1928).

$$Q = -\frac{4}{3} \cdot \frac{ab^3}{\mu} \cdot \frac{dp}{dz} \left\{ 1 - \frac{192}{\pi^5} \cdot \frac{b}{a} \left(\tanh \frac{\pi a}{2b} + \frac{1}{3^5} \right. \right. \\ \left. \left. \times \tanh \frac{3\pi a}{2b} + \dots \right) \right\}. \quad (4)$$

The maximum velocity, which occurs at the centre, is found from (3) by putting $x=0$, $y=0$:

$$w_{\max.} = -\frac{32\tau b^2}{\pi^3} \left\{ \frac{1}{\cosh(\pi a/2b)} - \frac{1}{3^3} \right. \\ \left. \times \cosh \frac{1}{(3\pi a/2b)} + \dots \right\} + \tau \cdot b^2. \quad (5)$$

Again, the mean velocity $= \frac{Q}{4ab}$, or, from equation (4),

$$w_{\text{mean}} = -\frac{1}{3} \frac{b^2}{\mu} \frac{dp}{dz} \left\{ 1 - \frac{192}{\pi^5} \cdot \frac{b}{a} \left(\tanh \frac{\pi a}{2b} \right. \right. \\ \left. \left. + \frac{1}{3^5} \tanh \frac{3\pi a}{2b} + \dots \right) \right\}. \quad (6)$$

Dividing (5) by (6) gives the ratio :

$$\frac{w_{\max.}}{w_{\text{mean}}} = -3 \frac{\left\{ \frac{16}{\pi^3} \left\{ \frac{1}{\cosh(\pi a/2b)} - \frac{1}{3^3} \frac{1}{\cosh(3\pi a/2b)} + \dots \right\} - \frac{1}{2} \right\}}{\left[1 - \frac{192}{\pi^5} \frac{b}{a} \left(\tanh \frac{\pi a}{2b} + \frac{1}{3^5} \cdot \tanh \frac{3\pi a}{2b} + \dots \right) \right]} \quad (7)$$

$$\left(\text{since } \tau = -\frac{1}{2\mu} \cdot \frac{dp}{dz} \right).$$

III.

If a is very great compared with b and may be regarded as tending to infinity, then

$$\frac{w_{\max.}}{w_{\text{mean}}} \rightarrow -3 \frac{\left[\frac{16}{\pi^3} (0) - \frac{1}{2} \right]}{\left[1 - \frac{192}{\pi^5} (0) \left(1 + \frac{1}{3^5} + \dots \right) \right]}, \rightarrow \frac{3}{2}. \quad (8)$$

The velocity at any point in the cross-section is then given simply by

$$w = -\frac{1}{2\mu} \cdot \frac{dp}{dz} \cdot (b^2 - y^2), \quad (9)$$

as in the standard formula for steady flow between two infinite parallel plates distant $2b$ apart.

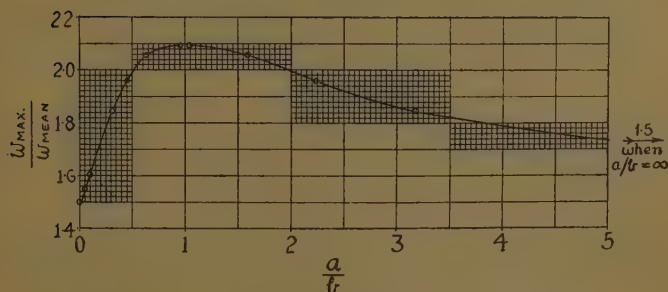
In that case the filament of mean velocity may readily be found to occur at a distance $\sqrt{\frac{1}{3}} \cdot b$, or $0.577b$ from the axis.

Similar conclusions must clearly apply when a is finite but b tends to infinity, although the solutions of equations (3) and (4) become indeterminate when $b = \infty$.

IV.

A general inspection of equation (7) shows that the ratio $\frac{w_{\max.}}{w_{\text{mean}}}$ depends essentially upon the relative magni-

Fig. 1.



tudes of a and b . Moreover, from the physical nature of the problem the value of $\frac{w_{\max.}}{w_{\text{mean}}}$ must be the same, for $\frac{a}{b} = \text{any value}, \alpha$, greater than unity, as for $\frac{a}{b} = \frac{1}{\alpha}$.

A maximum or minimum value of $\frac{w_{\max.}}{w_{\text{mean}}}$ must, in fact, occur when $a = b$, i. e., when the section of the pipe is square.

In order to draw the accompanying diagram (fig. 1), representing the general solution of equation (7), the

magnitude of $\frac{w_{\max.}}{w_{\text{mean}}}$ has been calculated for values of the ratio $a : b$ stated in the following table :—

$\pi a/2b.$	Ratio $a : b.$	Ratio $w_{\max.} : w_{\text{mean.}}$
1.5	0.9548 (or 1.047)	2.093
2.5	1.592 (or 0.6284)	2.058
3.5	2.228 (or 0.4488)	1.960
5.0	3.183 (or 0.3142)	1.844
	10.0 (or 0.100)	1.601
	20.0 (or 0.0500)	1.549
	Unity	2.10
	Infinity (or zero)	1.5

V.

The equation of the contour of those points in a cross-section at which the filament of mean velocity may be found is

$$\begin{aligned}
 & \frac{32b^2}{\pi^3} \left(\frac{\cosh(\pi x/2b)}{\cosh(\pi a/2b)} - \cos \frac{\pi y}{2b} - \frac{1}{3^3} \cdot \frac{\cosh(3\pi x/2b)}{\cosh(3\pi a/2b)} \cos \frac{3\pi y}{2b} + \dots \right) \\
 & - (b^2 - y^2) = - \frac{2}{3} b^2 \left\{ 1 - \frac{192}{\pi^5} \cdot \frac{b}{a} \left(\tanh \frac{\pi a}{2b} \right. \right. \\
 & \left. \left. + \frac{1}{3^5} \tanh \frac{3\pi a}{2b} + \dots \right) \right\} \dots \dots \dots (10)
 \end{aligned}$$

The position of the filament of mean velocity on the x -axis of the cross-section is, therefore, given by

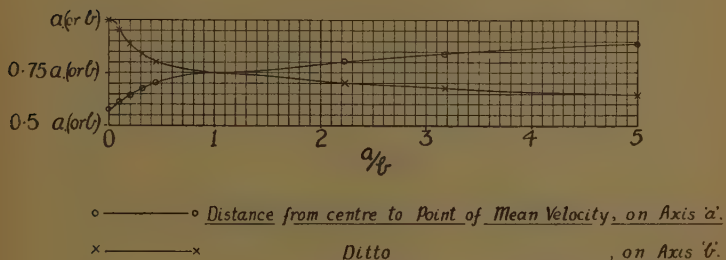
$$\begin{aligned}
 & \frac{32b^2}{\pi^3} \left(\frac{\cosh(\pi x/2b)}{\cosh(\pi a/2b)} - \frac{1}{3^3} \frac{\cosh(3\pi x/2b)}{\cosh(3\pi a/2b)} + \dots \right) - b^2 \\
 & = - \frac{2}{3} b^2 \left\{ 1 - \frac{192}{\pi^5} \cdot \frac{b}{a} \left(\tanh \frac{\pi a}{2b} + \frac{1}{3^5} \tanh \frac{3\pi a}{2b} + \dots \right) \right\} \dots \dots \dots (11)
 \end{aligned}$$

The position of the filament of mean velocity on the y -axis of the cross-section is given by

$$\frac{32b^2}{\pi^3} \left(\frac{1}{\cosh(\pi a/2b)} \cdot \cos \frac{\pi y}{2b} - \frac{1}{3^3} \frac{1}{\cosh(3\pi a/2b)} \cdot \cos \frac{3\pi y}{2b} + \dots \right) - (b^2 - y^2) = -\frac{2}{3} b^2 \left\{ 1 - \frac{192}{\pi^5} \cdot \frac{b}{a} \left(\tanh \frac{\pi a}{2b} + \frac{1}{3^5} \tanh \frac{3\pi a}{2b} + \dots \right) \right\}. \quad (12)$$

The values of x and y necessary to satisfy equations (11) and (12) respectively have been determined by successive trials for $a=b$, $\frac{\pi a}{2b} = 3.5$, $\frac{\pi a}{2b} = 5$, $\frac{a}{b} = 5$, and $\frac{a}{b} = 10$,

Fig. 2.



while the case of “ a ” infinite and “ b ” finite has already been dealt with in paragraph III.

From these calculations have been plotted the curves of fig. 2 representing the general solution of equations (11) and (12) for any value of the ratio $a : b$, thus enabling the points of mean velocity along the axes of a cross-section to be at once calculated.

VI.

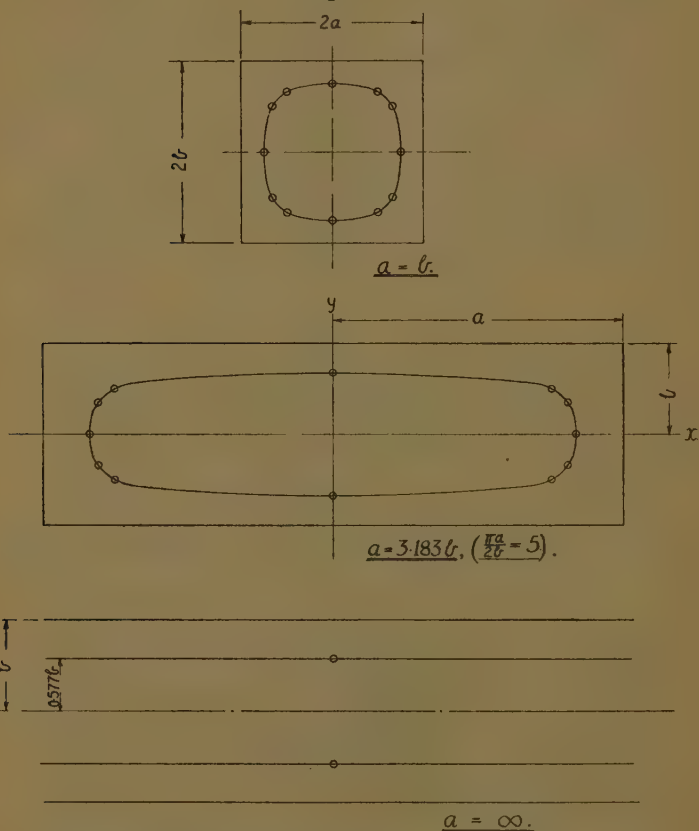
It is also of interest to plot the contours of points of mean velocity in a cross-section, and this has been done

in fig. 3, for a square section ($a=b$), for $a=3.183b$ ($\frac{\pi a}{2b} = 5$),

and for a pipe in which one side is very long compared with the other (“ a ” infinite, “ b ” finite), the method of

plotting consisting of calculating a number of points on the curves with the aid of equation (10).

Fig. 3.



Cross-sections of rectangular pipe, showing contours of mean velocity (laminar flow).

VII. Broad, Open Channel.

There is evidence * to show that in streamline flow in an open channel the filament of maximum velocity

* See Allen, "Streamline and Turbulent Flow in Open Channels," *Phil. Mag.* [7] xvii. p. 1081 (1934).

may not be found in the water surface, but at a distance of about 0.3 of the depth below the surface.

In such a case, if the channel is of infinite width and the curve of velocity distribution is assumed parabolic, it may easily be shown that the maximum velocity is only 1.34 times the mean velocity, and occurs at 0.65 depth below the surface.

VIII. *Summary.*

In laminar flow through a pipe of rectangular cross-section the ratio of maximum to mean velocity depends on the ratio of the lengths of the sides. Thus, for a square section the maximum velocity is 2.10 times the mean velocity; when one side is very long compared with the other the ratio tends to the value 1.5, as in steady flow between infinite parallel plates.

Similarly, the position of filaments of mean velocity is shown to vary with the ratio $a : b$; for a square section it may be found at points on the axes distant very nearly 0.375 of the length of the sides, from the centre. In a pipe having one side whose length may be regarded as infinite, the mean velocity occurs at points distant 0.289 of the total depth, measured from the transverse axis.

In streamline flow along an infinitely wide open channel, the maximum velocity may be less than 1.5 times the mean—there is evidence to support a value of 1.34, the filament of mean velocity being then situated at 0.65 of the depth below the surface.

XLVI. *Latent Energy due to Lattice Distortion of Cold-worked Copper.* By W. A. WOOD, M.Sc., *Physics Department, National Physical Laboratory, Teddington, Middlesex* *.

[Plate VIII.]

Introduction.

LATTICE distortion is produced during the plastic deformation of most metals and alloys. This paper is concerned with a comparison of the lattice

* Communicated by Dr. G. W. C. Kaye, O.B.E., M.A.

dimensions before and after cold working; it shows, for example, that in the case of copper an expansion takes place.

The presence of lattice distortion leads to a diffusion of the lines in the monochromatic X-ray spectrum of the metal. The position of a line in this type of spectrum depends only upon the spacing of the atomic planes in the lattice. Therefore the line broadening may be regarded as the result of deviations of the spacings from the normal values. The deviations may be such that the average value of the spacings is maintained unchanged, or such that the spacings vary more in one direction, increase or decrease, than in the other. In the first case the spectrum line from a typical set of spacings will broaden about its original position in a symmetrical way; in the second the line will shift in a way conforming with the major change in spacing. This is the point investigated.

A directional variation in lattice dimensions introduces the conception of a latent energy due to lattice distortion, for the distorted lattice is equivalent to one in which slight local expansions have occurred—that is, it will resemble one in which small increases in temperature have taken place from point to point. Therefore the distortion will confer an extra latent energy which the lattice with normal spacings does not possess.

The X-ray measurements indicate the degree by which the distorted spacings deviate from the normal, and therefore the magnitude of the temperature increments; the latter follow from the standard formula connecting the linear expansion of the metal with temperature. The latent energy of the lattice due to the distortion can then be calculated from a knowledge of these temperature changes and the specific heat of the material. A practical aspect of the results arises from the fact that the changes in physical properties produced by cold work appear to be associated with the lattice-distortion state of the metal.

Experimental Procedure.

The specimens used were copper in the form of strip. Before being worked they were given a preliminary heating *in vacuo* until they were free from distortion. The cold working was performed by rolling. This process

preserves a flat surface, preferable for accurate X-ray measurements, and also brings the metal quickly into the state of maximum distortion. In previous papers ^(1, 2) it has been shown that the distortion begins almost at once on rolling, and, after some 20 to 30 per cent. reduction, rises to a maximum, termed the lattice distortion limit. Specimens representing various stages in the distortion were prepared. A photograph of each was then taken in the X-ray camera described below and compared with a similar photograph of the undistorted material. The copper $K\alpha$ radiation was used; this wave-length brings the (420) line of copper into a position showing sufficiently high resolution for the purpose of the comparison.

X-ray Camera.

The X-ray camera was designed to ensure that experimental conditions for the different specimens were constant. The arrangement adopted is shown to scale in fig. 1. It consists essentially of three brass blocks—slit system, specimen-holder, and plate-holder—screwed down to a flat metal plate. The slit is formed by six parallel slots, 1 mm. deep, which are milled along the side of the block at intervals of 0.5 mm. The slots are parallel to the base-plate, and the middle one is at a height of 1 inch above it; they are closed at the side by a flat sheet of lead fastened to the block. X-rays diverging from the source are thus limited by the slots to a series of fine pencils before meeting the specimen.

The specimen-holder allows the face of a specimen to be pressed flush against a metal plate forming the front of the holder; the surface of each specimen can therefore be brought into a standard position. The front plate contains an aperture large enough for the incident beam to hit the specimen and for the reflected rays to emerge unobstructed. The holder could be screwed to the base-plate in one of four positions; these positions are reached by rotating the holder about a pin in the base-board; they incline the surface of the specimen at angles of 22.5° , 45° , 67.5° , and 90° respectively to the incident beam. The axis of rotation forms a vertical line which coincides with the face of the specimen and through which passes the direct X-ray beam.

The spectra are recorded on a photograph plate placed in a holder in the position indicated in the diagram

by P. The plate is pressed by springs against a flat rectangular frame of brass which constitutes the front of the holder. Sharp shadows are cast by the inner edges of the frame on to the plate during an exposure; they provide convenient calibration marks. Further reference points are given by grooves and small tapered holes in the framework. The normal from the centre of the

Fig. 1.

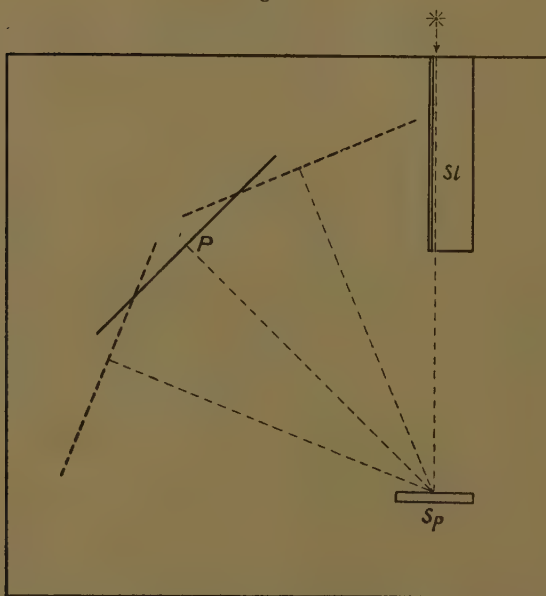


Fig. 1: showing relative position of Slit System Sl, Specimen Sp, and three possible settings of Photographic Plate P.

plate passes through the axis of the specimen-holder. This applies to each of the three positions, indicated in the diagram by the dotted lines, representing the normal to the plate, in which the holder can be fixed. The normal to the plate in these positions makes angles respectively of 112.5° , 135° , and 157.5° to the direction of the incident beam. Provision is therefore made by

these movements of plate- and specimen-holder for the recording of spectrum lines formed by deviation through angles of 90° to 180° , and, by the choice of suitable positions, for obtaining any given line in sharp focus. The spectrum beyond 90° is the part investigated because only in this portion does the resolution of the lines reach the highest degree.

The base was a square plate of brass, $\frac{1}{4}$ -in. thick; it could be kept at a constant temperature by water-cooling, which served also to control the temperature of the contiguous blocks forming slit, specimen-, and plate-holder systems. Temperature control was required because the accuracy by which the lattice spacings could be compared was of the same order as the changes which would arise as a result of a few degrees variation in the temperature of the whole specimen.

Measurement of Negatives.

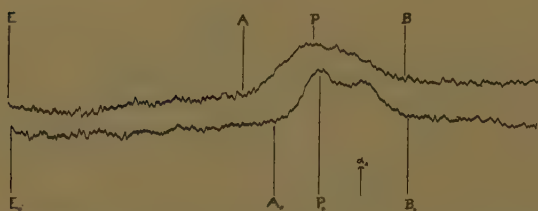
Measurements were made not only on the relative position of a spectrum line but also upon the intensity distribution or shape of the line. To illustrate the method typical photographs of a specimen before and after working are reproduced in figs. 2 *a* and 2 *b* (Pl. VIII.); they show the (420) doublets of copper and also the calibration edge E formed by the sharp shadow of the inner edge of the plate-holder frame. Now a change in the spacings of the (420) planes would result in a change of the distance of the corresponding line from the edge E. This was one distance measured. The second distance determined was that between the calibration edge E and the nearer boundary of the line. The third was the distance to the further boundary from E.

These three measurements involved the investigation of the shape of the line; for this a Moll microphotometer was utilized. The instrument possesses an accurate screw which carries the negative stage along a direction normal to the photometering light beam, and, at the same time, by appropriate gear mechanism, rotates a recording drum through a corresponding angle. Variations in the opacity of the negative are recorded on bromide paper wrapped round the drum by the trace of a spot of light reflected from a galvanometer in circuit with the thermopile of the photometer. Owing to the gear ratios between

screw and drum ($7\times$ or $50\times$), distances on the negative can be measured with accuracy on the microphotometer record. The determination is facilitated in the case of a spectrum doublet by the possibility of picking out the α peak, even when the doublet is diffused through lattice distortion, from the record.

To obviate sources of inaccuracy arising from the mounting of the bromide paper or from the effects of shrinkage produced by the development processes the same record was used for the comparison of different negatives. Thus, the spectrum from a cold-worked specimen was photometered from the calibration edge to the (420) line; then, without disturbing the bromide paper on the drum, this negative was replaced by a corresponding one from a normal undistorted specimen and photometered over the same range as before. The bromide paper

Fig. 3.



gave, therefore, two traces, one from the distorted and one from a standard specimen. The intensity of the light beam in the photometer was adjusted so that one trace lay just below the other. Each distorted specimen was recorded in the same way along with a concomitant trace from a normal specimen with which comparison could be directly made. A typical result is reproduced in fig. 3. The trace of the galvanometer reflexion begins at the right; as it moves towards the left it shows first the α_2 and then the stronger α_1 component of the (420) line; still moving to the left it records the distance between the line and the calibration edge. At the edge itself the spot of light passes sharply off the scale, owing to the sudden decrease in density of the plate as the shadow of the plate-holder frame is entered. The abrupt termination of the trace at this point provides the origin from which the comparison measurements are made.

After fixing the calibration edge the boundaries and peak of the line were found. The boundary on the side of the calibration edge is denoted in fig. 3 by A. It could be fixed on the record to the nearest 0.5 mm.; the limiting factor is the irregularity of the base-line due to negative granularity which had to be allowed for by averaging the results from repetition photographs. The same method was used for placing of B, the boundary of the line away from the edge E. The point P, on the other hand, which represents the position of maximum intensity of the α_1 component of the doublet, could be fixed in the case of a diffuse line to 0.1 mm. The α_2 peak was ignored, because its position is complicated by the presence of the stronger α_1 . The point A is concerned only with the inner boundary of the α_1 component, and the point B with the outer limit of the α_2 part of the line. It can be shown that the position of A is not affected by the presence of the α_2 satellite; similarly B is uninfluenced by the spread of the α_1 component. Both α_1 and α_2 lines are broadened in the same way by any distortion of the (420) planes, since the $K\alpha_1$ and $K\alpha_2$ wave-lengths in the incident X-ray beam are so nearly alike. It is therefore convenient, when considering broadening of the line in the direction of E, to measure up to the point A, and when considering diffusion in the other direction to take the point B. A movement towards E corresponds to an increase in lattice spacings, and a movement away to a decrease.

If E, A, P, B refer to the distorted specimen, and E_0 , A_0 , P_0 , B_0 to the normal specimen on the microphotometer record, the measurements made may be written :

$$\begin{aligned} EA - E_0A_0 &\text{ or } \Delta EA, \\ EP - E_0P_0 &\text{ or } \Delta EP, \\ \text{and} \quad EB - E_0B_0 &\text{ or } \Delta EB. \end{aligned}$$

Results.

(1) The line from the distorted lattice does not broaden symmetrically about the original position of the sharp line from the normal specimen; it tends to shift towards the side corresponding to an increase in spacing. Therefore the lattice spacings of the cold-worked metal deviate in the direction of expansion.

Fig. 3 is the case of a specimen reduced in thickness by 90 per cent., the lower trace in the figure being from the standard normalized material. A comparison of these two traces illustrate this first observation.

(2) The shift is of the following nature:—Taking the symbols defined above, we find that ΔEA is large, ΔEP is small but definite, whilst ΔEB is zero. Therefore the line broadens only by extending itself in the direction of the calibration edge—that is, the spacings of the distorted lattice exhibit only increases.

The magnitude of the shifts in the case of the specimen reproduced in fig. 3 are as follows:—

$$\Delta EA = 9 \text{ mm.}, \Delta EP = 1.5 \text{ mm.}, \Delta EB = 0.$$

Measurements made on other specimens are given in the accompanying table. It is seen that the effect increases to a steady value as the specimen is reduced by rolling.

Reduction (per cent.).	ΔEA .	ΔEP .	ΔEB .
	mm.	mm.	mm.
0	—	—	—
4.9	3	0.5	0
9.8	6.0	1.0	0
13.1	8.0	1.3	0
14.8	7.5	1.6	0
15.2	9.0	1.4	0
18.0	8.5	2.0	0
50	9.0	1.8	0

(3) An estimate can be made of the fractional changes in spacing to which these movements correspond, and also of the equivalent increases in latent energy of the lattice. From the Bragg relation, $2d \sin \theta = \lambda$, where λ is the wave-length used, d the normal spacing, and θ the diffraction angle, we have

$$\frac{\delta d}{d} = -\cot \theta \delta \theta.$$

The change $\delta \theta$ produces a shift on the negative and one, δx say, on the microphotometer record. For the

(420) line, taking 11.5 cm. as the radius of the camera and a gear ratio of the microphotometer of seven times, we find for the conditions of the present experiments

$$\frac{\delta d}{d} = 1.86 \times 10^{-4} \times \delta x,$$

where δx is in mm.

In the steady state of distortion, as represented by fig. 3, we substitute the values for the increments in EA and EP, and obtain

$$\frac{\delta d}{d} = 16.7 \times 10^{-4} \text{ for the point A,}$$

and
$$\frac{\delta d}{d} = 2.8 \times 10^{-4} \text{ for the point P.}$$

The temperature changes which these expansions represent are then obtained, taking for the linear coefficient of expansion of copper the value of 16.7×10^{-6} , with the result

$$\delta t = 100^\circ \text{ for A,}$$

and
$$\delta t = 16.8^\circ \text{ for P.}$$

The latter is the more important figure, as indicated below, because it refers to the main bulk of the material. The figure of 100° applies only to the small proportion represented by the low intensity at the boundary of the spectrum line. The distortion occurring in the main mass corresponds therefore to an equivalent temperature rise of about 17°C .

An accurate estimation of the latent energy involves a complete knowledge, on the view taken above, of the way in which the equivalent temperature increments are distributed throughout, say, unit mass of the metal—that is, it is necessary to know what proportion of the material has undergone a given deviation of lattice spacing. A guide to this problem is given by the shape of the spectrum line; for it may be regarded as the resultant curve formed by superposing the displaced spectrum lines from the several spacings in the specimen. It is hoped by future improvements in technique to obtain a closer analysis of this curve; at the moment it is possible, at any rate, to get an indication of the distribution of

distortion. Thus, a comparison of the peak intensities of the (420) line from the distorted and normal specimen, measured from the microphotometer records, gives a density ratio of 1.5:1.6. The proportion of matter in the distorted metal which contributes to the peak reflexion will therefore be of the order of 15/16ths of the normal. The remaining 1/16th will have spacings ranging between the minimum and maximum deviations observed. Consequently of 1 gramme of material approximately 15.16ths undergoes an equivalent temperature rise of 17° C., and 1/16th exhibits temperature increments distributed in some way from 0° to 100°. The former proportion absorbs a heat energy of 1.4 calories, taking a value for the specific heat of 0.09 calories per gram; the latter, assuming for a first approximation a linear distribution, represents an energy of 0.3 calories. The increase of latent energy due to the production of maximum lattice distortion in copper is therefore of the order of 1.7 calories per gram.

The following issues are raised: first, a technical point, the X-ray line broadening may be due to lattice distortion, as the above work assumes, or to the low resolving power consequent upon a grain size less than about 10^{-4} cm. The question of which factor is relevant to a cold-worked metal is to be considered. The present work confirms the assumption of lattice distortion; it provides also a future criterion for differentiating the two factors, for the line broadening due to fine grain should be of the symmetrical type. That actually observed, characteristic of cold-worked metal, is distinctly asymmetrical.

Second: it has been shown by Rosenhain and Stott, and by Taylor and Quinney⁽³⁾, that heat is absorbed in the mechanical process of cold working. A direct measurement of the proportion absorbed in the case of copper under torsion was made by the latter workers. It is suggestive that their result is of the same order as the latent energy attributed to lattice distortion.

Summary.

The lattice dimensions of cold-worked and normal copper are compared with the aid of a precision X-ray camera. It is shown that the process of working produces an irregular expansion of the lattice. The expansion

is interpreted in terms of the equivalent heat energy required to produce a similar state. The conception of a latent energy due to lattice distortion is advanced; its magnitude for the case of copper is deduced from measurements on the broadening and shift of the X-ray spectral lines.

In conclusion, the author expresses his thanks to Dr. G. W. C. Kaye for his interest and for the provision of facilities for the researches of which the above is part; also to Mr. J. A. G. Smith for technical assistance in much of the work.

References.

- (1) W. A. Wood, *Proc. Phys. Soc.* xliv. (1) p. 67 (1932).
- (2) W. A. Wood, *Phil. Mag.* xiv. p. 656 (1932).
- (3) G. I. Taylor and H. Quinney, *Proc. Roy. Soc. A*, cxliii. p. 307 (1934).
May 1934.

XLVII. *On the Comparison of Liquid Viscosity Data.* By MARY D. WALLER, B.Sc., F.Inst.P., Lecturer in Physics, London (R. F. H.) School of Medicine for Women*.

SUMMARY.

It has been found that if the melting-points and boiling-points of liquids are treated as corresponding temperatures respectively, a comprehensive view of viscosity in the liquid state is obtained which has yielded certain interesting results.

1. *Intrinsic Viscosity.*—A liquid is intrinsically more viscous than another when its viscosity, both at the melting- and the boiling-point, is greater. For example, mercury is intrinsically more viscous than water. If the critical temperatures be taken as a third corresponding temperature, data exist for showing that the intrinsic viscosities of three halogens both in the liquid and in the gaseous state are in the order iodine, bromine, chlorine.

2. *Characteristic Viscosity Ratio.*—The range of variation of viscosity in the liquid state may be expressed by taking the ratio of the melting- to that of the boiling-point viscosity. The ratios obtained are characteristically low (1.6–3 approx.) for metals, halogens, and benzene, and much higher (>9) for paraffins and certain other liquids

* Communicated by A. C. Egerton.

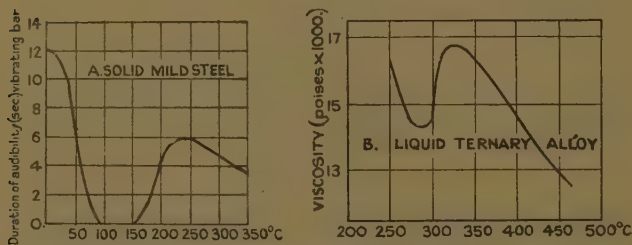
investigated, and this regardless of the liquid temperature range.

The results suggest a method of estimating the symmetry of the molecule in the liquid state, which is described in a subsequent paper.

§1. Introduction.

THE author has lately been engaged in a study of the variation with temperature of the internal damping in solid metals and alloys ⁽¹⁾. This has led on to a more general consideration of the viscosity of matter, more especially in the liquid state, the results of which are described below.

Fig. 1.



Temperature variation in internal friction of solid and liquid metallic alloys indicating transformation points. The data for figure B were obtained from Losana's fluidity numbers.

Whereas the viscosity of gases increases, that of solids * and liquids decreases with increasing temperature unless they are passing through some transformation point.

Examples of solid and liquid transformation points respectively are shown in fig. 1 (A) and (B). The general similarity of the curves is of interest, though the scales of course are different. Fig. 1 (A) shows the variations with temperature in the internal damping of a solid mild steel

* The "viscosity" of solids is sometimes spoken of as increasing with increasing temperature, meaning thereby that the internal damping, as measured by the logarithmic decrement of the flexural or torsional vibrations of wires and bars, increases with rising temperature. The distinction between this conception of viscosity and the usual one is at once made apparent by considering a case such as glass, the viscosity of which increases continuously as it is cooled from the molten to the solid condition. The internal friction in solids is complicated and depends on many factors.

bar as measured by the duration of audibility in seconds of the note (2800~approximately) given out when it is suspended from the nodes and struck with a hammer ⁽¹⁾; while fig. 1 (B) shows the viscosity-temperature curve for the alloy, 92 per cent. tin, 3 per cent. copper, 5 per cent. antimony. The viscosity values for the latter curve have been derived from Losana's ⁽²⁾ fluidity data. Curves of this type have also been obtained by Iokibe and Kikuta by measuring the torsional vibrations of fine metal wires (see International Critical Tables). The surface effects for these, however, are very large, as can be seen by comparing the entirely different curves given for wires of one material but of $\frac{1}{2}$ and 1 mm. diameter respectively. The most familiar curve showing the enormous viscosity alterations which may occur at transformation points is probably that of sulphur, which, although an element, has a complicated molecule. A very large maximum in the viscosity-temperature curve exists at about 190° C., due to allotropic modification.

Apart from such exceptional points, however, the viscosity of solids and liquids decreases regularly with increasing temperature, and the transition from the solid to the liquid, as also that from the liquid to the gaseous state, is of particular interest. Even in the solid state the atoms are not rigidly set in lattices, but their amplitude of vibration, due to thermal energy, gradually increases, as was shown practically by Sir William Bragg ⁽³⁾ in the early days of X-ray crystal analysis by means of the great reduction in the height of the diffraction peaks due to this thermal agitation. When the amplitude of vibration increases until, according to Lindemann, there is collision between neighbouring atoms the material melts. Even in the liquid state there may be enough "orderliness" to produce X-ray diffraction, as has been shown by Stewart and his collaborators ⁽⁴⁾. Stewart speaks of temporary unions between the molecules, which he terms the "cybotactic state," while Andrade ⁽⁵⁾ pictures the condition as a "temporary and fluctuating crystallization." Indeed, Andrade ⁽²²⁾ has lately developed a theory of viscosity at the melting-point for simple substances founded on the Lindemann theory of fusion and the assumption that the atomic oscillation frequencies do not change when the substance passes from the solid to the liquid state.

The large discontinuities in viscosity which occur at the melting- and boiling-points suggest that these points should be treated as corresponding temperatures, although it must be noted that some liquids pass gradually from the solid to the liquid state, and that some, consisting of complicated long chain molecules, assume a "liquid crystal" condition between that of the solid and the liquid condition.

§ 2. *Corresponding Temperatures.*

Reference may be made to Hatschek's 'The Viscosity of Liquids' (1928) and to Bingham's 'Fluidity and Plasticity' (1922) for an account of the work which has been done, more especially on organic liquids, in the measurement and comparison of liquid viscosities. It is interesting to note that Kammerlingh Onnes (see Bingham, p. 131, and Bibliography) derived a relation between the viscosities of all substances founded on the principle of corresponding states. The formula, however, does not apply at low temperatures, and probably only perfectly as the critical temperature is reached. Liquids belonging to the same homologous series often have equal viscosities at the boiling-points, so that these have naturally been regarded as corresponding temperatures. Most organic liquids for which data exist have low melting-points, while the viscosity data generally cease at the arbitrary temperature of 0° C. Accordingly little attention has been paid to the melting-point viscosities of organic liquids.

Melting-points have, however, been used as corresponding temperatures in connexion with other studies of the liquid state—see, for example, Clarke ⁽⁶⁾ and Walden ⁽⁷⁾; and the suggestion to use both melting-points and boiling-points as corresponding temperatures is not a new one, although it does not appear to have been applied before in the comparison of liquid viscosities.

§ 3. *Available Viscosity Data.*

In most cases either viscosities near the melting-points (metals) or those near the boiling-points (organic liquids) only are available. There are, however, some substances—notably mercury, bromine, iodine, and benzene—for which experimental measurements of viscosities have

been made throughout all or most of the liquid range. It may be mentioned that only one value of viscosity each has been measured for oxygen and hydrogen, and, unfortunately, no data for inert gases are available. The data used in this paper have in many cases been collected from the International Critical or the Landolt-Börnstein tables.

The viscosity values for mercury have been taken from Erk's paper ⁽⁸⁾ and those for tin from Slotte's ⁽⁹⁾ recent evaluations in terms of Sauerwald's values. Losana's data for tin, zinc, cadmium, and bismuth, which were originally given in terms of fluidity relative to tin, are of great value because of the large range of temperature over which they extend. There is no reason to doubt their sufficient accuracy for purposes of the present study; Slotte's and Losana's values for tin are both plotted in fig. 3, and are used for Table I.

Other data relative to metals to be found in tables either extend over too small a temperature range to be of use for present purposes or differ widely as given by different workers.

Steacie and Johnson's ⁽¹⁰⁾ data have been used for the halogens, including the actual boiling-point viscosities given by them.

It is evident that only in the case of very few liquids therefore has it been possible to obtain experimental values of both the melting-point and the boiling-point viscosities, and that the figures necessary for the present study had to be largely obtained by extrapolation. The familiar empirical Slotte-Thorpe and Rodger formula, constants for which are given in the tables for many of the liquids, has been found to be useless for purposes of extrapolation. It has, however, often been possible to obtain the desired data with reasonable accuracy and certainty by using the exponential relation which exists between liquid viscosity and temperature, reference to which is made below (§ 4).

§ 4. *Viscosity and Temperature.*

Guzman ⁽¹¹⁾, Raman ⁽¹²⁾, Dunn ⁽¹³⁾, Andrade ⁽⁵⁾, and Sheppard ⁽¹⁴⁾ have independently proposed the exponential formula

$$\eta = A \exp \frac{B}{T},$$

whence $\log \eta = \log A + \frac{B}{T}$,

relating viscosity to absolute temperature. A and B are constants for a particular substance. A formula of this type is frequently applicable in cases where the Maxwell-Boltzmann distribution law is valid; the different ways in which it has been derived by different investigators is of much interest. B is a work function ($=W/R$), where R =the gas constant. Guzman, in his original paper in 1913, first showed that $W=RB$ is often equal to the molecular latent heat of fusion. Dunn calls it the "latent heat of loosening," Lederer⁽¹⁵⁾ the "association-heat," Herzog and Kudar⁽¹⁶⁾ speak of "fluiditäts-wärme." Sheppard has pointed out that the relation is an approximate one, and Dunn states that the departure from linearity when $\log \eta$ is plotted against $1/T$ is concave to the T axis in the case of associated liquids. An example of a similar formula is the vapour pressure formula for simple liquids, and especially metals (Jäger⁽¹⁷⁾, Egerton⁽¹⁸⁾). It is interesting to notice that even the diffusion of various metals in lead have been shown by von Hevesy and Seith⁽¹⁹⁾ to obey a similar law with regard to temperature.

Iyer⁽²⁰⁾ has determined a large number of values of A and B , but although these were derived from published viscosity data, they have not been found reliable, as can be verified by substituting their values in the formula. The author finally decided to obtain the viscosities at the melting- and boiling-points by extrapolation of the straight or nearly straight lines obtained by plotting η against $1/T$ on paper, the ordinates of which were ruled logarithmically. In spite of the labour involved, it is much more satisfactory to obtain the values thus graphically, as the degree of extrapolation and any departure from linearity are at once apparent*.

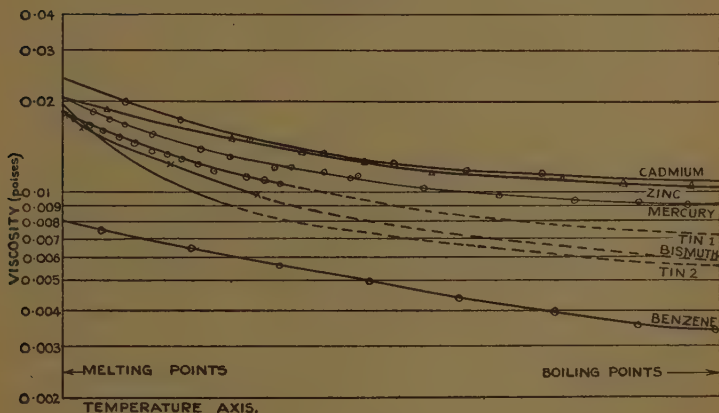
§5. Results.

Since the main purpose of the present study is to obtain a comparative idea of the viscosities of different liquids

* Since the above was written two papers dealing with the theory of liquid viscosity have been published (see Andrade, Phil. Mag. xvii. pp. 497, 698 (1934)). He proposes the formula $\eta v^{\frac{1}{3}} = Ac/vT$ for the variation of viscosity with temperature, v being the specific volume. The formula is not available for present purposes on account of the unknown melting- and boiling-point specific volumes.

throughout the liquid range certain results have been plotted in figs. 2, 3, and 4 which refer to metals and benzene; chlorine, bromine, and iodine; and various long-chain molecule liquids respectively. In all cases an equal distance is taken along the temperature axis to represent the interval between the normal melting- and boiling-temperature. The viscosities in poises, spaced logarithmically, are marked along the ordinates. The purpose of using a logarithmic spacing in the graphical exhibition of viscosity results is in order that liquids

Fig. 2.



Metals and benzene.

which differ widely in viscosity may be compared on the same diagram, and that curves which run parallel to each other throughout the liquid range may indicate equal percentage variations in viscosity between the melting- and boiling-temperatures.

Metals, Benzene, Halogens.

The data relative to figs. 2 and 3 are given in Table I. The melting-point, t_f , boiling-point t_b , and interval between them are shown in the second to the fourth columns, while the viscosity at the melting-point, η , and at the

Fig. 3.

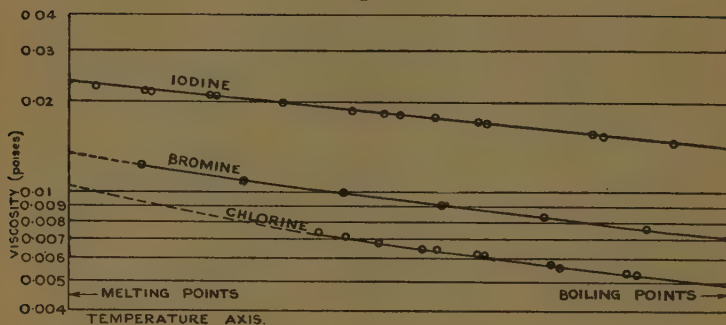


Fig. 4.

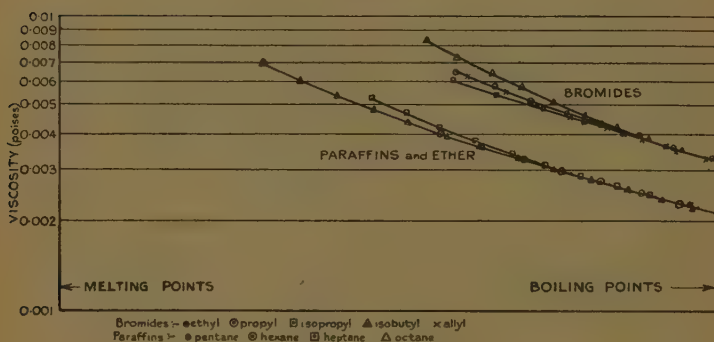
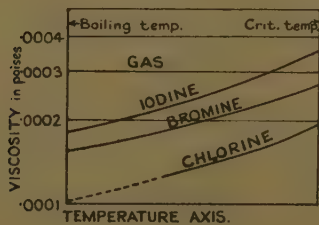


Fig. 5.



Intrinsic viscosities.

boiling-point, η_b , and the ratio between them, r , are shown in the fourth to the seventh columns.

The small variation in r (1.64 to 3 approx.) as compared with the great variations in the liquid temperature range (66° C. to 2028° C.) is the outstanding feature of the figures.

Losana has also given figures for *aluminium* and *lead* which, if they did not increase more rapidly near the melting temperature would yield the same low values for r . Losana states that the aluminium was not pure.

TABLE I.
Elements and Benzene.

Material.	$t_f^\circ\text{C.}$	$t_b^\circ\text{C.}$	$t_b - t_f$	η_f	η_b	$\frac{\eta_f}{\eta_b} = r.$	$\frac{F_f}{T_f}$
1. Zinc ...	419	907	498	·0204	·0103	c. 1·93	2·5
Cadmium	321	767	446	·0228	·0105	c. 2·17	2·6
Tin * ..	232	2260	2028	·0187	·0072	2·7	3·4
Tin †	232	2260	2028	·0195	·0056	3·5	3·4
Mercury..	— 38·9	356·9	396	·0210	·0091	2·32	2·4
Bismuth .	271	1380	1111	c. ·02	c. ·06	c. 3·3	> 3
2. Benzene..	5·1	79·6	74·1	·0082	·0034	2·2	
3. Chlorine..	— 101·6	— 34·6	67	·0106	·0049	2·16	
Bromine .	— 7·3	58·7	66	·0136	·0072	1·88	
Iodine ..	113·5	184·3	70·8	·0232	·0142	1·64	

* Losana.

† Stott.

Possibly Webster's⁽²¹⁾ recent researches concerning phenomena occurring when metals melt may be relevant to these data. He states that crystallization nuclei persist when bismuth, lead, and tin are melted, that in tin the nuclei are easily destroyed, but that in the cases of bismuth and lead the nuclei are only very slowly destroyed as the melt is superheated. If so, we may possibly assume that under careful conditions of melting and absolute purity of material the same low r values will be obtained for all metals. It may be noted that the melting-point viscosities should not be higher in order to conform to Andrade's⁽²²⁾ proposed melting-point formula. The possibility of transformation points must, however, be borne in mind.

The data available for *copper* and *iron* indicate melting-point viscosities of about 0.03 and 0.026 respectively, *i. e.*, in the same range, or a little above the metals of fig. 2. It is almost certain therefore that these metals have low r values, since boiling-point viscosities always lie within a narrow range, and it is unlikely that any of the curves will cross at higher temperatures.

It has been thought of interest to add the well-known ratio for metals between the molecular latent heat of fusion, F_f , and the absolute temperature of fusion, T_f , in the last column of Table I.

Paraffins, Mono-bromide Paraffin derivatives, Ether.

The curves obtained (fig. 4) are in marked contrast to that of benzene (fig. 2). Recorded measurements cease at 0° C., and as the liquids have low melting-points experimental data for the lower temperatures are not available. The list of liquids will be found under the figure. The boiling-point viscosities of each of the series, as is well known, are sensibly equal, while the curves diverge at lower temperatures. The ratios, r , vary from 9 to 60, in marked contrast to the low values obtained for the elements and benzene. They will be referred to in detail in the next paper dealing with the subject of molecular symmetry.

§ 6. *Intrinsic Viscosity.*

When the viscosities of liquids are compared, as they usually are, at an arbitrary temperature it does not follow that the one which has the higher viscosity is intrinsically the more viscous. For example, water is more viscous than mercury at 0° C. and mercury than water at 20° C.

If the viscosities are compared at corresponding temperatures, however, mercury is always more viscous than water. This may be expressed by saying that mercury has a higher intrinsic viscosity than water.

Fig. 3 shows the order of the intrinsic liquid viscosities of three halogens, *viz.*, iodine, bromine, and chlorine. Rankine's ⁽²³⁾ work on the viscosities of halogens in the gaseous state makes it possible to extend the conception of intrinsic viscosity to gases, using boiling- and critical-temperatures as corresponding temperatures. Fig. 5 shows that the intrinsic viscosities are in the same

order in the gaseous as in the liquid state. The relevant figures are shown in Table II., there being some uncertainty in the matter of extrapolation down to the boiling-point in the case of chlorine. The ratio of the liquid to the gaseous boiling-point viscosity is shown in the seventh column and that of the critical-temperature to the melting-temperature is shown in the last column.

The results are sufficiently significant to show that the general conception of intrinsic viscosity is a useful one, though when complicated liquids are compared, the viscosity-corresponding temperature curves will sometimes cross, indicating a greater intrinsic viscosity at some, and

TABLE II.

Name.	Liquid.		Gas.		$\frac{\eta_l}{\eta_b}$	$\frac{T_c}{T_f}$
	η_f	η_b	η_b	η_g		
Chlorine	·0106	·0049	(c. ·0001)	·00019	(50)	2·44
Bromine	·0136	·0072	·000167	·000287	43	2·17
Iodine	·0232	·0142	·000178	·000358	80	2·15

a less intrinsic viscosity at other, corresponding temperatures of one liquid as compared with another.

§ 7. Conclusion.

The method of presenting viscosity data given above provides, on account of its inclusion of the whole liquid range, a comprehensive view which is eminently satisfactory for the comparison of the viscosities of different liquids. It has been shown, for example, that three halogens for which data are available may be arranged in an order of increasing intrinsic viscosity by comparing them at the melting- and boiling-points respectively.

Moreover, the investigation has been rewarded by the discovery that liquids may be classified according as their viscosity alters little or much between the melting- and boiling-temperature, and this regardless of the actual temperature interval involved. This classification appears to be full of possibilities for gaining a knowledge of the

symmetry of molecules in the liquid state, which subject will be dealt with further in the next paper.

References.

- (1) Proc. Phys. Soc. xlv. p. 124 (1934).
- (2) *Il Notizario Chimico-Industriale*, ii. pp. 1, 63, 121 (1927).
- (3) 'The Crystalline State,' i. p. 218 (1933).
- (4) Phys. Rev. xxxviii. p. 1575 (1931), and references therein.
- (5) 'Nature,' cxxv. pp. 309, 580 (1930).
- (6) J. Amer. Chem. Soc. xviii. p. 618 (1896).
- (7) *Zeit. f. Elektrochemie*, xiv. p. 717 (1908).
- (8) *Z. f. Physik*, xlvii. p. 886 (1928).
- (9) Proc. Phys. Soc. xlv. p. 530 (1933).
- (10) J. Amer. Chem. Soc. xlvii. p. 754 (1925).
- (11) *Ann. Soc. Españ. de Fis. y Quim.* xi. p. 353 (1913); see also Drucker. *Z. f. Phys. Chem.* xcii. p. 287 (1918).
- (12) 'Nature,' cxi. pp. 532, 600 (1923).
- (13) Trans. Far. Soc. xxii. p. 401 (1926).
- (14) 'Nature,' cxxv. p. 709 (1930).
- (15) *Kolloid-Beihefte*, xxxiv. pp. 5, 270 (1931).
- (16) *Z. f. Physik*, lxxx. p. 217 (1933).
- (17) Taylor, Phys. Chem. i. p. 245 (1931).
- (18) Phil. Mag. xlviii. p. 1048 (1924).
- (19) *Zeits. f. Elektrochem.* xxxvii. p. 528 (1931).
- (20) Ind. J. of Phys. v. p. 371 (1930).
- (21) Proc. Roy. Soc. A, cxl. p. 653 (1933).
- (22) 'Nature,' cxxviii. p. 835 (1931); see also Phil. Mag. xvii. p. 497 (1934).
- (23) Proc. Roy. Soc. A, lxxxvi. p. 162 (1912); lxxxviii. p. 575 (1913); xci. p. 201 (1915).

April 1934.

XLVIII. Study of the Magneto-ionic Theory of Wave-propagation by means of Conformal Representation. By V. A. BAILEY, M.A., D.Phil., F.Inst.P., Associate Professor of Physics, University of Sydney*.

1. **G**ENERAL formulæ describing the propagation of electric waves in an ionized region of space, in the presence of a magnetic field, have been derived by Breit †, Appleton ‡, Golstein §, and Hartree ||. When the effects of collisions between the ions and molecules are taken into account, a frictional term is introduced,

* Communicated by the Author.

† Proc. Inst. Rad. Eng. xv. p. 709 (1927).

‡ U.R.S.I. Washington Proceedings, 1927.

§ Proc. Roy. Soc., A, cxxi. p. 260 (1928).

|| Proc. Camb. Phil. Soc. xxvii. p. 143 (1931).

and the resulting equations for the refractive index and polarization become complex. The method of introducing this frictional term has been given by Baker and Green *, and by Appleton †.

Surveys of the variations of refractive index of the medium and polarization of the wave, for various wave-frequencies and ionization densities, and for directions of propagation making various angles with the constant magnetic field, have been made by Mary Taylor ‡ and Ratcliffe §. The published surveys have been so far restricted to cases where the collision-frequency is zero. The complexity introduced by the frictional term is such that much labour is required for the computation of the refractive indices, absorption coefficients, and polarizations which is needed in order to examine the effect of the ionosphere on the passage of radio-waves.

At the suggestion of Dr. D. F. Martyn I have investigated this problem with the object of finding a more convenient method of making the survey and computations. This object has been attained by using the method of conformal representation.

Appleton || gives the formulæ which determine the refractive index μ , the absorption coefficient κ , and the polarization R in the following form :

$$\gamma_L^2 = \left(\alpha + i\beta - \frac{1}{c^2 q^2 - 1} \right) \left(\alpha + i\beta - \frac{1}{c^2 q^2 - 1} - \frac{\gamma_T^2}{1 + \alpha + i\beta} \right), \quad (1)$$

$$R = \frac{H_z}{H_y} = \frac{1}{i\gamma_L} \left(\frac{1}{c^2 q^2 - 1} - \alpha - i\beta \right), \quad . \quad . \quad . \quad . \quad . \quad . \quad (2)$$

where

$$\begin{aligned} c^2 q^2 &= (\mu - i\chi)^2, & \chi &= \kappa c/p, \\ \alpha &= -(p^2/p_0^2) - 1/3, & \beta &= p\nu/p_0^2, \\ \gamma_L &= \gamma \cos \theta, & \gamma_T &= \gamma \sin \theta, \end{aligned}$$

in which

$$p_0^2 = 4\pi N e^2/m, \quad p_1 = H e/mc, \quad \gamma = p p_1/p_0^2,$$

* Radio Research Board, Australia, Report 3, Bulletin No. 60, Commonwealth C. S. I. R. (1932).

† J. I. E. E. lxxi, p. 642 (1932).

‡ Proc. Phys. Soc. xlv, p. 245 (1933).

§ Wireless Eng. x, p. 354 (1933).

|| See Appleton, J. I. E. E. lxxi, p. 642 (1932).

and

m, e = mass and charge respectively of an ion ;

N = density of ionization ;

H = intensity of the constant magnetic field present ;

θ = angle between H and the direction of propagation ;

p = angular frequency of the wave ;

ν = frequency of collision of an electron with molecules.

2. The Polarization.

On eliminating $c^2q^2 - 1$ between (1) and (2) and rearranging the terms we get

$$R + \frac{1}{R} = \frac{i\gamma_T^2/\gamma_L}{1 + \alpha + i\beta} = \frac{2}{x + iy}, \quad . \quad . \quad . \quad (3)$$

where

$$x = \nu\sigma/p_1, \quad y = (p/p_0 - 2p_0/3p)\sigma/p_2 \quad . \quad . \quad (4)$$

and

$$\sigma = 2 \cos \theta / \sin^2 \theta, \quad p_2 = p_1/p_0 = H/c\sqrt{4\pi Nm}.$$

Let

$$z = x + iy, \quad \zeta = \xi + i\eta = z^{-1}, \quad R = \rho e^{-i\phi} = e^{iw}, \quad . \quad (5)$$

where

$$\rho > 0, \quad w = u + iv,$$

and $x, y, \eta, \rho, \phi, u$, and v are all real.

Then (3) becomes

$$\zeta = \cos w, \quad . \quad . \quad . \quad . \quad . \quad (6)$$

where

$$z\zeta = 1. \quad . \quad . \quad . \quad . \quad . \quad (7)$$

We now represent w and z conformally in the ζ -plane. Since (6) is equivalent to the pair of equations

$$\xi = \cos u \cosh v, \quad \eta = -\sin u \sinh v, \quad . \quad . \quad (8)$$

it follows that the u -curves and v -curves are given respectively by the following system of confocal hyperbolas and ellipses*:

$$\frac{\xi^2}{\cos^2 u} - \frac{\eta^2}{\sin^2 u} = 1, \quad . \quad . \quad . \quad . \quad (9)$$

$$\frac{\xi^2}{\cosh^2 v} + \frac{\eta^2}{\sinh^2 v} = 1. \quad . \quad . \quad . \quad . \quad (10)$$

* See, for example, Jeans's 'Electricity and Magnetism,' 3rd ed. pp. 267 and 270.

The x -curves and y -curves are similarly found to be given respectively by the following system of co-axial circles * :

$$\xi^2 + \eta^2 = x^{-1} \xi, \quad . \quad . \quad . \quad . \quad . \quad (11)$$

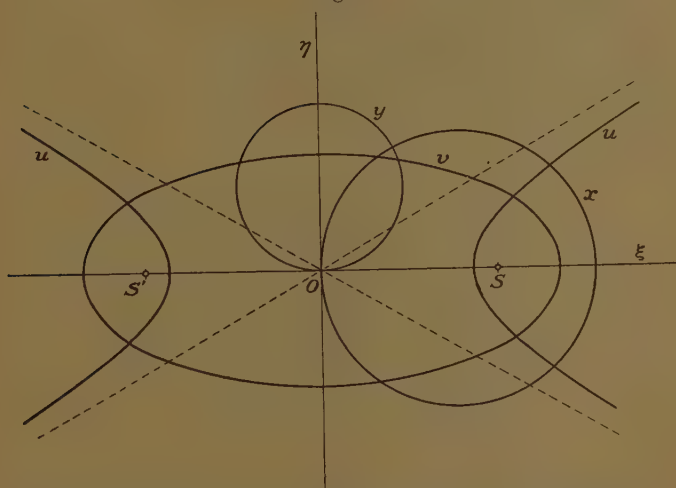
$$\xi^2 + \eta^2 = -y^{-1} \eta. \quad . \quad . \quad . \quad . \quad (12)$$

Fig. 1 gives examples of these curves.

From the definitions (5) we have

$$\phi = -u, \quad \rho = e^{-v},$$

Fig. 1.



and so the semi-axes a, b of the ellipse (10) are given by

$$2a = \rho^{-1} + \rho \quad 2b = \rho^{-1} - \rho.$$

Hence

$$\rho = a - b \quad \text{and} \quad \rho^{-1} = a + b.$$

If R_1, R_2 be the two roots of (3), then clearly $R_1 R_2 = 1$; hence

$$\rho_1 \rho_2 e^{-i(\phi_1 + \phi_2)} = 1.$$

Since ρ_1 and ρ_2 are both positive, therefore

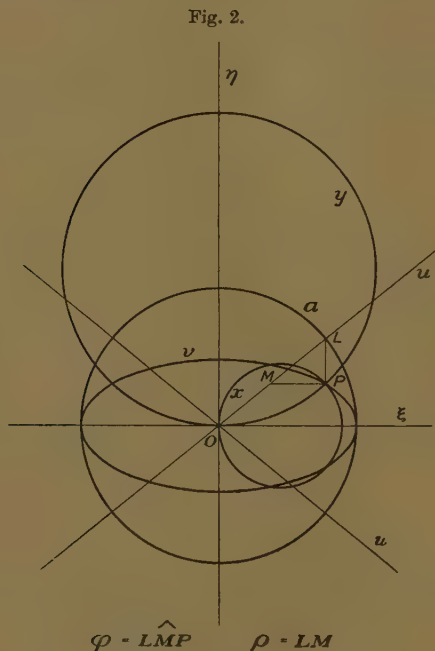
$$\rho_1 \rho_2 = 1 \quad \text{and} \quad \phi_1 + \phi_2 = 0,$$

* Jeans, *loc. cit.*

i. e.,

$$\text{and} \quad \left. \begin{aligned} \rho_1 &= a-b, & \phi_1 &= -u, \\ \rho_2 &= a+b, & \phi_2 &= u. \end{aligned} \right\} \dots \dots (13)$$

Since the semi-axes are essentially positive quantities, v is always positive.



The foci of the system of ellipses and hyperbolas lie on the ξ -axis at the points $\xi = \pm 1$.

The asymptotes of (9) are the lines $\eta = \pm \xi \tan u$, *i. e.*, the lines through the origin which makes angles $\pm u$ with the ξ -axis.

The circles (11) have their centres on the ξ -axis, have diameters equal to x^{-1} , and all pass through the origin. The circles (12) form a similar system with their centres on the η -axis.

If then a chart be constructed which gives the curves for a large series of values of u , v , x , and y , it can be used to determine the polarization, as follows :—

First, by means of (4) the quantities x and y are calculated. If the corresponding curves intersect in the positive quadrant at P, then the ellipse and hyperbola which pass through this point at once give ρ_1 , ϕ_1 , ρ_2 , and ϕ_2 by means of (13).

In such a chart the hyperbolas may be replaced by the auxiliary circles of the ellipses, *i. e.*, the concentric circles of radii a and the radial lines u as illustrated by fig. 2.

For it is easy to show by means of (8) that the vertical line drawn through P will pass through the intersection L of the auxiliary circle a and the radial line u whose angle of inclination to the ξ -axis is $-u$, and that if the horizontal line through P cuts the line u at M then $LM=a-b$. Thus

$$\phi_1 = \widehat{LMP} \quad \text{and} \quad \rho_1 = LM$$

are at once given by such a chart.

If $R=r-is$, then $r=MP$, $s=PL$, and so r and s are also easily obtained.

3. The Refractive Index and Absorption Coefficient.

The equation (2) may be written as

$$(\alpha + i\beta + iR\gamma_L)(\overline{\mu - i\chi^2} - 1) = 1,$$

and so, on setting

$$R=r-is, \quad X=\alpha-s\gamma_L, \quad Y=\beta+r\gamma_L, \quad . \quad (14)$$

$$\xi=\mu^2-\chi^2-1, \quad \eta=-2\mu\chi, \quad . \quad . \quad . \quad (15)$$

it becomes

$$Z\zeta=1,$$

where

$$Z=X+iY.$$

This is identical in form with (7), so X and Y are conformally represented in the ξ -plane by the same circles as those for x and y .

From (15) we find that the μ -curves and χ -curves are given respectively by the parabolas

$$\eta^2=4\mu^2(\mu^2-1-\xi) \quad . \quad . \quad . \quad . \quad (16)$$

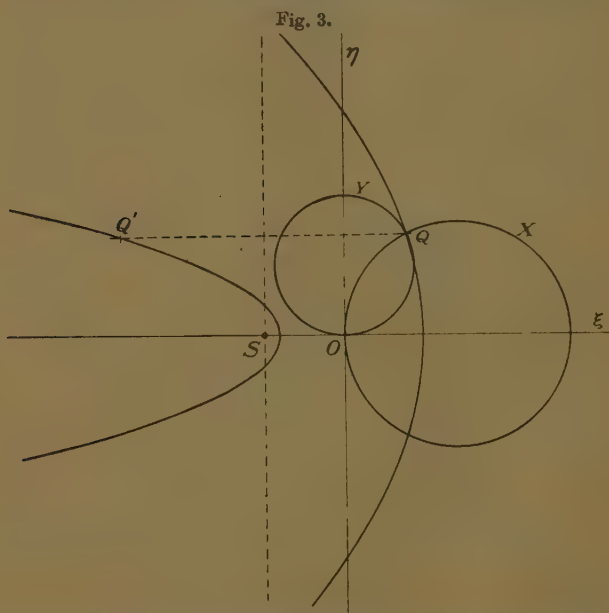
$$\text{and} \quad \eta^2=4\chi^2(\chi^2+1+\xi), \quad . \quad . \quad . \quad . \quad (17)$$

whose axes lie along the ξ -axis and whose common focus is the point $(-1, 0)$. It is clear that the χ -curves are the

exact images of the μ -curves in the line $\xi = -1$, and so need not be drawn.

If a chart be constructed, as in fig. 3, giving the curves for X, Y, and μ^2 , it can be used to determine μ^2 as follows :—

First r and s are determined with the aid of fig. 2, as already explained ; then X and Y are calculated by means of (14). The intersection Q of the corresponding circles in fig. 3 will lie on the parabola whose value of μ^2 is that



which is required. The image Q' of Q in the dotted line will then give a parabola whose value of μ^2 gives the required value of χ^2 .

4. Other Aids.

The quantity $\sigma = 2 \cos \theta / \sin^2 \theta$ which occurs in (4) can be determined graphically as follows :—

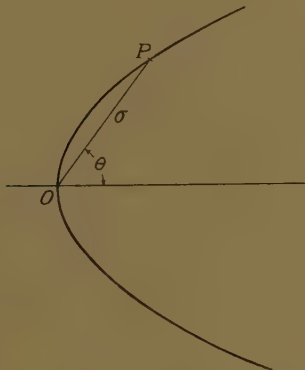
Writing $\sigma = r$,
 we have $r^2 \sin^2 \theta = 2r \cos \theta$,
i. e., $y^2 = 2x$,

where (x, y) are the Cartesian coordinates of a point whose polar coordinates are (r, θ) .

This is the parabola shown in fig. 4. The radius vector OP , which is inclined to the axis at an angle θ , gives the value of σ . Such a parabola can also be found in the chart in fig. 3, being that whose vertex is at the point $(-\frac{1}{2}, 0)$, and for which $\eta^2 = \frac{1}{2}$.

If a pantograph be available it could also be used to handle the factor σ which occurs in both x and y , and so enable the effect of varying θ to be studied.

Fig. 4.



5. *Summary and Conclusion.*

By means of conformal representation a graphical method is established for the rapid detailed study of the propagation of plane electric waves in an ionized region of space where a constant magnetic field is also present. The two charts needed for the determination respectively of the polarization and the refractive index are easily drawn, as they involve only circles, ellipses, and parabolas.

In another paper Dr. Martyn will give an account of an actual survey of the circumstances of propagation by means of such charts.

I am much indebted to Dr. Martyn for some useful criticisms, and to Mr. R. St. C. Pitt for drawing the diagrams.

XLIX. *Notices respecting New Books.*

The New Background of Science. By Sir JAMES JEANS, D.Sc., F.R.S. Second edition, Jan. 1934. [Pp. viii+312.] (Cambridge : at the University Press. Price 7s. 6d.)

IN the preface to the first edition, which appeared only about a year ago, Sir James stated that "after undergoing a succession of kaleidoscopic changes, theoretical physics appears to have attained a state of comparative quiescence in which there is fairly general agreement about essentials." In the intervening year some new discoveries have been made, especially that of the neutron (which carries no electric charge of either sign), and when atoms are exposed to intense bombardment, as by the cosmic rays, yet another constituent appears known as the positive electron or positron—it carries the same positive charge as the proton but has a mass only about equal to that of the negative electron, *i. e.*, about one eighteen-hundredth part of the mass of a proton. There is evidence that it is only a temporary form of matter. "If further research confirms this, then, whatever primary qualities matter may possess, permanence in time, uncreatability, and indestructibility must no longer figure in the list."

These new discoveries have necessitated some restatement in matters of detail, but none on the main argument of the book.

Uncle Joe's Nonsense for Young and Old Children. By J. W. MELLOR, D.Sc., F.R.S. [Pp. 231, with 129 drawings and 2 photographs.] (London : Longmans, Green & Co., 1934. Price 12s. 6d.)

THIS book, by an eminent authority on ceramics (or keramics), proves that he is not all clay. Its publication has been arranged by the Ceramic Society as a memento of services rendered by the author, and consists mainly of letters sent at various times to his nephews and nieces in New Zealand. These letters are grave and gay (chiefly gay). Only occasionally does their subject-matter fall within the range dealt with in this Magazine, and the way in which it is treated might not satisfy all readers. Nevertheless the book contains many wise statements. It is to the pictures (by the author) that we turn with the greatest delight (and there are more than one hundred of them). The author displays a genius of high order for pictorial caricature which we had not been led to expect by his other books.

The Principles of Geometry.—Vol. VI. By H. F. BAKER, F.R.S. [Pp. 308.] (Cambridge University Press. Price 17s. 6d. net.)

THE volume under review is the sixth in Prof. H. F. Baker's great panorama of Algebraic and Synthetic Geometry. The first volume deals with "Foundations"; the second with "Plane Geometry, Conics, Circles, Non-Euclidean Geometry"; the third with "Solid Geometry, Quadrics, Cubic Curves in Space, Cubic Surfaces"; the fourth with "Higher Geometry," being illustrations of the utility of the consideration of Higher Space, especially of four and five dimensions; the fifth with the "Analytical Principles of the Theory of Curves"; the sixth with the "Introduction to the Theory of Algebraic Surfaces and Higher Loci." The present volume contains seven chapters. Chapter I. treats of "Algebraic Correspondence"; Chapter II. of "Schubert's Calculus and Multiple Correspondence"; Chapter III. of "Transformations and Involutions for the most part in a Plane"; Chapter IV. of "Preliminary Properties of Surfaces in Three and Four Dimensions"; Chapter V. of "Introduction to the Theory of the Invariants of Birational Transformation of a Surface, particularly in Space of Three Dimensions"; Chapter VI. of "Surfaces and Primals in Four Dimensions, and Formulæ for Intersections"; Chapter VII. of "Illustrative Examples and Particular Theorems."

The general plan of Prof. Baker's volumes will therefore be clear. He begins with the very simplest configurations of straight lines, planes, conics, and quadrics in his earlier volumes, and develops their properties in considerable detail. Many of these properties are well known to the general student of mathematics, but the author's aim throughout is to extend and deepen this elementary knowledge and to relate it to more fundamental theorems of greater simplicity and generality. This is nowhere better evidenced than in his careful exposition of the somewhat complicated and lopsided properties of the cubic surface, in space of three dimensions, which become simplified almost beyond recognition, when the surface is regarded as the projection of the surface of intersection of two hyperquadrics in space of four dimensions. Properties which appear accidental in the case of the cubic surface assume the character of inevitability when viewed as derived from the four-dimensional surface. The general principle hereby exemplified of simplification through projection from a higher space to a lower is characteristically present throughout all the volumes. As the volumes proceed the investigation of the detailed properties of individual curves, surfaces, etc. recedes into the background, and theorems of greater and greater generality are made to occupy the attention of the

reader. Volumes V. and VI. are indeed very general in aim and character.

Volume VI. is a most important contribution to the general theory of Algebraic Geometry. It cannot be regarded as in any sense easy reading, but the fundamental character and generality of its contents preclude easy treatment. Nevertheless, the skill of the experienced expositor is everywhere apparent. There is a really first-rate and most interesting glimpse into "research-psychology" given in the introduction to Chapter V., where the invariant $p = \frac{1}{2}w - m + 1$, i. e., the genus of a plane curve, is defined first of all from the standpoint of the tangents that can be drawn from any assigned point to the curve, and then the definition is widened to include the points of intersection with the curve of linear systems of curves. Starting from this viewpoint, the author shows how one would naturally attempt to do precisely the same thing in dealing with the corresponding problem for surfaces, and he thereafter gives some account of the work of Zeuthen, Noether, and Clebsch from their respective standpoints. The discovery of the two invariants of a surface P_g and P_n and the importance of $P_g - P_n$ in birational transformation is thereafter explained. This is a particularly interesting portion of the book from other standpoints than the purely mathematical, and its perusal may be specially commended to the young student just launching himself on his career as an investigator.

Another interesting feature of the book is the continual and entirely unexpected appearance in theory of great generality of particular and concrete properties. Thus, in the general theory of Algebraic Correspondences we suddenly stumble upon the following delightful property of the plane quartic curve:—

"It is known that there are sets of six pairs of the bitangent of a plane quartic curve, such that the eight points of contact, of any two of these pairs, lie upon a conic. The points of contact of the 28 bitangents of the curve lie on the degenerate curve of order 14 which is composed of seven such conics, properly taken (and in various ways)."

These sudden and continual obtrusions of the concrete keep alive the reader's faith, when the analysis is at its most abstract, and his mind is being most severely taxed.

A particularly important section is that on Schubert's Calculus, which has not hitherto been very readily accessible to the majority of English readers.

Perhaps the most debatable problem presented by the treatment adopted in the book is as to whether or not adequate space has been given to the part that can be played in the theory of geometry by Abelian Integrals in two and three

dimensional space. The main object of the present volume is of course to develop Algebraic Geometry, but there are many concepts which require a very artificial introduction and definition when presented from the purely geometrical standpoint, but which obtrude themselves immediately and simply when viewed from the standpoint of Abelian Integrals. One need only instance the genus of a curve and from some standpoints the theory of linear systems of points on a curve. Some readers might therefore have welcomed an increase in the volume and a fuller treatment of the Abelian Theory. Perhaps it is the author's intention to develop these themes on the lines of Picard-Simart in a later volume.

It is impossible to say more in a general review. Prof. Baker has laid the whole mathematical world under a very deep debt of gratitude for his prolonged and sustained effort, stretching over six substantial volumes, and for rendering accessible to general readers information and viewpoints that otherwise would have been capable of approach only by the expert.

Actualités scientifiques et Industrielles.
(Hermann et Cie, Paris, 1934.)

No. 76. *L'ancienne et la nouvelle logique.* By RUDOLF CARNAP. [Pp. 37.] (Prix 8 fr.)

No. 97. *Théorie de la connaissance et physique moderne.* By PHILIPP FRANK. [Pp. 54.] (Prix 8 fr.)

No. 152. *Les énoncés scientifiques et la réalité du monde extérieur.* By MORITZ SCHLICK. [Pp. 53.] (Prix 10 fr.)

Trans. E. VOUILLEMIN. Introd. M. BOLL.

THE essays in these booklets are all translations from articles in the journal *Erkenntnis*. Each is preceded by an illuminating biographical note on the author by M. Boll. The three essays are closely related, as they present various aspects of the outlook of the "Vienna circle," which claims to have broken away almost completely from traditional philosophy. Essentially a critical philosophy is built up which aims at the logical analysis of scientific propositions. The traditional logic, which dealt almost exclusively with predicative forms, is inadequate; a method for dealing with "relations" is required such as has been developed primarily in connexion with mathematics. The view is stressed throughout that science can raise no questions which cannot be answered by the methods of science itself; a transcendent metaphysic is not required. Metaphysical doctrines, in pronouncements such as those about the "real," are set aside as useless, not because they are false, but because they are meaningless. The general outlook may be roughly described as that of logical empiricism,

Carnap gives an account of the elements of the logical technique. He shows clearly the distinction between logical propositions (which can be tautological or contradictory) and experimental propositions (which can be true or false). Frank outlines the historical development of the new outlook. He considers the scientific system as consisting of symbols such that there is a one-to-one correspondence between the symbols and experiences. He also discusses the causality question, showing that many of the difficulties arise from questions being put in such a way as to render impossible any significant answer; this part of the essay forms a good introduction to his book 'Das Kausalgesetz und seine Grenzen.' Schlick, with admirable lucidity, considers the logical form and content of scientific propositions, and discusses the significance of "reality" and the "external world" from the new point of view.

These essays should be of considerable value as giving a clear and short introduction to the definitive and explicit development of a philosophical treatment of science which will make a wide appeal to scientific readers.

Theoretical Physics. By W. WILSON, F.R.S.—Vol. II. *Electromagnetism and Optics (Maxwell - Lorentz)*. [Pp. 308 + diagrams.] (Methuen & Co., Ltd., 1933. Price 18s. net.)

THIS admirably produced text-book is a worthy successor to its predecessor, which dealt with Mechanics and Heat, and was first published in 1931.

The treatment, as the title suggests, is theoretical in character, and is intended for university students—the matter being in the main drawn from Professor Wilson's own lectures on the subject.

The main part of the volume—234 pages—is devoted to the usual topics in electrostatics, magnetism, and electromagnetic effects. Within these sections are included useful and illuminating chapters on Clerk Maxwell's Theory and the electron theory.

The last seventy-three pages deal with geometrical and physical optics in a rather abbreviated manner. In geometrical optics Fermat's principle is stated, and followed up by a brief consideration of reflexion and refraction. Spherical and chromatic aberrations are dismissed in a few lines.

In Physical Optics the briefest account of the phenomena of interference is given, followed by final—but too short!—chapters on the propagation of light.

The book can be thoroughly recommended to advanced university students of applied mathematics and physics.

[The Editors do not hold themselves responsible for the views expressed by their correspondents.]

E.

Fig. 2a.



2b.



E

